RIVER BASIN PLANNING OF SUBANSIRI RIVER UNDER CLIMATE CHANGE SCENARIOS

A thesis submitted in partial fulfillment of the requirement

for the award of the degree of

Doctor of Philosophy

By

Shivam

Department of Civil Engineering

Indian Institute of Technology Guwahati

January 2017

Department of Civil Engineering
Indian Institute of Technology Guwahati
Guwahati-781039, Assam, India

Certificate

It is certified that the work contained in the thesis entitled "**River basin planning of Subansiri river under climate change scenarios** " by Shivam, Roll Number 126104039, a student in the Department of Civil Engineering, Indian Institute of Technology Guwahati for the award of the degree of Doctor of Philosophy has been carried out under our supervision and that this work has not been submitted elsewhere for a degree.

Prof. Arup Kumar Sarma
Professor
Department of Civil Engineering
Indian Institute of Technology
Guwahati-781039

Dr. Manish Kumar Goyal
Assistant Professor
Department of Civil Engineering
Indian Institute of Technology
Guwahati-781039

Date:

Declaration of Authorship

I, Shivam, declare that this thesis titled '**River basin planning of Subansiri river under climate change scenarios**' and the work presented in it has been carried out by me under the supervision of Prof. Arup Kumar Sarma and Dr. Manish Kumar Goyal, Department of Civil Engineering, Indian Institute of Technology Guwahati. This work has not been submitted elsewhere for the award of any degree.

Shivam

Department of Civil Engineering

Indian Institute of Technology

Guwahati-781039

Date:

Acknowledgment

I would like to place on record my deep sense of gratitude and sincere thanks to my thesis Supervisors Prof. Arup Kumar Sarma, Professor, and Dr. Manish Kumar Goyal, Assistant Professor, Department of Civil Engineering, Indian Institute of Technology Guwahati for their invaluable guidance and full hand cooperation throughout the all aspects of this research work. I also admire their patient explanation of the concepts and basic principles.

I am grateful to the Chairman of my Doctoral committee Prof. Subashisa Dutta and members Prof. Rajib Kumar Bhattacharjya and Dr. Sreeja P. for their valuable suggestions and kind support during completion of the research work.

I am thankful to National Hydro-power Corporation, for providing the necessary data during the research work.

Particularly I am indebt to my parents Shri S.B. Gupta and Smt. Sukhda Devi, sister Shweta, brothers Vivek and Prateek for their blessings and unconditional support for bringing me to such level. Without their faith in me, I would not have been able to carry out this study. Special thanks to Vishal Singh, Vivek Gupta, Uttam Puri Goswami, Ashutosh Sharma, Juna Devi, Manas Khan, Venkatesh, Bhargava and Gilbert Hinge.

I am thankful to the scientific staff of the Dept. of Civil Engineering. I am thankful to the Indian Institute of technology Guwahati for providing the magnificent facilities and beautiful atmosphere to carry my research work.

Abstract

In this research work, Subansiri river which is the largest tributary of Brahmputra river in Northeastern part of India was selected for the study. Impact of climate change on the hydro-climatic parameters of the river basin was investigated using the statistical downscaling technique. Fifth phase coupled model inter-comparison project (CMIP5) general circulation model (GCM) datasets with their representative concentration pathway (RCP) scenarios as archived by Intergovernmental panel on climate change (IPCC) has been utilized in the study. Three GCMs namely ESM2G, ESM2M and GFDL-CM3 datasets were used for the impact assessment for low, moderate and high emission scenarios. Statistical downscaling model (SDSM) was implemented for the downscaling of the maximum temperature (Tmax), minimum temperature (Tmin) and precipitation of the five selected climate stations of the river basin for the long term period of 2011-2100. Before projecting the long term Tmax, Tmin and precipitation downscaling models were calibrated and validated for the historical observed period.

Downscaling results of the Tmax, Tmin and precipitation indicate the rise in temperature over the river basin for all RCP scenarios. Average annual maximum temperature is likely to increase in the coming time along with the minimum temperature. Precipitation trend also shows the increase in the precipitation for all the scenarios. Apart from this, extreme precipitation indices such as total precipitation, simple daily intensity index, consecutive dry days, consecutive wet days, heavy precipitation days, very

heavy precipitation days, wet days and very wet days were calculates to investigate the changes in the extreme events in the future for different climate change scenarios.

After projection of the Tmax, Tmin and precipitation, Hydrological modeling of the Subansiri river basin was carried out using soil and water assessment tool (SWAT). SWAT model requires digital elevation map (DEM), soil map, land use land cover map and weather data such as precipitation temperature etc for the simulation of the streamflow at the given outlet of the catchment along with the other hydrological parameters such as evapotranspiration, soil moisture etc. SWAT hydrological model was calibrated for the period of 2002-2010 and validation was carried out for the period of 2011-2013. After successful calibration and validation of the hydrological model, future streamflow of the river were projected for the period of 2016-2100 utilizing the downscaled precipitation and temperature series as the primary input in the model. Streamflow projection results exhibit increase in the streamflow for the river basin as the increase precipitation will enhance the surface runoff process. All the emission scenarios projects increase in the streamflow of the basin along with the water yield from each sub-basins.

Taking in to consideration the impact of climate change, major concern for the policy makers and planners is the management of the water resources for the future water demand of increasing population and other sectors. Subansiri river basin consists one reservoir at the Gerukamukh in Assam, this study focuses on the projection of the future water demand of the river basin and suggest the available water resources and the demand of the water for future which will be helpful for the policymakers to decide the strategies to overcome the water scarcity situation in the future. Three districts in the command area of the reservoir were taken for the study and their population data were collected for the last two census i.e. 2001 and 2011. On the basis of these two census,

a projection of the population were made for the future. Inflow to the reservoir were projected with the hydrological model for the emission scenarios and with the help of reservoir physical characteristics such as elevation capacity curve, the water availability in the reservoir were calculated. Further a coupled approach of hydrological modeling and water management modeling were suggested for the management of the available water resources for different emission scenarios.

Contents

List of Figures

List of Tables

List of Abbreviation

$ALPHA_BF$	Baseflow alpha factor
$ALPHA_BNK$	Baseflow alpha factor for bank storage
CH_K2	Effective hydraulic conductivity
CH_N2	Mannings roughness coefficient
GW_DELAY	Groundwater delay
GW_REVAP	Groundwater revaporation coefficient
R^2	Coefficient of determination
SOL_AWC	Available water capacity of the soil layer
SOL_BD	Soil bulk density
SOL_K	Soil hydraulic conductivity
95PPU	95 percent prediction uncertainty
A1, B1, A2, B2, A1B	Emission Scenario from third assessment report
AMC	Antecedent moisture content
ANN	Artificial neural network
APHRODITE	Asian precipitation highly resolved observational data integration towards evaluation of water resources
AR	Assessment report
AR4	Fourth assessment report

BSDP	Bayesian Stochastic Dynamic Programming
CANMX	Maximum canopy storage
CGCM3	Coupled Global Climate Model phase 3
CMIP3	Coupled model inter-comparison project phase third
CMIP5	Coupled model inter-comparison project phase fifth
CN	Curve number
CN2	Curve number for AMC 2 condition
CRB	Columbia River Basin
CSM	Climate System Models
CWD	Consecutive wet days
DHSVM	Distributed hydrology–soil–vegetation model
DTR	Diurnal temperature range
EMP	Ecological sustainable management practices
ESCO	Soil evaporation compensation factor
ESM	Earth System Models
FAO	Food and agriculture organization
GA	Genetic algorithm
GCM	General circulation model
GFDL	Geophysical Fluid Dynamics Laboratories
GLUE	Generalized likelihood uncertainty equation
GWQMN	Threshold depth of water in shallow aquifer
HadCM3	Hadley center climate model
HRU	Hydrological response units

IDW	Inverse distance weighting
IDWA	Inverse distance weighted average
IMD	India meteorological department
IPCC	Intergovernmental Panel on Climate Change
KHEP	Koyna Hydro-Electric Project
LARS-WG	Long Ashton Research Station Weather Generator
LHS	Latin Hypercube Sampling
LSHE	Lower Subansiri hydro-electric project
LULC	Land use and land cover
MHI	Moisture homogeneity index
MK	Man-Kendall
MW	Mega Watt
NCAR	National Center for Atmospheric Research
NCEP	National center for environmental prediction
NHPC	National Hydro-power commission
NLP	Non-linear Programming
NSE	Nash-Sutcliff Efficiency
PEST	Parameter estimator
PRCPTOT	Total annual precipitation
PRP	Percentage reduction in partial correlation
R10mm	Heavy precipitation days (precipitation more that 10mm)
R20mm	Very heavy precipitation days (precipitation more that 20mm)
RCP	Representative concentration pathways

rhsmax	Relative humidity maximum
rhsmin	Relative humidity minimum
RMSE	Root Mean Square Error
RSR	Square error observations standard deviation ratio
RVM	Relevance vector machine
SCS	Soil conservation services
SDII	Simple daily intensity index
SDP	Stochastic Dynamic Programming
SDSM	Statistical downscaling model
SFTMP	Snowfall temperature
SMFMN	Melt factor for snow on 21 December
SMFMX	Melt factor for snow on 21 June
SMTMP	Snowmelt base temperature
SNO50COV	Fraction of snow volume
SNOCOVMIN	Minimum snow cover content
SNOCOVMX	Maximum snow cover content
SRES	Special report on emission scenario
SRTM	Shuttle radar topographic mission
SSVM	Smooth Support vector machine
SUFI2	Sequential uncertainty parameter fitting approach
SURLAG	Surface lag
SVM	Support vector machine
SWAT	Soil and Water Assessment Tool

SWATCUP	SWAT Calibration and uncertainty program
SWE	Snow water equivalent
TAR	Third assessment report
tas	Temperature at surface
tasmax	Maximum temperature at surface
tasmin	Minimum temperature at surface
TIMP	Snow pack temperature lag factor
TVI	Temperature variability index
USDA	United States Department of Agriculture
VIC	Variable infiltration capacity

List of Symbols

Symbols	Description
CO_2	Carbon di-oxide
T_{deb}	Debiased daily time series of temperature
T_{SCEN}	Downscaled temperature scenario
$\bar{T}_{CONT}$	Long term monthly mean of historical model temperature
$\bar{T}_{obs}$	Monthly mean of historical observed temperature
P_{deb}	Debiased daily time series of precipitation
P_{SCEN}	Downscaled precipitation series
$\bar{P}_{obs}$	Monthly mean of historical precipitation
$\bar{P}_{CONT}$	Long term monthly mean of historical model precipitation
T_{o_i}	ith data point of observed temperature
T_{p_i}	ith data point of observed precipitation
$\bar{T}_{o_i}$	Mean of observed variable (temperature/precipitation)
$\bar{T}_{p_i}$	Mean of model variable (temperature/precipitation)
R^2	Coefficient of determination
S_{w_t}	Final soil water content (mm H_2O)
S_{w_a}	Initial soil water content (mm H_2O)
R_{day}	Amount of precipitation in day i (mm H_2O)

Q_{surf}	Amount of surface runoff on day i (mm H_2O)
E_a	Amount of evaporation on day i (mm H_2O)
W_{seep}	Amount of percolation and bypass exiting the soil profile bottom on day i
Q_{gw}	Amount of return flow on day i (mm H_2O)
Q_s	Total surface runoff (mm)
R	Daily rainfall (mm)
I_a	Initial abstraction such as infiltration prior to runoff (mm)
S	Retention parameter on combination of soil
Q_{min}	Lower limit of parameter value
Q_{max}	Upper limit of parameter value
Q_{absmin}	Lower limit temperature of parameter value
Q_{absmax}	Upper limit temperature of parameter value
g_θ	Objective function
J_{ij}	Sensitivity matrix
ΔQ_j	95 % predictive interlog parameter θ
C	Parameter covariance matrix
S_g	Variance of objective function
Q_j	Parameter Q_j for best estimates
v	Degree of freedom
$Y^M_{t_1,97.5\%}$	Upper boundary of 95 percent population
$Y^M_{j,2.5\%}$	lower boundary of 95 percent population
σ_{obs}	Standard deviation of measure data
S_t	Storage mm^3
km	Kilometer

CHAPTER 1

Introduction

1.1 Purpose of the study

Indian sub-continent is drained by several perennial Himalayan river such as Ganges, Indus, and Brahmaputra. Indus River drains the northern part of India, Ganga River drains the North-central part of India whereas Brahmaputra River drains the North-eastern part of the India. Brahmaputra River is considered as the life line of the north-eastern India as it is the largest source of surface water. Tributaries of the Brahmaputra river are mostly glacier and snow-melt contributed and perennial in nature which makes this region a potential hydropower generation region (Singh et al., 2013). Brahmputra River drains eight states of the north-east which include the states of Assam, Arunachal Pradesh, Meghalaya, Manipur, Nagaland, Tripura, Mizoram and Sikkim.

Intergovernmental Panel on Climate Change (IPCC) reported an unequivocal warming trend of global temperature since 1950. Fifth assessment report (AR5) of IPCC concluded that the ongoing warming trends are going to affect the hydrology of the mountainous region (IPCC, 2014). Extreme events are likely to increase in the near future for the projected climate change scenarios. Major impacts of warming trends

will be on the snow packs and glacier of the mountainous systems.

Rivers originating from the Himalayan mountains are mainly snow and glacier fed. Changes in the snowfall and snowmelt amount would cause serious alterations in the ecology and hydrology of the region. Several studies on climate change implicates the adverse impacts of the global warming on the Himalayan glaciers and this phenomena subsequently affecting the water resources of the major river basins. Himalayan region is very much vulnerable to the climate change impacts, recent studies on the climate change impacts on the precipitation and temperature of the Himalayan range shows that this region is also not untouched with the impacts of global warming (Bhutiyani et al., 2007; Dahal et al., 2016; Khadka et al., 2014). Increased precipitation and temperature are eventually affecting the hydrology and water resources in the region (Bhutiyani et al., 2010; Rajbhandari et al., 2015).

Increasing population, urbanization, industrialization, deforestation will eventually impose immense burden on the available water resources. Drastic increase in the electricity demand, irrigation water requirement, and drinking water supply will cause the pressure on the government and policy makers to search for optimal use of available resources. Situation worsen when threat of climate change impacts are combined along with the demographic and socio-economic changes. Taking into consideration the above mentioned facts, objectives of this research work focus on the assessment of the changes in temperature and precipitation, its impact on the hydrology of the Subansiri river basin and development of a simulation-optimization model for water resources management of the river basin under different climate change scenario.

1.2 Problem statement

This research work will focus mainly on the four sectors i.e., change in precipitation and temperature for the climate change scenarios, hydrological modeling of the Subansiri river basin, future projections of the streamflow for the climate change scenarios using hydrological modeling, change in the water demands for different sectors, and river basin planning under climate change scenarios.

Subansiri River is the largest tributary of Brahmputra river which contributes largest amount to the river discharge as compared to the other tributaries of Brahmputra (Singh et al., 2013). It originates in the Tibet plateau and mainly fed by snow and glacier melt. Downscaled precipitation and temperature data for the river basin scale from the coarse resolution CMIP5 GCMs will help to understand the possible changes in the pattern of these meteorological variables and eventually the discharge in the Subansiri river.

This study proposes a coupled approach for the simulation-management model and its application on the Subansiri river basin to assess the changes in water demand for the various sectors along with the changes in the streamflow of the river for different climate change scenarios.

1.3 Research objective

Following objectives have been decided for the present research work

- Estimation of the changes in precipitation and temperature in Subansiri river basin for IPCC AR5 emission scenarios.
- Assessment of the trends in precipitation and temperature extreme events for

historical and future timeseries.

- Streamflow simulation of Subansiri river basin and estimation of changes in water resources by streamflow projections for different emission scenarios.

- To develop the simulation-management approach by using the hydrological model and water resources planning model and its application in river basin planning of Subansiri river.

1.4 Organization of the thesis

Present research work is divided in several chapter which are explained in brief as below

- Chapter 2 gives the brief literature review of the works done previously on topic selected in the present work. Literature review covers the topic related to the climate change impact assessment on precipitation and temperature. Downscaling of the precipitation and temperature from coarse resolution of the GCM to the basin scale, hydrological modeling and uncertainty analysis of river basins, changes in streamflow for climate change scenarios, optimization methods for water resources management.

- Chapter 3 comprises of the detailed description of study area Subansiri river basin and data collection. Details of basin characteristics, topographical details major land use land cover classes, soil type is discussed in the chapter along with the hydro-climatological data collection and data used in the study.

- Chapter 4 describes the detailed methodology used for the downscaling of temperature and precipitation for the Subansiri river basin. Downscaling includes

predictor selection, model preparation and projection of the precipitation and temperature for the climate change scenarios over the period of 2011-2100.

- Chapter 5 provides the explanation of the hydrological modeling and uncertainty analysis of Subansiri River using Soil and Water Assessment Tool (SWAT) model and SWAT Calibration and Uncertainty Program (SWAT-CUP) model. Future projection of the streamflow for different emission scenarios.
- Chapter 6 contains the details of water resources management modeling, integrated simulation-management approach for management, changes in water demand for different sectors for various climate change scenarios.
- Chapter 7 summarizes the discussion and conclusion of the entire research work and future scope of the research work.

CHAPTER 2

Literature review

2.1 General

The literature review comprises of the climate change impacts on precipitation and temperature on a Himalayan river, hydrological modeling and climate change impacts on the water resources of the river basin, socio-economic changes in the basin and its impact on the available water resources. Thus the literature review is organized in the way covering the global climate change issues, climate change impact on the water resources on global scale, on Indian sub-continent and on Himalayan river systems.

2.2 Greenhouse gas emission and climate change

Changes in the atmospheric abundance of greenhouse gases and aerosols, in solar radiation and in land surface properties alter the energy balance of the climate system. The exact definition of the climate change given by Intergovernmental Panel on Climate Change IPCC (2007), "Climate change refers to a change in the state of the climate that can be identified (e.g., by using statistical tests) by changes in the mean and/or the

variability of its properties, and that persists for an extended period, typically decades or longer". IPCC suggests the possible increase in the emission of greenhouse gases in the future considering the various anthropogenic factors, which are known as the emission scenarios (Cayan et al., 2008; IPCC, 2007). These emission scenarios are helpful tools for impact assessment and deciding the mitigating measures. Basic driving factors of greenhouse gas emissions are industrialization, urbanization, social and economic development and technological change. Emissions scenario projections are the products of very complex dynamic systems, consists of socio-economic changes, technological changes and demographic changes. Scenarios are sources to depict the future projections that is how driving forces enhances the emission which subsequently assist in impacts assessment studies, adaptation, and mitigation.

It is evident from the analysis of the historical data that the greenhouse gases compositions in the atmosphere has increased rapidly along with the increase in global temperature and the period from 1983 to 2012 was likely the warmest 30-year period of the last 1400 years in the Northern Hemisphere (IPCC, 2014). The land and ocean surface temperature data show a warming of 0.65°C to 1.06°C between the period of 1880-2012 (IPCC, 2014). IPCC (2007) report revealed that the eleven years during the period of 1995-2006 were the warmest eleven years, these eleven years are ranked among the twelve warmest years in the surface temperature since 1850. Trend analysis of the temperature of 1906-2005 shows warming at higher rate (i.e. 0.74°C) compared to the warming trend of 0.6°C in the period of 1901-2000, this warming is higher in northern hemisphere and land regions have warmed faster than the oceans. Global average sea level has risen since 1961 at an average rate of 1.8 mm/yr but rise in sea level observed to increase rapidly after 1993 i.e. 3.1 mm/yr, reason behind this rapid

increase is supposed to be the glacier melting and ice caps melting and polar ice sheets melting.

2.3 IPCC fifth assessment report (AR5) and CMIP5 emission scenarios

Assessment report of IPCC provide an insight of the possible increase in greenhouse gas concentration for the future period on the basis of evaluation of the future probable changes in various natural factors and anthropogenic activities utilizing the scientific approach. Fifth assessment report (AR5) provides a new approach to represent the greenhouse gas concentration i.e. in terms of the representative concentration pathways (RCP) (IPCC, 2014). In earlier IPCC reports greenhouse gas concentration were represented in terms of emission scenarios A1, A2, B1 and B2 (CMIP3 datasets). In AR5, greenhouse gas emission scenarios has been culminated in the terms of RCPs. Presently four RCP scenarios has been introduced namely RCP2.6, RCP4.5 RCP6.0 and RCP8.5. Suffix with the RCP represents the radiative forcing at the end of the 21st century societal responses. The labels associated with the RCPs provide an estimate of the radiative forcing in the year 2100 (relative to preindustrial conditions). The radiative forcing in RCP8.5 increases throughout the twenty-first century before reaching a level of about 8.5 W/m^2 at the end of the century. RCP2.6 is known as the low radiative forcing scenario, where radiative forcing reaches a maximum in the mid of the century and reaches to a nominal value of 2.6 W/m^2, RCP4.5 and RCP6.0 are the intermediate scenarios and RCP8.5 is termed as the high scenario. AR5 report includes the mitigation strategies along with the emission sources to produce the emission scenarios (Taylor et al., 2012). Major advantage of the CMIP5 datasets is the fine

resolution of GCM models (Taylor et al., 2012).

2.4 Climate change impact on water resources

IPCC in their third assessment report (TAR) addressed the severity of climate change on the water resources (IPCC, 2007). Trend analysis of the streamflow in major rivers show significant trends whereas in few rivers, streamflow reflected a statistically significant relation with temperature and precipitation trend (Bates et al., 2008). Anthropogenic activities are also one of the major factors influencing the streamflow apart from change in temperature and precipitation (Bates et al., 2008). Changes in mountainous hydrology is also a prime concern of the climate change researchers, enhanced glacier melt and shifting in melting season because of the increasing temperature is observed in the recent decades (Box et al., 2006; Kaser et al., 2003). Streamflow analysis at the catchment and global scale show significant change in the river flows, studies also found significant links with temperature and precipitation. Changes in flow also caused because of the drastic changes in land-use change and dam construction in the previous few decades (Bates et al., 2008).

Precipitation pattern around the world is changing significantly which is substantially altering the flow regimes in the rivers (Whitehead et al., 2015). Excessive urbanization and deforestation are causing the enhancement in runoff generation processes, thus the effective land-use planning and management strategies are required for climate change impact mitigation (Arnell and Lloyd-Hughes, 2013). A brief conclusion of the climate change impacts on water resources suggest that this phenomena will alter the hydro-climatological variables such as precipitation, temperature, evapo-transpiration and streamflow. On the contrary to the increased precipitation events, increasing tem-

perature trends would cause the scarcity of water in arid regions, as the increase temperature will enhance the evapotranspiration from the surface and water bodies (IPCC, 2014). In contrast to this in glacier fed rivers, streamflow tend to increase because of the increased amount of snowmelt (Singh and Bengtsson, 2005).

2.4.1 Climate change impact on water resources around the world

Impacts of climate change on water resources has been addressed broadly in fifth assessment report of the IPCC. Report reveals a significant changes in the water resources around the world under climate change scenarios. Increase in streamflow in mountainous region and decrease in inland catchments are likely to happen because of the changes in temperature and precipitation (Arnell, 2003). Worldwide studies about impact of climate change on water resources justify the findings of the IPCC AR5 concerns to a larger extent. Dettinger (2012) suggests significant changes in temperature and precipitation in Southwestern America and at local scale these impacts could be more severe. Climate change projection for United Kingdom shows significant decrease in summer precipitation followed by increase in winter precipitation (Murphy et al. 2009), and increase in temperature will subsequently enhance the evapotranspiration (Watts, 2010; Vidal et al., 2011).

Kron and Berz (2007) reported the increased flood events during the period of 1996-2005 as compared to the previous records of 1950-1980 globally and as a result, related economic losses have increased manifolds. Zhang et al. (2009) analyzed the observed discharges of 40 years and reported an increase in the lower Yangtze basin. At regional scale, significant increase in the annual maximum streamflow has been obtained in northwestern Europe by several researchers (Hattermann et al., 2013; Ellison et al.,

2012). Significant decrease trends in snowmelt-flood magnitudes at almost one-fifth of 160 stations has been recorded in Canada (Cunderlik and Ouarda, 2009). Hattermann et al. (2013) identified consistent trends in precipitation extremes and flooding in Germany. Decrease trends for spring and annual maximum flows were also recorded by Burn et al. (2010). Dai et al. (2009) conducted a study on the projection of streamflow and reported that the top rivers of the world such as Congo, Mississippi, Yenisei, Parana, Ganges, Columbia and Niger showed significant increments in the simulated streamflow.

Elsner et al. (2010) simulated the 21st century hydrological projections utilizing the 20 GCMs for Pacific Northwest Yakima River and Puget Sound River and projected the different water balance component such as runoff, streamflow and soil moisture for A1B and B1 emissions scenarios. Results reveals the possible shifting in streamflow timing in snowmelt dominant and rain–snow mixed watersheds whereas increase in runoff by 2–3% by the 2040s with a projected increase in winter precipitation. Similarly, (Barnett et al., 2005) also showed that soil water equivalent (SWE) to precipitation ratios have been declining in the historic record due to observed warming, and that these changes are predominantly related to human influence on the climate.

Payne et al. (2004) studied the climate change impact on Columbia River Basin (CRB) using GCMs and three emission scenarios and found that temperature changes dominated the simulated hydrologic effects by reducing winter snow accumulation, thus shifting summer streamflow to the winter. Vano et al. (2010) conducted a study on the sensitivities of water supply systems in the Puget Sound basin, historical and projected future streamflow variability and water demands, study shows that all systems are projected to experience declines and eventual disappearance of the springtime snowmelt

peak. Several impact assessment studies have been conducted in China which indicates water stress scenario for the coming future for different emission scenarios (Thomas, 2000).

Fischer et al. (2007) analyzed the agricultural water demand under different climate change scenarios. Future agricultural requirement were computed as a function of both projected irrigated land and climate change for period of 1990-2080. Projected water demand for agriculture were calculated with the consideration of implication of mitigation strategies. Finding of the study suggested that the mitigation reduced the impacts of climate change on agricultural water requirements significantly as compared with unmitigated climate.

2.4.2 Climate change impact on water resources in Indian sub-continent and Himalayan region

Mehrotra and Mehrotra (1995) examined that an increase in mean annual surface air temperature has resulted in increasing precipitation totals over the whole of India, especially along the western coast of the subcontinent. Indian sub-continent as well as Himalayan region is also influenced with the changing climate and global warming (Singh and Kumar, 1997). Mehrotra (1999) conducted a study on India to assess the impact of climate change on water resources. Study was carried out dividing the country in 11 agro-climatic zones, results showed that analysis on inter-annual and long-term variability of monsoon and annual rainfall have pointed out that the variations in rainfall for the Indian subcontinent are within the statistical limit.

Gosain and Basuray (2003) quantified the impact of climate change on the water resources of the India using SWAT (Soil and Water Assessment Tool) hydrological model.

Calibrated SWAT model for different river basins of India were used for the future projection of the streamflow with the assumption of no change in land use cover. Study revealed that the emission scenarios may enhance the extremity of floods and draughts in several part of the country. Rehana and Mujumdar (2013) conducted a study to assess the change in irrigation water requirement in Bhadra reservoir command area of Krishna River for A1B scenario and downscaling of temperature and precipitation showed increase in average maximum and minimum temperature along with monthly rainfall, subsequently, evapotranspiration is projected to increase. Irrigation demand in command area assessed on monthly time-scale likely to increase because of the projected increase/change in temperature.

Duhan and Pandey (2013) analyzed the precipitation trends in 45 districts of state of Madhya Pradesh on different time scale using Mann-Kendall (MK) test and Sen's slope estimator test and an increase was observed on annual precipitation. Ghosh et al. (2009) examined the trends in summer monsoon of India and effect of global warming and local urbanization, deforestation impacts on precipitation. Study found the increasing trend of heavy rainfall and decreasing trend of occurrence of moderate rainfall. Patra et al. (2012) detected rainfall trends using 1871-2006 data and reported declining trend in annual and monsoon rainfall, increasing trend in the post-monsoon season was also observed.

Khadka et al. (2014) carried out a study on Himalayan river basin named Tamakoshi Nepal to identify the climate change impact on snow cover and its effect on the streamflow of the river. Statistical downscaling method was used for temperature and precipitation projection to the basin scale and results suggest increase in both temperature and precipitation. Temperature and snow cover relationship showed that snow cover in

winter and spring are more vulnerable to the climate change. Immerzeel et al. (2012) developed the hydrological model to estimate the snowmelt contribution to runoff in a glacier river basin, analysis showed that temperature and precipitation are likely to increase in the future scenario which will result in the retreat of the glacier area and increase in river runoff because of the increased precipitation and ice melt.

Neupane et al. (2015) calibrated the SWAT model for two Himalayan rivers namely Tomar and Seti river basins in Nepal and checked the probable impact of climate change scenarios B1 and A1B along with land use changes on the river runoff. While assessing the probable land use change agricultural land and grassland were considered preferably. Study reported significant increase in the runoff when combined the effect of emission scenarios along with the land use changes. Mishra and Lilhare (2016) conducted the impact assessment study on the major river basins of India for RCP emission scenarios using CMIP5 datasets and SWAT hydrological modeling. Results describes the significant changes in the streamflow for almost all the RCP scenarios.

2.5 Downscaling and future projection of temperature and precipitation

Intergovernmental Panel on Climate Change (IPCC) has suggested several CO_2 emission scenarios and different general circulation model (GCM) has generated several simulation of the climatic variable on the basis of these emission scenarios but these climatic variables are given at a very coarse resolution of around 350 × 250 kilometer grids, which is quite large for the basin scale study because local conditions also play important role in hydrology of the basin. So, for the climate change studies it is necessary to downscale these data at basin scale. Several downscaling techniques have

been developed for projecting the climatic parameters for future climate change scenarios at basin scale. Mainly two types of downscaling techniques are there, statistical downscaling and dynamic downscaling techniques. Dynamic downscaling techniques are used less because of its complexities and large requirement of data, while statistical downscaling techniques are popular because of its feasibility and less data requirement. Several sophisticated software and models have made statistical downscaling technique easier. Several studies on the downscaling of climatic parameter are summarized here which gives the state of the art of this technique.

Anandhi et al. (2008) developed downscaling model for Malprabha river basin to project the maximum and minimum temperature using the National Center for Environmental Prediction (NCEP) dataset predictors for calibration and validation. For future projections GCMs COMMIT and CGCM3 for three emission scenarios A1B, A2 and B2 scenarios were utilized. The impact of trend in predictor variables on downscaled temperature was studied. Sachindra et al. (2011) in their study downscaled the rainfall and temperature for the general circulation model predictors to the basin scale for modeling the streamflow of the basin for future climate scenario. A statistical relationship was developed between the basin hydro-climatic data and NCEP predictors and future streamflow was developed using the statistical model. Ghosh and Mujumdar (2008) used support vector machine in downscaling of the climatic variables and used it for generating the future streamflow generation over Mahanadi river basin. Principal component analysis was used for selecting the appropriate predictors from the best correlated predictors. Efficiency of relevance vector machine (RVM) and support vector machine (SVM) were checked and it was observed that RVM has the advantage over SVM.

Mahmood and Babel (2013) developed the monthly and annual based regression model for minimum temperature, maximum temperature and precipitation for the Jhelum river basin of Pakistan using statistical downscaling model (SDSM). Bias correction approach was used for improving the performance of model and removing the biasness in the future projected data. It was stated that monthly regression model performs better over annual regression model and this is because there is a variation occurs in summer, winter and monsoon season temperature and rainfall. Chu et al. (2009) used statistical downscaling method for downscaling of temperature, rainfall and evapotranspiration for Haihe river basin in China. For the 11 stations of the basin GCM predictors for HadCM3 model were selected and regression equation was established for three predictands i.e. mean temperature, rainfall and evaporation. Study shows that for the different stations selected predictors which are best correlated may vary.

Khan et al. (2006) carried out a study to check the capability of three different downscaling tools i.e. statistical downscaling model (SDSM), Long Ashton Research Station Weather Generator (LARS-WG), and artificial neural network (ANN). Several extreme indices were calculated for the comparison from different model results. Observed and downscaled data from 1961-2000 were used for analysis and the results suggested that the SDSM is the most capable of reproducing various statistical characteristics of observed data in its downscaled results with 95% confidence level.

Goyal and Ojha (2012b) compared the performance of ANN method and linear multiple regression methods for the temperature projection on a lake catchment. Results of the study showed that ANN-based models are better to LMR-based models, further ANN model was applied to obtain future projections of Tmax and Tmin and it was observed that Tmax and Tmin are likely to increase in A1B, A2, and B1 scenarios, along with

precipitation whereas no trend has been observed for pan evaporation in future.

Samadi et al. (2013) used two downscaling models, statistical downscaling model (SDSM) and an artificial neural network (ANN) model, to describe the uncertainty in regression-based statistical downscaling of daily precipitation and temperature over a semiarid catchment in the west of Iran. Thirty years of observed and downscaled daily precipitation and temperature data set obtained from NCEP reanalysis predictors for the years of 1961 to 1990 were used to estimate the biases in mean, variance, and wet/dry spells. The uncertainty in daily temperature was evaluated from the comparison of monthly mean and variance of downscaled and observed daily data at a 95% confidence level. The uncertainty in daily precipitation was evaluated based on monthly mean dry and wet spell lengths and their confidence intervals, cumulative frequency distributions of monthly mean of daily precipitation, and the distributions of monthly wet and dry days for observed and modeled daily precipitation. Their results indicate that the uncertainty in downscaled precipitation is higher compare to temperature. They have also shown that daily temperature simulations can accurately reproduce the extreme events. Comparing SDSM and ANN, their study shows that the SDSM is the most efficient model at reproducing various statistical characteristics of observed data at a 95 % confidence level, whereas the ANN model is the least efficient in this context.

Chen et al. (2012) have evaluated and compared water balance components in upper Hanjiang basin in China simulated using different downscaling methods, hydrological models and GCMs. Statistical downscaling techniques, i.e. SSVM (Smooth Support Vector Machine) and SDSM (Statistical Downscaling Model) were calibrated and validated using NCEP/NCAR reanalysis data for the period 1961–2000. The A2 emission scenarios from CGCM3 and HadCM3 for the same period are used as input to the

statistical downscaling models and the downscaled local scale climate scenarios are obtained. These local scale climate scenarios are given as input to Xin-anjiang and HBV hydrological models. Further, their results have shown that there is great variability in the simulated runoffs obtained using different statistical downscaling techniques for same GCM. SDSM was shown to have better comparison compared to SSVM based on most widely used statistics in the literature, however in case of Nash–Sutcliffe efficiency (NSE) and root mean square error-observations standard deviation ratio (RSR) SSVM outperformed. SDSM downscaled rainfall has lower efficiency in runoff simulation compared to SSVM. Further, they have concluded that NSC and RSR can be used as key statistics for the evaluation of statistical downscaling models performance when the downscaled rainfall is used as an input to hydrological model.

2.6 Studies on temperature and precipitation extremes

Easterling et al. (1997) found significant variations in minimum and maximum temperature and observed that the diurnal temperature variations. Vose et al. (2005) examined the trends of maximum and minimum temperature of historical data series and found rapid increase in Tmin as compared to Tmax which indicates significant decrease of diurnal temperature range (DTR) during the period of 1950-2004. Apart from change in DTR uniform increase in Tmax and Tmin was observed all over the part of globe. Alexander et al. (2006) analyzed the temperature and precipitation extreme events on global scale. Extreme events data were gridded for the globe and trend analysis was conducted for the period of 1951-2003. It was observed that the occurrence of the cold nights are decreasing significantly, significant change in the warming trends were also observed along with the extreme events associated with the minimum temperature.

Palazzi et al. (2013) evaluated CMIP5 GCMs over Karakoram-Himalaya and gradual increments in the summer precipitation throughout the 21st century scenarios. Though, properly simulation of seasonal precipitation and its spatial and temporal distribution using GCMs has demonstrated many difficulties. Deng et al. (2016) analyzed the frequency of extreme precipitation over Ontario using GCMs and observed annual heavy precipitation days, very heavy precipitation days, very wet day and extreme wet days in the progressive manner over major parts of the Ontario.

Song et al. (2015) also used observed precipitation datasets to detect the recent changes in extreme precipitation and droughts during 1960 to 2013 over Songhua river basin, China. Study found that the observed that wet days are increased and the regionally averaged consecutive dry days significantly increased. Qian et al. (2007) found that the frequencies of extreme precipitation events increased in eastern China. Kharin et al. (2013) prepared extreme precipitation indices to detect the annual, seasonal and intra-annual variability in 21st century precipitation scenario utilizing CMIP5 RCPs. The authors observed relative changes in the intensity of precipitation extremes and the annual mean precipitation is increased.

2.7 Hydrological modeling

After getting the hydro-climatic data next step is modeling of the hydrologic process for the study area including calibration and validation of the hydrological model. After calibration and validation model can be used for generating the future stream flow, evaporation and other hydrologic process by using the future projected hydro-climatic data. Several studies have been carried out all over the world using different hydrological models for generating the future water availability of the certain river basin or the

study area.

Abbaspour et al. (2015) applied soil and water assessment tool (SWAT) model for hydrological modeling of Europe to simulate the water resources component of the major river basins. Crop yield and water quality were simulated at the hydrological response unit (HRU) scale and authors also discussed the comprehensive framework for the leaching of nitrate to the groundwater. Abbaspour et al. (2007b) used SWAT hydrological model for simulating streamflow, sediment and nutrient load in Thur river basin in northeast Switzerland and applied sequential uncertainty fitting (SUFI2) approach for calibration and uncertainty analysis. Abbaspour et al. (2004) addressed the uncertainty involved in the parameter estimation process in hydrological modeling. Authors proposed an approach to quantify the uncertainty in parameter estimation using uniform distribution and fitting the simulated streamflow bracketed with 95% prediction uncertainty of parameter values.

Bahremand and De Smedt (2010) for their study used WetSpa model to the Torysa river basin and Parameter estimation, sensitivity and predictive analysis of the model parameters were performed using a model-independent parameter estimator (PEST). It was found that the correction factor for measured evaporation data has the highest relative sensitivity. Parameter uncertainty and predictive analysis give an insight of a proper parameter set and parameter uncertainty intervals and prove that the parameter uncertainty of the model does not result in a significant level of predictive uncertainty.

Patil et al. (2014) explained the difference in the result of distributed hydrological modeling and lumped hydrological modeling. Study was carried out for the 41 catchment of Pacific Northwest of the USA. Lumped and distributed hydrological model was applied on all the basins. Two metrics i.e. moisture homogeneity index (MHI) and tempera-

ture variability index (TVI) were used to check the performance of models. Comparison of results shows that the distributed model performs well. It was concluded that the distributed hydrological model are better for the catchment with low homogeneity of moisture distribution.

According to Zhang et al. (2014) the fundamental task in surface water hydrology is to understand the behavior of a catchment in terms of its underlying hydrological signatures which could be beneficial in water resource management, catchment classification, and prediction of runoff time series. Zhang et al (2013) applied three approaches for analyzing six hydrological signatures in southeastern Australia. The applied approaches included spatial interpolation with three weighting schemes, index model that estimates hydrological signatures using catchment characteristics and classical rainfall–runoff modeling. Six hydrological signatures were categorized as long-term aggregated signatures annual runoff coefficient, mean of log-transformed daily runoff, and zero flow ratio. The signatures obtained from daily flow metrics i.e. concavity index, seasonality ratio of runoff, and standard deviation of log-transformed daily flow. Approach was applied on more than two hundred basins and it was found from the results that for the log-transformed daily runoff and runoff coefficient which were two long-term aggregated signatures, the index model and rainfall–runoff modeling performed similarly. The results were better than the spatial interpolation methods too in this case.

Yang et al. (2007) addressed the inherent errors and uncertainty in the calibration and parameterization of the hydrological models. They also addressed the complexity in calibration for arid regions. To address this issue, authors suggested the procedure to overcome the parameters identifiability in distributed modeling and the problem of

auto-correlated errors and problems of seasonal variation. Authors applied this procedure on the soil and water assessment model calibration for Chaohe river basin in North China. Results demonstrated better results to overcome the problem of uncertainty and errors in hydrological modeling.

2.8 River basin planning and management

Climate change study with river basin management planning requires a detailed study of changing climatic variables and its impact on available water resources with the future projected climate change scenario. Downscaling and hydrological modeling provides both these information discussed above. Main factor which affects the available water is temperature and rainfall. With the increasing temperature evapotranspiration from the bare soil and vegetation increases which consequently affects the water availability for the plants and living beings. Several studies related to the changing climate and its impact on the available water resources of river basin have been carried out.

Sarma et al. (2013) stated in their article about the ecological imbalance in the hilly region of Brahmputra river basin because of unplanned urbanization and massive deforestation. Deforestation has caused the increased runoff and thus the sediment yield in the region. Ecological sustainable management practices (EMP) were suggested for the micro-watershed of Guwahati. These management practices are grass land, forest land and detention pond. A multi-objective optimization model was developed for the maximization of the carbon sequestration and minimization of the cost of the suggested EMPs. Constraints selected were sediment yield, peak discharge constraints, EMP suitability area constraints, and owner's choice for constraints.

Ahmed and Sarma (2005) introduced a genetic algorithm (GA) model for finding op-

timal operating policy of a multipurpose reservoir for Pagladia Project at Assam in India. Which has been compared with the policy derived using stochastic dynamic programming (SDP). They found that the GA based policy is better as compared to the conventional one. Ray and Sarma (2011) presented an optimum reservoir policy to minimize the diurnal variation of stream flow at downstream for Lower Subansiri Hydroelectric project. Simulation model was developed and performed with Standard Operating Policy proposed for the project. The results highlights during lean period the release discharge increased about eight times as compare to normal flow, whereas its zero during non-operating period. To minimize the deviation of flow, structural and non-structural measures were adopted and compared with seven performed criteria and found that structural measures provides the best result. Also, the adoption of non-structural measure can provide the significant improvement as compare with baseline standard operation scenario.

Mujumdar and Nirmala (2007) have adopted a stochastic optimization tool (Bayesian Stochastic Dynamic Programming (BSDP)) to develop the operating policy for a multi-reservoir system with forecast and inflow uncertainty. The BSDP includes Bayesian approach with Stochastic Dynamic Programming (SDP) formulation. This stochastic optimization tool includes state variables such as - initial storages of individual reservoirs at the time t, cumulative inflow to the system during period t and forecast for cumulative inflow to the system for the next time t+1. In this study, inflow randomness is presented by a posterior flow transition probability, whereas flow forecast uncertainty presented through both posterior flow transition probability and predictive probability of forecasts.

Kumar et al. (2013) used artificial neural network (ANN), fuzzy logic and decision tree

algorithm as main tools to optimize the reservoir policy. Optimum release is the function of state variable and hydrologic inputs, which allows to control the water release in terms of available informations. The optimal release, inflow series and modified reservoir characteristics (e.g. elevation-area capacity table, zero elevation level) obtained from optimal control theory. ANN with back propagation algorithm, Fuzzy Logic and decision tree algorithms (M5 and REPTree) were used to control the operating rules for irrigation and power supply and found fuzzy logic provides best results as compare to other two techniques.

Rani and Moreira (2009) presented a survey of simulation and optimization modeling approaches used in reservoir systems operation problems. Optimization methods have been proved of much importance when used with simulation modeling and the two approaches when combined give the best results. The main objective of the review article was to discuss simulation, optimization and combined simulation– optimization modeling approach and to provide an overview of their applications reported in literature. In addition to classical optimization techniques, application and scope of computational intelligence techniques, such as, evolutionary computations, fuzzy set theory and artificial neural networks, in reservoir system operation studies were reviewed. Conclusions and suggestive remarks based on this survey were outlined, which could be helpful for future research and for system managers to decide appropriate methodology for application to their system.

Jothiprakash and Arunkumar (2013) addressed the complexity of the multi-objective optimization problem in water resources which involves irrigation, hydro-power and flood control. Nonlinear programming problem were developed for solving the multi-reservoir system and the model was applied on Koyna Hydro-Electric Project (KHEP)

for maximizing the hydropower production and solved for three different dependable inflow scenarios under various operating policies. Complex situation of the study arises in the case of irrigation and hydropower release were in opposite direction. In order to get the optimal operation policy, annual, seasonal and monthly inflow and power production were compared and it was found that power production can be increased to a minimum of 22% by slightly relaxing the tribunal constraint on releases towards the western side.

Vano et al. (2010) in their study explained the consequence of changing climate and by using VIC model (Variable Infiltration Capacity) model which is the macroscale distributed hydrological model assessed that there will be water scarcity in the region as per the B1 emission scenario. Without adaptations, for IPCC A1B global emission scenarios, water shortages increase to 27% (13% to 49% range) in the 2020s, to 33% in the 2040s, and 68% in the 2080s. For IPCC B1 emissions scenarios, shortages occur in 24% (7% to 54%) of years in the 2020s, 31% in the 2040s and 43% in the 2080s. Historically unprecedented conditions where senior water rights holders suffer shortfalls occur with increasing frequency in both A1B and B1 scenarios. Economic losses include expected annual production declines of 5%–16%, with greater probabilities of operating losses for junior water rights holders.

Elsner et al. (2010) estimated the sensitivity of the hydrology of the Pacific Northwest as the region dominates in runoff from the snowmelt and temperature plays important role in the region for melting of snow and subsequently runoff. Datasets from the fourth assessment report of IPCC were utilized for the impact assessment for two emission scenarios Total twenty GCM were selected for the study. Impact assessment were specifically focused on Washington and the greater Columbia River watershed,

with additional focus on the Yakima River watershed and the Puget Sound which are mainly sensitive to climate change. All the three component of the water balance i.e. soil water equivalent, soil moisture and streamflow were calculated for estimating the changes in future scenarios as compared to baseline period of 1917-2006. Study finds out that SWE decreasing upto 46% by 2040 for two emission scenarios i.e. B1 and A1B, and seasonal shifting in the streamflow is also observed, annual runoff projected to increase by 2-3%.

Block (2011) compared the benefits and reliability of actual forecast based optimization approach over climatological approach for the Blue Nile river basin, model utilizes rainfall, runoff modeling, forecasting the hydrological variables and hydropower model. Steinschneider and Brown (2012) suggested management approach for the climate change scenarios and hydrological changes in a watershed. Study suggested that the water resources management can be enhanced with the seasonal forecast of the hydrological variables and adapting to the reservoir managements. In order to decide the adaptability options for the future management plans, two approaches were used. In first approach, system was optimized on the basis of the projections of variables like streamflow using the GCM ensembles and in the other approach the stationarity of the system was considered assuming the baseline historical behavior of the system. Model was applied on the Westfield River in the northeast United States. Results declare that deciding the adaptation strategy on the basis of the seasonal forecasting is better option than the adaptation based on the stationary approach.

Brekke et al. (2009) represented the risk based planning for adaptive water resources management under climate change scenarios. Study focuses on the water management strategies for the California's Central valley project and state water project systems un-

der the threat of different climate change scenarios and flood-conditions in the coming future for the flexible climate change risk assessment using ensembles of projections, which could be helpful for the policymakers. Risk was analyzed for the two decisions such as whether the climate change will influence the flood control and water supply or whether it is required to use the weighted scenarios of climate change ensembles. It was found that the flexible approach in decision making provide various dimensions of adaptations to mitigate the impact of climate change scenarios.

Yates et al. (2005) introduced a model which can simulate the hydrological processes and integrates the water management plans considering the various sectors and their priorities. Model named Water evaluation and planning (WEAP) integrates watershed-scale hydrological simulation and management of water resources considering all the points in the watershed such as reservoir, streams environmental flow and demand sectors. Yates et al. (2009) used WEAP model for assessing the water resources of the Sacramento River Basin in California, in the study river basin was divided into several sub-watershed along with the demarcation of the canals, diversions reservoirs characterized for the water management plans. Study found that WEAP model capable for the simulation of hydrology of the river basin and assessment of the management plans for the river basin considering all the stakeholders within the river basin.

Purkey et al. (2008) also applied the WEAP model in the Sacramento River basin for searching the different possible water saving options in traditional agricultural and irrigation practices. Study tested the different agricultural practices and cropping pattern and found that these methods could reduce the required water for agricultural practices and which subsequently increase the available water to fulfill the domestic water demand in the watershed.

Mehta et al. (2013) applied an integrated water management model for planning the framework of the water resources management in the Lake Victoria region of the Africa which is considered as the region having fastest growth in Africa. Integrated water management model was prepared with the help of WEAP model and three cities of the lake catchment were considered for the study. Model was provided with all the hydro-climatological input for all the sub-watersheds separately, demography of the cities and different demand sites were identified on the basin of the literature and filed surveys. An assessment of the water resources and demand up to 2050 were estimated on the basis of population projection and infrastructure development. It was found that the water resources will be enough to fulfill the demand till 2020, but after that the available water resources will be insufficient for the different sectors and various watershed management strategies will have to be adopted in order to meet the demand. Chinnasamy et al. (2015) conducted a study on the Koshi river basin which is a tributary of the Ganges river in Northern part of Indian subcontinent. Study was focused on the assessment of the water resources in the river basin and its sufficiency for fulfilling the hydropower production demand and drinking water demand. It was found that the available water resources are sufficient to fulfill the requirement of power production and population demand but for the future increase in the population, agricultural growth and industrialization will cause a deficit situation for the available resources by 2050. Bhave et al. (2016) integrated the participatory and modeling approaches for water resource management including all the stakeholder of the Kangasati river catchment in West Bengal. Methodology involved all the stakeholders of the river basin for the participation in the policy making along with the modeling of the hydrological processes in the catchment, process was followed by proposing the two adaptation measures in the

watershed in order to increase the water holding capacity and checking the drainage of the runoff water through construction of the check dams and increasing forest cover. Later final decision was taken on the basis of the meeting of all the stakeholders to find the no-regret adaptation option on the basis of the priority of the stakeholders and it was found that increasing forest cover will be more effective and acceptable to the participants.

Alemayehu et al. (2010) selected the Lake Tana catchment for the study of water resources management under the influence of economic growth scenarios. Study utilizes the WEAP model for the estimation of the water demand of different sectors in the different development scenarios. Water demand was simulated for the three sectors separately i.e. irrigation, hydropower and downstream drinking water demand. Harou et al. (2009) reviewed the popular hydro-economic models used all over the world in the field of water resources management. Review includes the methodologies being used for last 45 years in 23 countries across the world and found that these hydro-economic models not just provides a solution to the maximization of the profit, or minimization of loss from the existing system but also provide a framework to adapt immediately to the coming changes in the society as well as changing scenario of water demand.

2.9 Conclusion from the literature review

From the literature review on the various topics of climate change impact on water resources, following conclusions have been drawn

- IPCC AR5 suggests rise in temperature and precipitation for the 21st century which will subsequently enhance the extreme events in future. Studies on the Himalayan range indicate the impact of climate change will be higher in this

region because of the increased glacier melts and change in snowfall and snowmelt pattern.

- Streamflow in the rivers are likely to change because of the changes in temperature and precipitation patterns, which will subsequently alter the hydrological components such as evapotranspiration, surface runoff, infiltration etc. in a river basin. In snow and glacier fed rivers, impact of climate change becoming more severe because of the enhanced snowmelt and shifting in snowfall.

- Studies on the water resources availability also indicates that water resources are the primary sectors to be addressed for mitigation and adaptation strategies under climate change.

- Less studies have been found which focuses on the simulation-optimum approach for addressing the water distribution policies which includes all the demand sectors viz. municipal water, irrigation water, water for hydropower generation and environmental flow under the ambit of climate change impacts. No literature have been found where latest published fifth assessment report of IPCC climate change RCP scenarios have been used for addressing the changes in water resource availability.

- Simulation-optimization approach is required to address the streamflow projections and inflow to the reservoir, along with the change in demand for different sectors to decide an optimal release policy under the given constraints.

CHAPTER 3

Study area and data

The Subansiri river is the northern bank tributary of Brahmputra which is also the longest among all the tributaries (Sarkar et al., 2012). Nomenclature of Subansiri River originates from the fact that the river course was a potential site for Gold mining in the recent past which gives this river the name Subansiri derived originally from the Sanskrit world "Swarn" which means gold. Subansiri river is trans-Himalayan river which originates in the Tibet Himalayan plateau at an elevation of 5340 m and formed by joining the three small tributaries namely Lokong Chu (Char Chu), Chayal Chu and Tsari Chu in Tibet, after travelling through the Himalayan mountains it enters India passing the Miri hills in Arunachal Pradesh. Total length of Subansiri River from origin to the confluence to Brahmaputra, is 337 km, in this length, 208 km length falls in the mountainous terrain of Himalaya, and remaining length falls in the plain of Assam, where it joins the Brahmputra River near Jamuguri Ghat.

Total basin area of the river is about 35771 Km^2 as calculated from the basin delineated from the shuttle radar topographic mission (SRTM) digital elevation map, 21066 Km^2 area falls in Arunachal Pradesh, 4360 Km^2 lies in Assam state and remaining 10345 Km^2 falls in Tibet region (Ray and Sarma, 2011). Observed maximum discharge of

Subansiri river has been found to be approximately 18,500 m^3/sec and minimum of 131 m^3/sec, river contributes 7.92% of total discharge of the Brahmaputra river observed at Pandu Port (Singh et al., 2013). Several small tributaries contribute their water to the Subansiri River, few of them are Ranganadi, Dikrong, Kamala, Ghagar and Sampara Figure 3.1. In India, Subansiri River drains some parts of two states namely Arunachal

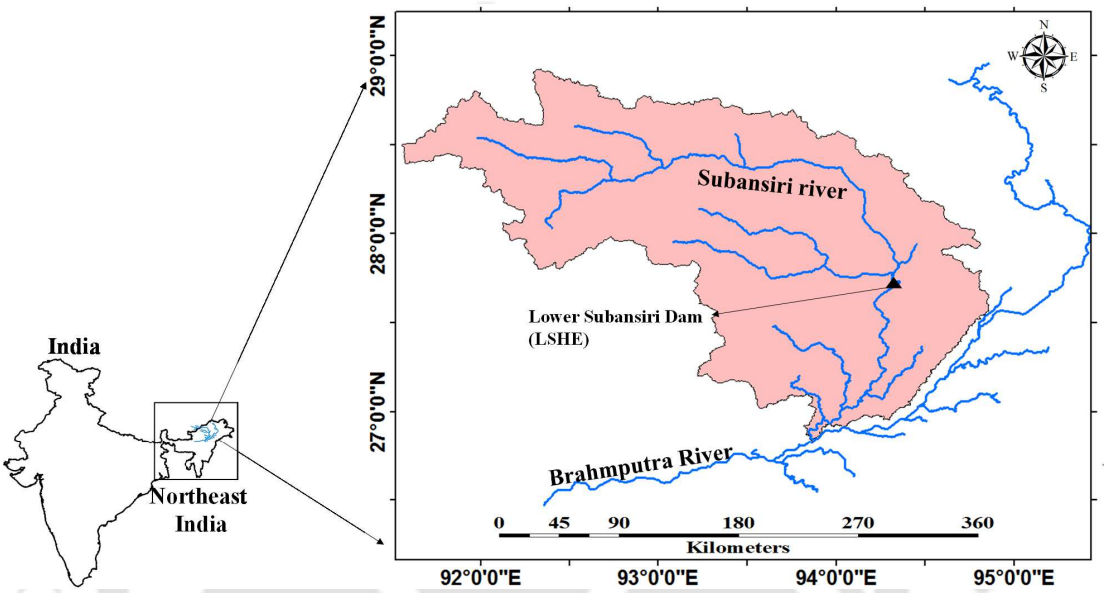

Figure 3.1: Subansiri river map with its tributaries

Pradesh and Assam. In Arunachal Pradesh, parts of Lower Subansiri district, Upper Subansiri district and Papum Pare is covered whereas in Assam some part of Dhemaji and North Lakhimpur district of Assam falls in Subansiri river basin. Figure 3.2 shows the districts which comes under the Subansiri river basin. A hydroelectric power plant is constructed on the Subansiri River at the foothill near Gerukamukh where it enters the Assam state, which is named as Lower Subansiri hydro-electric project (LSHE). Main objective of project is the electricity production and flood control, capacity of the power plant is 2000 MW (Ray and Sarma, 2011) .

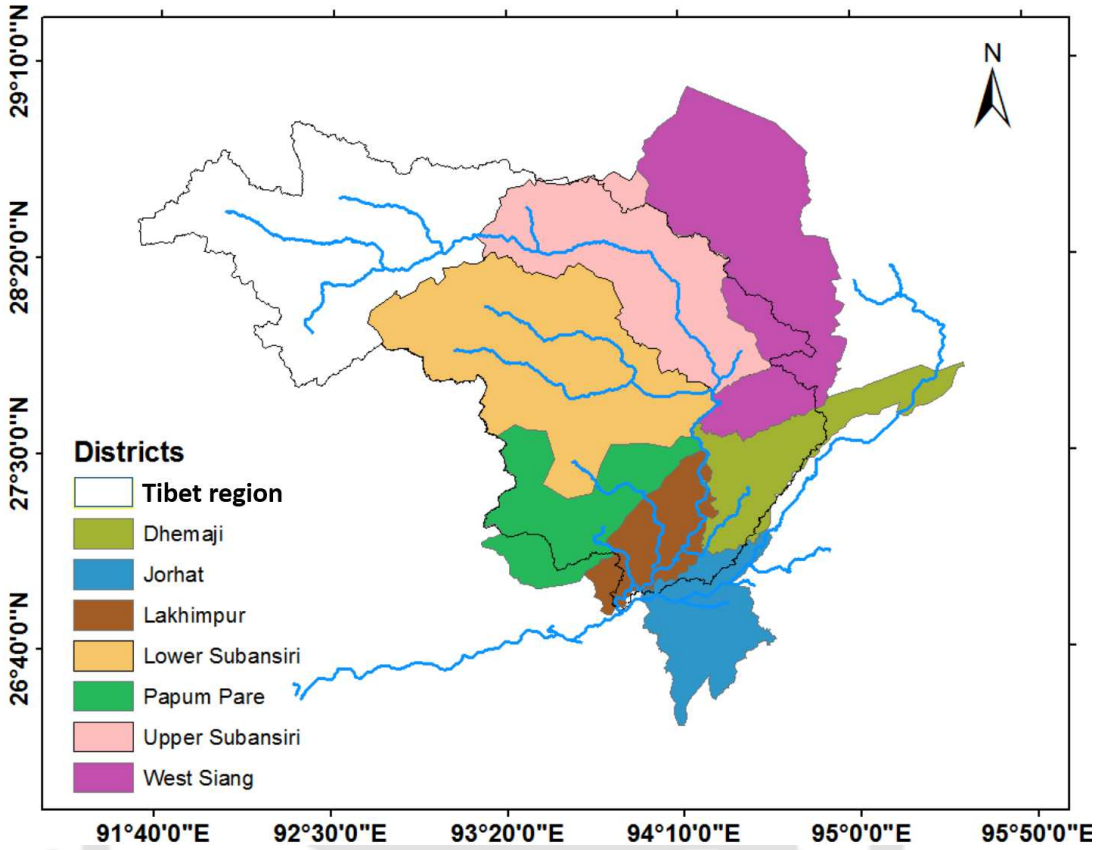

Figure 3.2: Regions covered in Subansiri river basin

3.1 Geological and morphometric characteristics

Subansiri River covers very diverse topography from its origin point to the confluence to the Brahmputra River. At the origin point elevation reaches above 5000 m whereas when it enters the plains of Assam the elevation reaches as low as 100 m amsl. In the upper part of the river basin, many big tributaries joins the Subansiri River and in the foothills, two major rivers Ranganadi and Dikrong river join the river. Shuttle radar topographic mission (SRTM) data analysis of the Subansiri river basin shows high relief in the upper catchment with sharp rise mountain tops is indicative of the hard rock terrain with low erosion rate, whereas the southern part of the basin has the low hill topography and flat hill tops (Goswami et al., 1999). Flood plain of the

Subansiri River is extensive about 63 Km in an east-west direction and 40-58 km in north-south direction. Thus, the geomorphic units mapped in the Subansiri basin can be classified broadly as dissected piedmont plain and dissected flood plain (Ray and Sarma, 2011). Terrain in the foothills to the south is mainly composed of alluvial deposits of Brahmputra River, Siwalik hill range located to the northern part of the area. Subansiri river alluvial plain area has more than 6 Km thick sedimentary sequence with very low gravity anomaly indicating thick mass of low density material. Subansiri River in the foothills follows a braided course (Gogoi and Goswami, 2014) . Subansiri River is typically meandering river with drastic channel shift, meandering continues in the downstream and depends on the amount of discharge and tributaries joining the river.

Morphological elements of Subansiri river consists point bars, natural levee, channel bars and back swamps. In the plane of Assam, Subansiri River shows very sinuous character and creates bar point deposition of varying size contains sand. In flood season, river flows above the natural bank of river thus its velocity is reduced and it deposits the coarse sediment on the bank of the river which is known as natural levee. Subansiri River creates a very broad levee because of the heavy sediment load from the upper mountainous catchment.

3.2 Socio-economic status

Major population of the river basin live in the downstream of the LSHE, this area is geographically a remote area and infrastructures are not very good, which makes this region less developed. Literacy rate is also very less and large population depend upon the agricultural practices and fishing. People on the bank of Subansiri River depend

largely on this river because of the availability of water for agricultural purpose and catching fish.

River basin covers the seven districts of Assam and Arunachal Pradesh, among these districts Lakhimpur of Assam has the highest population of approximately 1 Million (Census 2011), whereas population of Dhemaji district is approximately 0.7 Million. Population of the districts of Arunachal Pradesh is comparatively low as compared to the districts of Assam. Papum Pare district has a total population of 0.1 Million (Census 2011). Agriculture and livestock are the backbone of the economy of these villages. Large population depends totally on the agriculture and fish catching. Rice cultivation is practiced by the major population.

3.3 Land use and land cover (LULC)

Upstream of the Subansiri river basin (above dam) dominates with the forest cover with 5-10% area with snow and glacier, some part which comes under the Tibet plateau is rain shadow zone with least forest and mostly cold dessert with barren land and grasses. In the downstream of the Subansiri river basin, 50% area is covered under agricultural land. Village houses, huts and residential plots accounts for the 18% of the total area whereas 16% area is swamp or marshy land. Figure 3.3 shows the LULC map of the river basin and details of the legends used in Figure 3.3 are shown in Table 3.1. From the Figure 3.3 it can be shown that the basin part in Tibet are dominated with grass, whereas in the Indian part of the basin, different type of forest covers the major part of the basin (in the upstream part) and in the downstream portion major part covers with agricultural crop land.

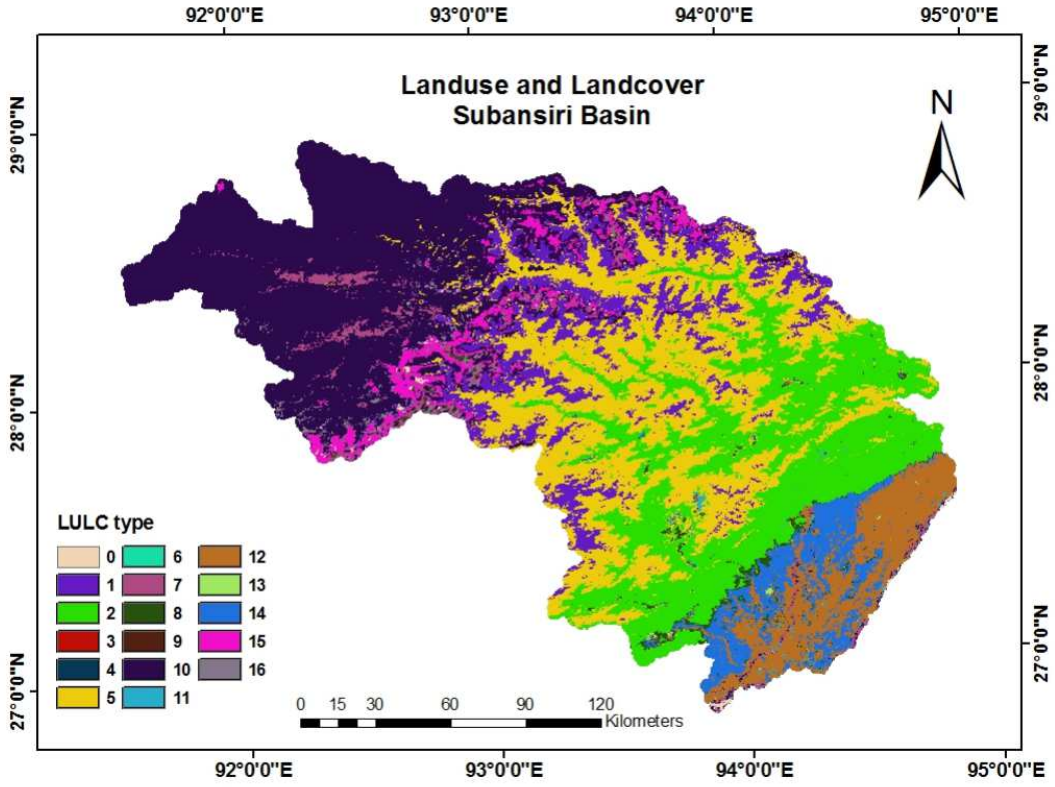

Figure 3.3: Land use and land cover map of Subansiri river basin

3.4 Soil type

Soil map obtained from food and agriculture organization (FAO) shows mainly seven dominant soil classes in the basin as shown in Figure 3.4. In the downstream area on the flood plain of the Brahmputra River major soil class is orthic acrisol (3651) at top layer with ferric luvisol and gleyic acrisol as secondary and lower layers. In the upstream of the river where river passes through the hilly terrain, major soil type at the top layer are orthic acrisol (3650) with leptic podsol and humic acrisol as secondary and lower layers. In North Lakhimpur area thickness of silt and silty clay zone is about 2 m and below to this a medium to coarse sand is found. In the flood plain of Subansiri near the confluence of Brahmaputra River, soil type eutric cambisol (3683) is found at top layer

Table 3.1: Land use/land cover details of Subansiri River

S.N.	**Symbol**	**LULC**	**Area** (%)
0	WATR	Water	0.19
1	FOEN	Evergreen needle leaf	12.22
2	FOEB	Evergreen broad leaf	13.92
3	FODN	Deciduous needle leaf	0.03
4	FODB	Deciduous broad leaf	0.01
5	FOMI	Mixed forest	29
6	SESB	Closed Shrub land	0.02
7	SHRB	Open Shrub lands	1.95
8	SAVA	Woody savanna	0.34
9	WEWO	Savannas	0.01
10	GRAS	Grassland	37.02
11	WETN	Perm. Wetland	0.03
12	CRWO	Cropland	0.03
13	URBN	Urban and built-up	0
14	CRGR	Cropland natural veg.	0.07
15	ICES	Snow and Ice	4.14
16	BSVG	Barren and sparsely vegetated	1.03

along with orthic luvisol and chromic luvisol at second and third layer. Apart from this, some part are permanently covered with glaciers (6998) and waterbodies (6997).

3.5 Meteorological characteristics of Subansiri river basin

Subansiri sub-basin shows very much diversity in rainfall characteristics because of its areal extends from tropical to temperate zones (Sarkar et al., 2012) . Average annual rainfall in the Subansiri catchment increase to the foothills from the plains of Assam. Relative humidity remains high throughout the year. Average annual maximum temperature ranges from 2°C to 25°C whereas average annual minimum temperature varies from −7°C to 5°C. Variation of temperature in the upper part of the basin is very low because of the high elevation zone which remains covered with snow and glacier throughout the year. Temperature variation in the basin can be explained separately for the upstream and downstream, as the upstream is mostly covered with the hilly

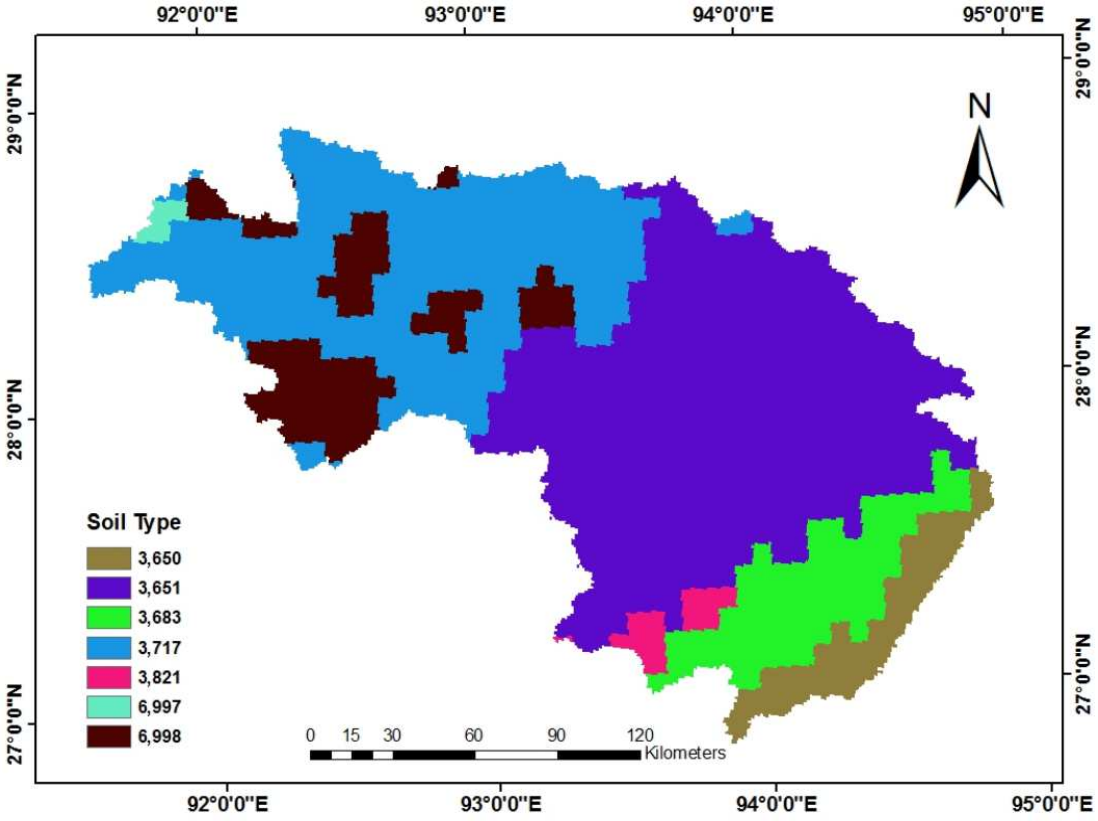

Figure 3.4: Soil map of Subansiri River

terrain so the temperature range does not go very high whereas in the downstream it could rise up to 35°C in the summer month. Monthly variation of maximum and minimum temperature along with the monthly precipitation are shown in the Figure 3.5.

3.6 History of natural hazards in the Subansiri river basin

In Indian sub-continent, where river basin are heavily populated and unplanned urbanization on the river banks are taking place, natural hazards are bound to happen (Singh and Awasthi, 2011). Situation become even worse when this flood phenomena occurs in the hilly region such as in Assam and other states of Northeast India. Northeastern part is very much prone to earthquake and heavy rainfall incidents, which makes this

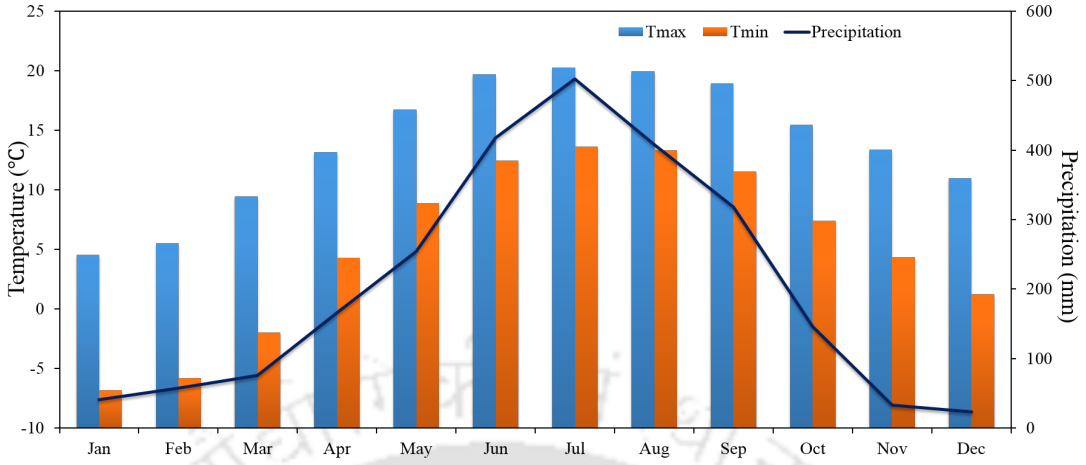

Figure 3.5: Average monthly precipitation, minimum and maximum temperature variation in the Subansiri river basin

region very much vulnerable to the natural hazard situations. Recent known biggest natural hazard in the Subansiri river basin happened in August, 1950 when a massive earthquake stroked the Assam state, which caused landslides in the hilly region. Landslide choked the path of Subansiri River at the gorge near Gerukamukh where the lower Subansiri hydroelectric project is situated. This dam like formation continued for the three days and amount of water stored behind the obstruction caused by blocking of rocks and stones was equal to the present capacity of the constructed hydropower dam (Ray, 2010). After three days the pressure of stored water broke the naturally formed dam, which resulted in catastrophic flood in the region. This flood caused a massive deposition of sediment and also it changed the morphology of the Subansiri River.

Apart from this catastrophic flood event, frequent flood is quite common in the Subansiri river basin. Subansiri River is a perennial river which is fed mainly by snow/glacier melt. Northeastern India region receives annual rainfall more than 2000 mm, which make this region prone to frequent flood events. Cities like Dhemaji and Lakhimpur face severe flood problem in monsoon season because of the high flow in the Suban-

siri River during monsoon season. Extreme events like heavy precipitation are very common in the region which causes flash flood like situation and fragile mountainous geomorphology causes frequent landslide events (Das et al., 2009). Recently on June 2004, flash flood occurred due to heavy rain in North Lakhimpur district which inundated approximately 50 villages and caused loss of lives, another event occurred in the same year 2004 in the month of October when flash flood occurred in the Subansiri river and surrounding small tributaries which cause inundation of several villages and loss of properties (Das et al., 2009).

3.7 Hydrological and meteorological datasets

India meteorological Department (IMD) gridded precipitation data of 0.50° latitude × 0.50° longitudes is used as observed data (for station 2, 3 and 4) as shown in Figure 3.6. IMD gridded data are the products of interpolation of high quality gauge station data from more than 1800 stations (Rajeevan et al., 2006). Apart from these gridded data one precipitation gauge station data (for station 5) is also available for study. Since there is no IMD gauge stations and IMD gridded datasets are available for the upper region, APHRODITE gridded (0.50° × 0.50°) precipitation dataset was used as observed data. Asian Precipitation- Highly Resolved Observational Data Integration Towards Evaluation of the Water Resources (APHRODITE) is the high resolution ($0.25°C \times 0.25°C$ and $0.5°C \times 0.5°C$) daily rainfall data sets developed for the Asian region which is based on the data collected at more than 5,000 stations (Yatagai et al., 2009). Apart from the meteorological datasets, observed daily streamflow datasets were collected from the National Hydro-power commission (NHPC) for the period of 2002-2012.

3.8 GCM and NCEP datasets description

Fifth phase of coupled model inter-comparison project CMIP5 datasets comprises of the substantial changes to the previous provided SRES datasets (IPCC AR4) and culminated in the form of Representative Concentration Pathways (RCPs) to characterize alternative future greenhouse gas emissions scenarios (Taylor et al., 2012). The estimated radiative forcing values by the year 2100 are 2.6 W/m^2 in the RCP2.6 experiment, peaking at about 3 W/m^2 before 2100 and declining afterwards, two intermediate emission scenarios 4.5 W/m^2 and 6.0 W/m^2 and a extreme radiative forcing scenario i.e. RCP8.5 is also proposed in fifth assessment report (Taylor et al., 2012) .

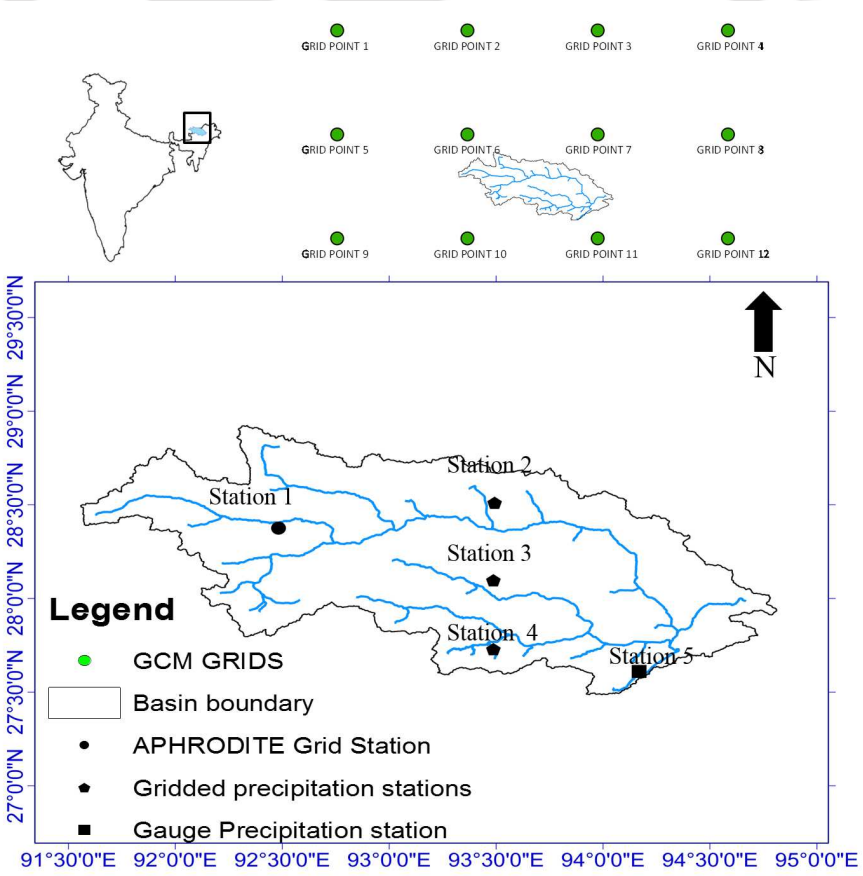

Figure 3.6: Observed, gridded and GCM precipitation and temperature stations location

Moreover, the CMIP5 models include the standard Climate System Models (CSMs) as used in CMIP3 (albeit mostly with updates, including higher spatial resolution) which incorporate additional biogeochemical components (e.g. aerosols, chemistry, and dynamic vegetation) (Taylor et al., 2012).

In this research work, two earth system model (ESM) GCM datasets namely ESM2G and ESM2M were downloaded from Geophysical Fluid Dynamics Laboratories (GFDL) data-portal (http:// nomads.gfdl.noaa.gov:8080 /DataPortal/cmip5.jsp) for three RCP scenarios i.e. RCP2.6, RCP6.0 and RCP8.5. Apart from these two ESM models, GFDL-CM3 GCM dataset was also utilized for the projection of temperature and precipitation. These GCM has a grid resolution of 2° latitude × 2.5° longitude. ESM2G and ESM2M GCM are the product of the Earth System Models (ESMs) (Dunne et al., 2012, 2013) which includes physical factors like precipitation and aerosols (atmospheric component), streams, lakes, rivers, and runoff (land component) and water fluxes, or flow; currents; sea ice dynamics; iceberg transport of freshwater for simulating the carbon emission and concentration. The National Center for Environmental Prediction (NCEP) reanalysis datasets variables with a resolution of 2.5° latitude × 2.5° longitude for the historical period (1981-2000) was used for preparing the downscaling model.

CHAPTER 4

Temperature and precipitation downscaling

4.1 General

The increase of the greenhouse gas concentration in the atmosphere is causing alterations in the occurrence and magnitude of many hydrological events as well as the water availability (Bhave et al., 2016). Temperature is one of the several climatic parameters which is supposed to be the most vulnerable to the climate change phenomena (Karl et al., 1993). The Intergovernmental Panel on Climate Change (IPCC) has reported an increase of 0.6°C in the global mean temperature over the last 100 years of the twenty-first century with 1998 being the warmest year; it is likely to increase further by 1.1° to 2.9°C for their lowest emission scenario and 2.4° to 6.4°C for their highest emission scenario (IPCC, 2007).

In the hydrological studies, local scale factors play a vital role in occurrence and distribution of the various hydrological events thus the coarse resolution of the GCMs makes them unsuitable for direct use in impact assessment studies (Mondal and Mujumdar, 2012; Samani et al., 2012). Goyal and Ojha (2012b) used the artificial neural network method to downscale the minimum and maximum temperature for the four emission

scenarios over lake-catchment and reported an increase in Tmax and Tmin for three of the four emission scenarios. Duhan and Pandey (2015) analyzed the downscaled maximum and minimum temperature over Tons River basin for A2 emission scenario and reported an increase in Tmax and Tmin for the period of 2001–2100. Shrestha et al. (1999) analyzed the long-term observed temperature data for Nepal and reported a high warming trend at the higher elevation region as compared to lower elevation part. The weather elements, i.e., precipitation and evapotranspiration are said to be highly correlated to the temperature (Kalma et al., 2008). The availability of water resources of a region highly depend on the temperature, precipitation, evaporation, and other hydrological factors (Milly et al., 2005). The assessment of changes associated with temperature for different climate change scenarios is helpful for estimating the changes in several hydrological events (Goyal and Ojha, 2012a).

In this chapter, maximum temperature, minimum temperature and precipitation were downscaled for the selected five stations of the Subansiri river basin for three RCP scenarios (RCP2.6, RCP6.0, and RCP8.5) and trends and magnitude of changes in the future domain were computed using Mann-Kendall test and Sen's slope method. Precipitation extreme indices were calculated for the historical period and future scenarios.

4.2 Statistical downscaling model

In this study, the Statistical Downscaling Model (SDSM) is used for downscaling of temperature. The SDSM is a statistical tool which establishes linear regression equation between observed datasets (predictands) and the GCM variables (predictors) (Wilby et al., 2002). There are two sub-modules for preparing the regression model between predictors and the predictand, i.e., conditional and unconditional. A conditional model

which accounts wet-dry spells for establishing the regression relation is used for precipitation downscaling whereas unconditional model is used for temperature downscaling (Wilby et al., 2002). SDSM includes two methods for parameter optimization viz. the ordinary least square method and simplex method (Wilby et al., 2002). SDSM model performs explained variance analysis, correlation matrix, and scatterplot between the predictors and predictand for selection of the predictors. Apart from the statistical analysis of the variables, ground knowledge of the region is important for understanding the physical significance of predictors and final selection of the predictor combinations.

4.3 Interpolation of the GCM and NCEP datasets

As shown in Figure 3.6 (Chapter 3) grid resolution of NCEP predictors and GCM predictors differ from each other, so it is important to bring these predictors to the same grid resolution hence the nearest four GCM grid points of the predictor variables were first interpolated to the NCEP grids using inverse distance weighted average (IDWA) method (Snell et al., 2000) spatial interpolation approach of GCM variables has been utilized in the previous studies (Duhan and Pandey, 2015; Singh and Goyal, 2016).

4.4 Bias correction

The CMIP5 GCMs data also contains some bias in their time series values (Torres and Marengo, 2014). Moreover, all model outputs involve a great deal of biases that, if not corrected, can lead to significant errors in impact assessments. Therefore, a bias correction of GCM outputs is necessary before analyzing regional/local impacts (Goyal et al., 2011). For this reason, bias corrections of the downscaled temperature and

precipitation datasets have done (Mahmood and Babel, 2013)

$$T_{deb} = T_{SCEN} - (\overline{T_{CONT}} - \overline{T_{obs}}) \tag{4.1}$$

$$P_{deb} = P_{SCEN} \times \frac{\overline{P_{obs}}}{\overline{P_{CONT}}} \tag{4.2}$$

where T_{deb} and P_{deb} are the de-biased (corrected) daily time series of temperature and precipitation respectively for future periods. SCEN represents the scenario data downscaled by SDSM for future periods (2006-2100), and CONT represents downscaled data by SDSM for the present period (1980-2005). T_{SCEN} and P_{SCEN} are the daily time series of temperature and precipitation generated by SDSM for future periods respectively. T_{CONT} and P_{CONT} are the long term monthly values for temperature and precipitation for the control period simulated by SDSM. T_{obs} and P_{obs} represent the long-term monthly observed values for temperature and precipitation respectively. The bar over P and T shows the long-term average. The frequency and intensity of precipitation are the two main factors affecting precipitation variability (Mahmood and Babel, 2013). The characteristic of this method of study is to correct the precipitation amount and not the frequency, and also to remove any systematic errors belonging to SDSM during downscaling.

4.5 Model performance evaluation

The Root Mean Square Error (RMSE), Nash-Sutcliff Efficiency (NSE) (Nash and Sutcliffe, 1970) and coefficient of determination (R^2) were checked for evaluation of the prepared downscaling model.

Nash-Sutcliff Efficiency

$$NSE = 1 - \frac{\Sigma_{i=1}^{n}(T_{O_i} - T_{P_i})^2}{\Sigma_{i=1}^{n}(T_{O_i} - \overline{T_O})^2} \tag{4.3}$$

Root Mean Square Error

$$RMSE = \sqrt{\frac{\Sigma_{i=1}^{n}(T_{O_i} - T_{P_i})}{n}} \tag{4.4}$$

Coefficient of determination

$$R^2 = \left(\frac{\sum_{i=1}^{n}(T_{O_i} - \overline{T_O})(T_{P_i} - \overline{T_p})}{\left(\sqrt{\sum_{i=1}^{n}(T_{O_i} - \overline{T_O})^2}\right)\left(\sqrt{\sum_{i=1}^{n}(T_{P_i} - \overline{T_P})^2}\right)} \right)^2 \tag{4.5}$$

Where T_{O_i} and T_{P_i} are the i^{th} data point of observed and model generated temperature dataset respectively and $\overline{T_O}$ and $\overline{T_P}$ are the mean of observed and model generated temperature data series respectively.

4.6 Screening of predictors

Statistical downscaling model performs the predictor selection on the basis of correlation between the observed variables (predictands) and NCEP/GCM variables (predictors) and partial correlations among the predictors. It is suggested that the correlation between the predictors and predictands should be maximum but correlation between predictors should be minimum in order to avoid the collinearity in the downscaled time series (Sachindra et al., 2011; Wilby et al., 2002). Purpose of the predictor selection is to identify the set of most relevant predictors which represents the local scale factor which influence the predictands (precipitation and temperature). The selection of first

predictor is comparatively easy but the selection of the next predictors are much more subjective. First suitable predictor is selected on the basis of the correlation check and the highest correlated predictor is selected as the first predictor and second third and next predictors are selected following the steps explained below

- Correlation matrix of the NCEP predictors and the predictands are prepared for each station predictor separately and the predictors are arranged in descending order predictor with highest correlation is ranked as the first predictor, this process is done for all the stations' predictands and after this step, correlation coefficient between the predictors and predictands and, correlation coefficient between individual predictors and the partial correlation between the predictors are calculated in order to decide the second, third and more predictors.
- After selecting the first predictor, percentage reduction in an absolute partial correlation (PRP) with respect to absolute correlation is calculated for each predictor by subtracting the correlation coefficient from the partial correlation coefficient and then dividing with the correlation coefficient.
- Predictor with minimum PRP value is considered as the second predictor which is least correlated with the first selected predictor to avoid any multi-collinearity in the series. This process is repeated for selection of the next predictors.

In order to select the GCM predictors, first the GCM predictors were interpolated to the GCM scale grid utilizing the inverse distance weighted average method (IDWA) (Willmott et al., 1985) to avoid any spatial variability between GCM and NCEP grids. Correlation and partial correlation between the predictands and predictors were checked to select the final set of predictors for preparing the model. Predictors namely tas (temper-

ature at surface), tasmax (maximum temperature at surface), tasmin (minimum temperature at surface), rhsmax (relative humidity maximum), rhsmin (relative humidity minimum) were chosen, prc (precipitation flux) were selected finally for preparing the precipitation and temperature downscaling models. The selected predictors and their screening results for minimum temperature, maximum temperature and precipitation are shown in Table 4.1. For all the stations first predictor for the precipitation were selected as tasmax. Whereas for maximum temperature and minimum temperature for all of the climate stations tas selected as first predictor. These predictors also covey a physical relationship regarding the local scale minimum temperature, maximum temperature and precipitation. As per the latest CMIP5 GCMs, several new predictors have been added (Taylor et al., 2012). In this study, the basic concept of predictor's selection is adopted as per the methodology proposed by (Mahmood and Babel, 2013).

Table 4.1: Predictor details with statistics for Tmax, Tmin and precipitation

Var.	Stations	Statistics	tas	tasmax	tasmin	pr	prc	rhs	rhsmax	rhsmin	rlds	rsds	vas	hfls
Tmin	Stn1	R	0.82	0.82	0.85	0.54	0.42	0.56	0.55	0.59	0.81	0.07	0.41	0.76
		Partial r	0.11	0.01	0.17	0.04	0.14	0.11	0.01	0.13	0.03	0.06	0.03	0.12
		PRP	0.87	0.99	0.80	0.93	0.67	0.80	0.98	0.78	0.96	0.14	0.93	0.84
	Stn2	R	0.87	0.87	0.90	0.58	0.45	0.59	0.62	0.58	0.85	0.08	0.44	0.80
		Partial r	0.08	0.05	0.16	0.03	0.15	0.11	0.13	0.01	0.02	0.06	0.04	0.12
		PRP	0.91	0.94	0.82	0.95	0.67	0.81	0.79	0.98	0.98	0.25	0.91	0.85
	Stn3	R	0.79	0.87	0.90	0.57	0.85	0.58	0.42	0.61	0.57	0.08	0.44	0.79
		Partial r	0.10	0.01	0.16	0.03	0.02	0.10	0.11	0.12	0.00	0.06	0.02	0.11
		PRP	0.87	0.99	0.82	0.95	0.98	0.83	0.74	0.80	1.00	0.25	0.95	0.86
	Stn4	R	0.88	0.87	0.90	0.58	0.08	0.59	0.45	0.62	0.85	0.44	0.58	0.80
		Partial r	0.05	0.07	0.03	0.11	0.02	0.01	0.10	0.12	0.11	0.14	0.04	0.13
		PRP	0.94	0.92	0.97	0.81	0.75	0.98	0.78	0.81	0.87	0.68	0.93	0.84

Continued on next page

Table 4.1 – *Continued from previous page*

Var.	Stations	Statistics	tas	tasmax	tasmin	pr	prc	rhs	rhsmax	rhsmin	rlds	rsds	vas	hfls
Tmax	Stn5	R	0.91	0.81	0.90	0.57	0.61	0.57	0.42	0.79	0.85	0.08	0.44	0.57
		Partial r	0.12	0.00	0.18	0.04	0.13	0.11	0.13	0.13	0.03	0.07	0.02	0.01
		PRP	0.87	1.00	0.80	0.93	0.79	0.81	0.69	0.84	0.96	0.13	0.95	0.98
	Stn1	R	0.75	0.83	0.75	0.05	0.46	0.44	0.69	0.47	0.33	0.45	0.33	0.66
		Partial r	0.07	0.16	0.08	0.01	0.05	0.08	0.07	0.06	0.13	0.05	0.02	0.02
		PRP	0.91	0.81	0.89	0.80	0.89	0.82	0.90	0.87	0.61	0.89	0.94	0.97
	Stn2	R	0.83	0.83	0.38	0.87	0.50	0.08	0.53	0.77	0.38	0.52	0.39	0.51
		Partial r	0.05	0.07	0.03	0.14	0.07	0.01	0.06	0.07	0.14	0.05	0.03	0.05
		PRP	0.94	0.916	0.92	0.84	0.86	0.88	0.89	0.91	0.63	0.90	0.92	0.90
	Stn3	R	0.83	0.86	0.83	0.49	0.51	0.50	0.77	0.52	0.36	0.08	0.39	0.73
		Partial r	0.07	0.16	0.08	0.08	0.04	0.05	0.07	0.06	0.13	0.01	0.02	0.02
		PRP	0.92	0.81	0.90	0.84	0.92	0.90	0.91	0.88	0.64	0.88	0.95	0.97

Continued on next page

Table 4.1 – *Continued from previous page*

Var.	Stations	Statistics	tas	tasmax	tasmin	pr	prc	rhs	rhsmax	rhsmin	rlds	rsds	vas	hfls
Pcp	**Stn4**	R	0.83	0.86	0.83	0.50	0.52	0.51	0.77	0.53	0.38	0.08	0.38	0.74
		Partial r	0.06	0.15	0.07	0.08	0.05	0.06	0.08	0.06	0.14	0.01	0.03	0.03
		PRP	0.93	0.83	0.92	0.84	0.90	0.88	0.90	0.89	0.63	0.88	0.92	0.96
	Stn5	R	0.82	0.86	0.83	0.50	0.49	0.51	0.77	0.52	0.35	0.08	0.39	0.72
		Partial r	0.08	0.16	0.09	0.05	0.08	0.05	0.07	0.06	0.12	0.01	0.02	0.02
		PRP	0.90	0.81	0.89	0.90	0.84	0.90	0.91	0.88	0.66	0.88	0.95	0.97
	Stn1	R	0.43	0.3	0.28	0.32	0.53	0.43	0.41	0.19	0.41	0.10	0.24	0.38
		Partial r	0.01	0.03	0.02	0.01	0.01	0.05	0.02	0.01	0.00	0.00	0.01	0.02
		PRP	0.98	0.9	0.93	0.97	0.98	0.88	0.95	0.95	1.00	1.00	0.96	0.95
	Stn2	R	0.43	0.31	0.28	0.32	0.67	0.43	0.20	0.41	0.41	0.10	0.24	0.38
		Partial r	0.02	0.03	0.03	0.01	0.01	0.05	0.01	0.03	0.01	0.01	0.01	0.03
		PRP	0.95	0.90	0.89	0.97	0.99	0.88	0.95	0.93	0.98	0.90	0.96	0.92

Continued on next page

Table 4.1 – *Continued from previous page*

Var.	Stations	Statistics	tas	tasmax	tasmin	pr	prc	rhs	rhsmax	rhsmin	rlds	rsds	vas	hfls
	Stn3	R	0.31	0.30	0.27	0.57	0.31	0.42	0.19	0.40	0.40	0.10	0.24	0.37
		Partial r	0.02	0.03	0.02	0.02	0.01	0.05	0.00	0.03	0.01	0.00	0.00	0.03
		PRP	0.94	0.90	0.93	0.96	0.97	0.88	1.00	0.93	0.98	1.00	1.00	0.92
	Stn4	R	0.31	0.41	0.20	0.67	0.32	0.28	0.43	0.43	0.41	0.10	0.32	0.38
		Partial r	0.03	0.03	0.01	0.00	0.01	0.02	0.05	0.02	0.01	0.01	0.01	0.03
		PRP	0.90	0.93	0.95	1.00	0.97	0.93	0.88	0.95	0.98	0.90	0.97	0.92
	Stn5	R	0.40	0.42	0.34	0.55	0.34	0.31	0.33	0.21	0.44	0.11	0.27	0.44
		Partial r	0.04	0.02	0.02	0.05	0.01	0.02	0.04	0.00	0.00	0.00	0.01	0.01
		PRP	0.90	0.95	0.94	0.91	0.97	0.94	0.88	1.00	1.00	1.00	0.96	0.98

4.7 Temperature downscaling model performance

For maximum temperature model the RMSE, R^2 and NSE values for the calibration period are 0.91 °C, 0.93 and 0.91 respectively. Validation results of RMSE, R^2, and NSE are found to be 1.07°C, 0.86 and 0.87 respectively. The graph plots of calibration and validation periods are shown in Figure 4.1(a). Figure 4.1(b) shows the graph plot of minimum temperature for calibration period (1981-1995) and validation period (1996-2000). The RMSE, R^2 and NSE values for the downscaling model of Tmin are 0.82°C, 0.97 and 0.97 respectively for the calibration period whereas for the validation period these are 0.72°C, 0.92 and 0.93 respectively. The performance of temperature downscaling models are in good agreement with the temperature downscaling works done over different regions of India (Duhan and Pandey, 2015; Mahmood and Babel, 2013; Goyal and Ojha, 2012b).

4.7.1 Future projection of temperature for RCP scenarios

Further, the calibrated and validated models are used for generating the temperature data series over the period of 2011-2100 for RCP scenarios RCP2.6, RCP6.0 and RCP8.5 using CMIP5/ESM2G datasets. Tmax and Tmin data series for the period of thirty years (2011-2040, 2041-2070 and 2071-2100) were analyzed for comparing the overall change in the minimum and maximum temperature with the observed temperature data for the period of 1981-2000. Figure 4.2(a) shows the plot of mean annual temperature of all the nine ensembles for the period of 2011-2100. Figure shows an increasing pattern of the warming trend in future, Figure 4.2(b) shows the average of three GCMs for respective RCP scenarios i.e. RCP2.6, RCP6.0 and RCP8.5 and it indicates increase in temperature for low to extreme emission scenarios, this increase in temperature

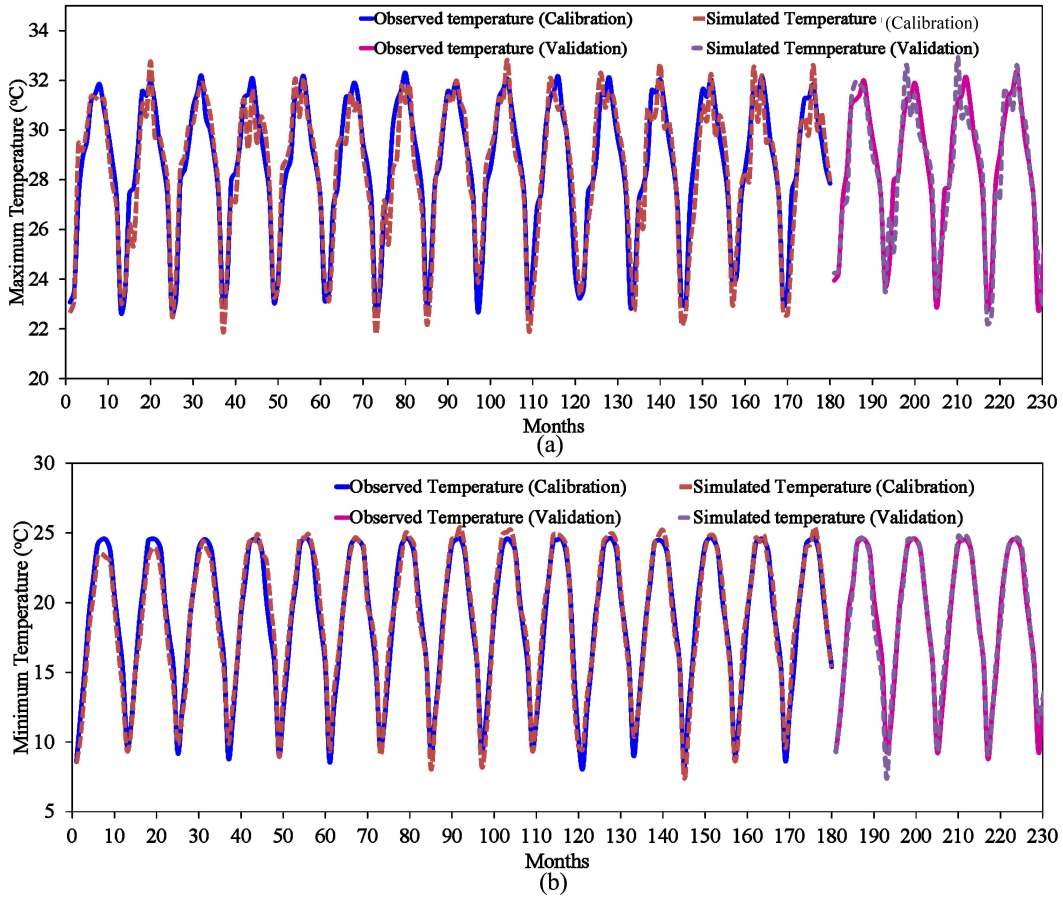

Figure 4.1: Calibration (1981-1995) and validation (1996-2000) result of (a) maximum temperature (b) minimum temperature downscaling models for Subansiri river basin.

varies from 14°C (for RCP2.6) to 14.6°C (for RCP8.5). Figure 4.2(b) represents the average of three GCMs for their respective RCP scenario and it shows that the change in magnitude is increasing for all emission scenario with magnitude increasing from low to high emission scenarios. Comparison of the mean of three inter-decadal period i.e. 2011-2040, 2041-2070 and 2071-2100 for RCP2.6, RCP6.0 and RCP8.5 along with the Tmax data for observed time period (1981-2000) shows that the lower limit of maximum temperature tends to increase whereas the upper limit shows a slight decrease over the time period. The increase in mean of the temperature for inter-decadal period shows uniform increasing trend from low to extreme emission scenario. The last three-decadal

period (2071-2100) shows the highest increase. The comparison by magnitude shows an overall increase in Tmax by 0.47°C over the period 2011-2100 for RCP2.6 and an increase of 0.72°C for RCP8.5. The inter-decadal time-steps also show a gradual increase in temperature from beginning of the century to the end of the century.

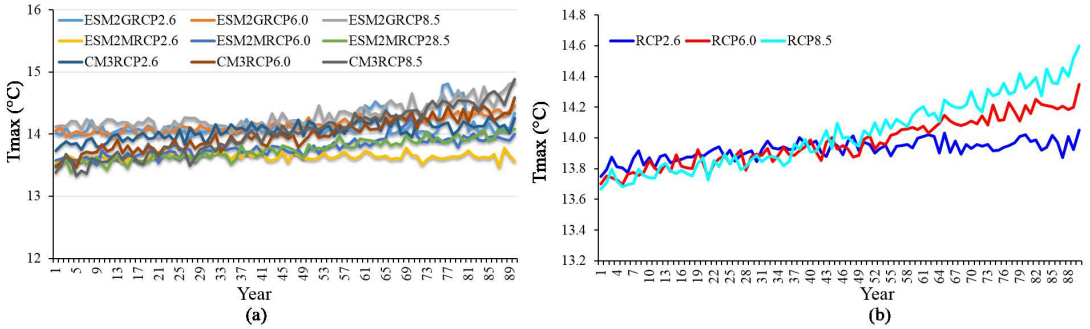

Figure 4.2: Change in maximum temperature for all GCM/RCP scenarios over 2011-2100 period (a) GCM/RCP ensembles (b) average of the GCMs of respective RCPs

Similar pattern can be seen for the Tmin in Figure 4.3. Figure 4.3(a) shows the annual Tmin pattern of all the nine ensembles for the period 2011-2100 and Figure 4.3(b) shows the average of three GCMs for the respective RCP scenario, it is clear from the figure that the Tmin likely to increase from 4.8°C for RCP2.6 scenario to 5.6°C for RCP8.5 for 2071s. Although the Tmax and Tmin shows clear increasing trends, the monthly analysis of the temperature for all the scenarios may provide clearer picture of the seasonal changes in temperature. The comparison of the minimum temperature

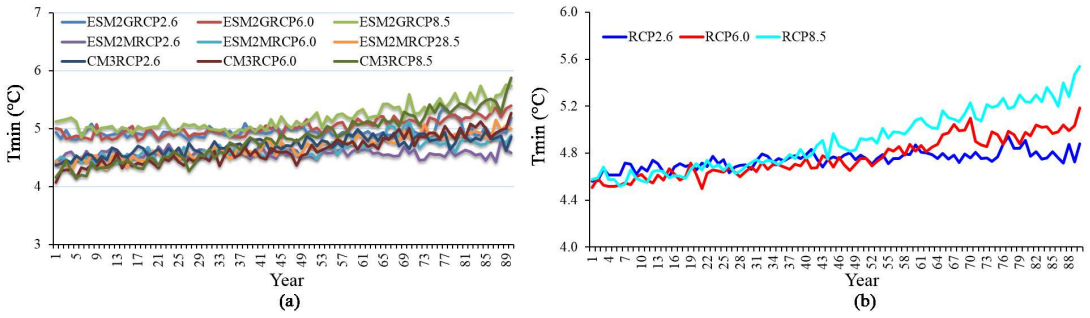

Figure 4.3: Change in minimum temperature for all GCM/RCP scenarios over 2011-2100 period (a) GCM/RCP ensembles (b) average of the GCMs of respective RCPs

along with observed period minimum temperature for three inter-decadal time scales as compared to observed Tmin shows a consistent increase in minimum temperature. An increase in median of the minimum temperature for RCP2.6 scenario is observed to be 0.36°C, for RCP6.0 and RCP8.5 it is 0.26°C and 0.72°C respectively.

4.7.2 Annual and monthly change in Tmax and Tmin

4.7.2.1 Trends in historical temperature

The non-parametric Mann-Kendall test (Mann, 1945; Kendall, 1968) was applied for detecting the statistically significant or insignificant trend in the time series.The Mann-Kendall test was applied to detect the long term trends in monthly and annual time series of Tmax, Tmin and precipitation. The significance level of TLR is evaluated as α = 0.05. Trends were checked on the 95% confidence interval. Based on this significance level (α), values larger than 1.96 or lower than 1.96, indicated a significantly ($p < 0.05$) increasing or decreasing behavior of the time series, respectively. The Mann-Kendall equations can be described below as The statistics (S) is defined as (Eq. 4.6):

$$S = \Sigma_{i=1}^{N-1}\Sigma_{j=i+1}^{N} sgn(x_j - x_i) \tag{4.6}$$

where N is the number of data points. Assuming $\theta = (x_j - x_i)$, the value of sgn (θ) is computed as follows (Eq. 4.7):

$$sgn(\theta) = \begin{cases} 1 & if\theta > 0 \\ 0 & if\theta = 0 \\ -1 & if\theta < 0 \end{cases} \tag{4.7}$$

This statistics represents the number of positive differences minus the number of negative differences for all the differences considered. For large samples (N 10), the test is

conducted using following Eq. 4.9.

$$E[S] = 0 \tag{4.8}$$

$$\text{var}(S) = \frac{(N(N-1)(2N+5) - \Sigma_{k=1}^{n}(t_k - 1)(2t_k + 5))}{18} \tag{4.9}$$

Where n is the number of tied (zero difference between compared values) groups and t_k the number of data points in the k^th tied group. The standard normal deviate (Z-statistics) is then computed as (Eq. 4.10):

$$Z = \begin{cases} \frac{S-1}{\sqrt{var(S)}} & if S > 0 \\ 0 \quad if S = 0 \\ \frac{(S+1)}{\sqrt{var(S)}} & if \theta < 0 \end{cases} \tag{4.10}$$

If the computed value of $|Z| > Z_{\alpha/2}$, the null hypothesis (H_0) is rejected at alpha (α) level of significance in a two-sided test.

The historical data series of Tmax, Tmin and DTR on the monthly and annual scale for all the selected stations were analyzed for auto-correlation test at 95% confidence interval where no significant correlation was found. Further, the MK trend test was applied to data series; Z-statistics and Sen's slope values for all the stations are shown in Table 4.2. At station 1 the annual Tmax shows significant increasing trend with a magnitude of 0.07°C/yr whereas on the monthly scale there is no clear pattern on summer or winter temperature were found. But the months of March, May, September, and December show a significant increasing trend. Similarly stations 2, 3 and 4 also show a significant increase in annual Tmax and on monthly scale no clear pattern was observed. At station 5 warming trends were found insignificant at annual scale although December month showed a significant increasing trend with 0.12°C/yr.

The Tmin shows comparatively clearer pattern of increasing trend as compared to the Tmax at annual scale as well as at the monthly scale. For the stations 1, 2, 3 and 4 the Tmin shows an increasing trend whereas Tmin trend at station 5 is not as much significant as the other stations. At station 1, the monsoon months (June to September) show significantly increasing trend and at stations 2 and 3 except in the month of January all other months show the increasing trend. The station 4 shows an increasing trend only at annual scale with magnitude of 0.05°C/yr with no significant increase in monthly scale but on the other hand at station 5 there was no such increasing trend observed.

The trend analysis of Tmax and Tmin for all the stations reveals an increasing trend at annual and monthly scale and it is found that the increase in Tmin is higher as compared to the increase in Tmax which clearly indicates a decrease in the diurnal temperature range (DTR). Trend analysis of DTR indicates decreasing trend at all the station but only station 3 and 4 were found significant.

4.7.2.2 Trends in downscaled temperature series

The average Tmax and Tmin of the river basin was calculated from the downscaled temperature data of the selected stations. The Mann-Kendall Z-statistic results of the average Tmax for RCP2.6, RCP4.5 and RCP8.5 are shown in Figure 4.4 as Z-statistics indicates the significance or non-significance of the existing trend at 95% confidence interval. Trends in downscaled temperature series of all the RCP scenarios were tested for inter-decadal time steps of 30-years i.e. 2011-2040, 2041-2070 and 2071-2100 as well as for the entire period of 2011-2100.

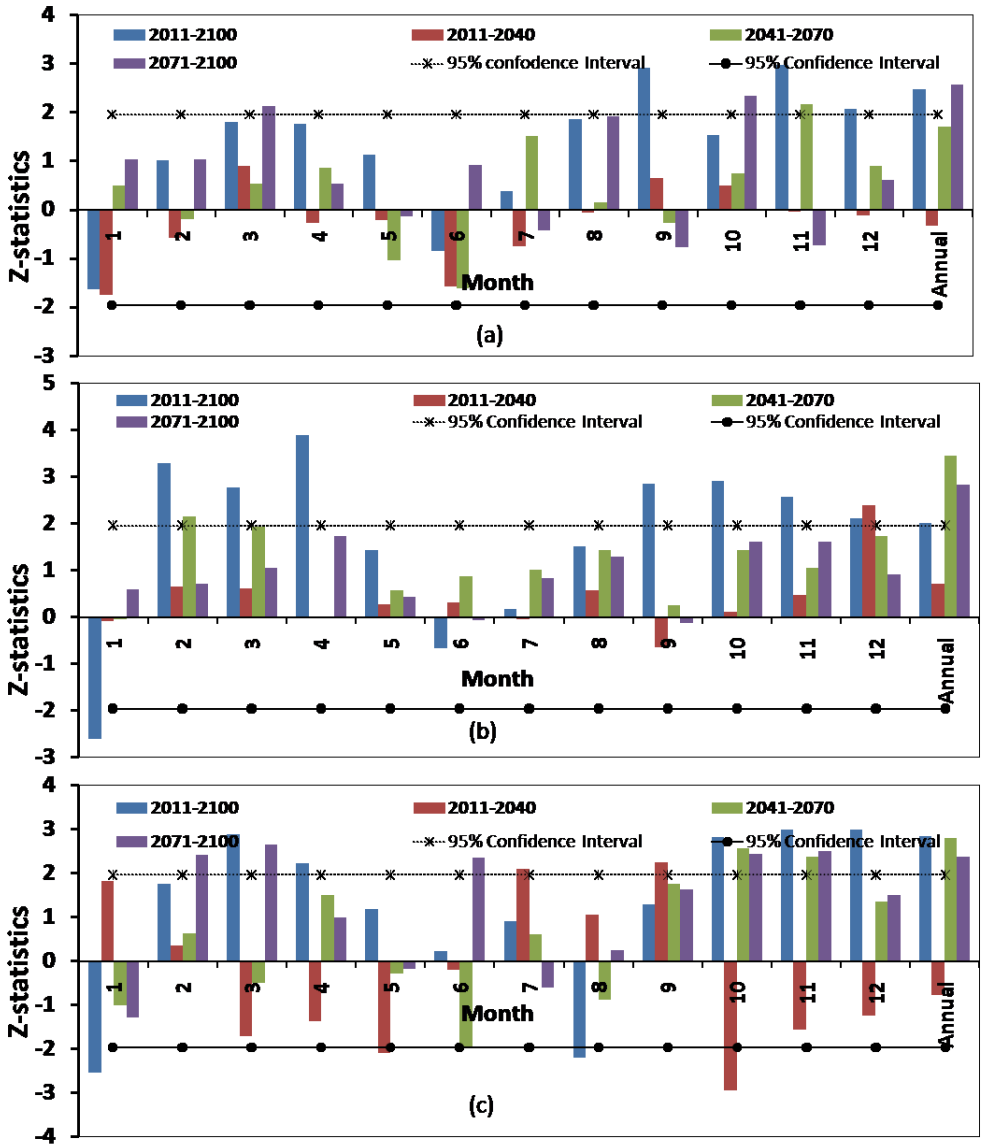

Figure 4.4: Mann-Kendall test Z- statistics showing significant and non-significant trend of maximum temperature for (a) RCP2.6 (b) RCP6.0 and (c) RCP8.5

The annual average maximum temperature shows a significant increase over long term period of 2011-2100 for RCP2.6 along with an increase in post monsoon months (September, October) and winter temperature (November and December), and the respective magnitude of changes (Sen's slope) are shown in Table 4.3(a). For RCP6.0 scenario, the increase in long-term maximum temperature was found to be significant with a magnitude of 0.004°C/yr following the warming of winter season months of December

(0.01°C/yr) and February (0.003°C/yr). The warming rate was found to be comparatively higher at the end of the century as compared to starting decades, with magnitude of 0.008°C/yr during 2041-2070 and 0.007°C/yr during 2071-2100 (Table 4.4 a). The annual average Tmax tends to increase significantly for the extreme emission scenario (RCP8.5) along with the significant increase in the months of March (0.008°C/yr), October (0.019°C/yr), November (0.013°C/yr) and December (0.007°C/yr) whereas there was a significant decreasing trend observed in January (0.005°C/yr) and August (0.003°C/yr) as shown in Table 4.4(a).

Table 4.2: Trend analysis results of historical period (1981-2000) monthly maximum temperature, minimum temperature and diurnal temperature variation (DTR) data series of all stations.(* shows the significant trends at 95% confidence interval)

			Jan	**Feb**	**Mar**	**Apr**	**May**	**Jun**	**Jul**	**Aug**	**Sep**	**Oct**	**Nov**	**Dec**	**Annual**
Station 1	Tmax	Z	1.25	1.89	2.85*	1.46	2.67*	0.52	0.75	1.43	2.90*	1.59	1.57	3.58*	3.14*
		Slope	0.08	0.08	0.14	0.07	0.11	0.01	0.02	0.03	0.06	0.05	0.06	0.15	0.07
	Tmin	Z	1.39	1.21	2.67*	1.21	2.60*	2.93*	2.46*	2.80*	3.21*	1.89	2.05*	3.07*	3.91*
		Slope	0.11	0.08	0.18	0.06	0.07	0.04	0.04	0.04	0.04	0.04	0.09	0.14	0.09
	DTR	Z	-0.64	-0.18	-1.73	-0.27	2.25*	-0.98	-1.21	-1.30	0.07	0.95	-1.55	-0.71	-1.75
		Slope	-0.02	-0.01	-0.06	-0.01	0.04	-0.02	-0.03	-0.02	0.00	0.01	-0.02	-0.01	-0.01
			Jan	**Feb**	**Mar**	**Apr**	**May**	**Jun**	**Jul**	**Aug**	**Sep**	**Oct**	**Nov**	**Dec**	**Annual**
Station 2	Tmax	Z	1.73	3.48*	2.52*	0.39	0.73	1.75	2.66*	2.89*	1.66	1.77	0.68	0.95	4.18*
		Slope	0.05	0.11	0.07	0.01	0.02	0.04	0.06	0.05	0.04	0.05	0.03	0.03	0.05
	Tmin	Z	1.68	2.09*	3.96*	2.27*	2.52*	3.89*	3.91*	3.10*	2.77*	2.80*	1.77*	3.18*	4.84*
		Slope	0.06	0.07	0.13	0.04	0.03	0.04	0.04	0.04	0.04	0.05	0.03	0.08	0.06

Continued on next page

Table 4.2 – *Continued from previous page*

			Jan	**Feb**	**Mar**	**Apr**	**May**	**Jun**	**Jul**	**Aug**	**Sep**	**Oct**	**Nov**	**Dec**	**Annual**
	DTR	Z	-0.91	2.02*	-2.82*	-0.89	-1.07	-0.43	0.41	1.43	0.09	0.39	-0.25	-2.71*	-1.82
		Slope	-0.02	0.05	-0.07	-0.02	-0.02	-0.01	0.01	0.02	0.00	0.01	-0.01	-0.05	-0.02
Station 3	Tmax	Z	1.56	3.20*	2.17*	1.68	0.71	2.97*	4.28*	2.77*	1.73	2.06*	2.05*	0.71	4.99*
		Slope	0.04	0.07	0.07	0.03	0.02	0.06	0.07	0.03	0.04	0.04	0.07	0.01	0.05
	Tmin	Z	1.85	2.88*	3.10*	2.56*	3.04*	4.47*	4.99*	3.93*	2.71*	2.23*	1.93*	2.03*	5.26*
		Slope	0.08	0.09	0.11	0.06	0.04	0.05	0.05	0.04	0.04	0.05	0.04	0.07	0.07
	DTR	Z	-1.49	-0.91	-1.05	-1.33	-1.31	1.18	1.26	-0.67	0.31	-0.27	-0.18	-3.07*	-2.80*
		Slope	-0.03	-0.02	-0.03	-0.03	-0.02	0.01	0.01	0.00	0.00	0.00	-0.01	-0.06	-0.02
			Jan	**Feb**	**Mar**	**Apr**	**May**	**Jun**	**Jul**	**Aug**	**Sep**	**Oct**	**Nov**	**Dec**	**Annual**
	Tmax	Z	1.96*	3.14*	1.80	0.17	0.41	2.00	3.85*	3.78*	2.50*	1.45	1.42	0.92	4.25*
		Slope	0.04	0.06	0.05	0.00	0.01	0.03	0.04	0.04	0.04	0.03	0.04	0.01	0.04
	Tmin	Z	1.99	3.55	2.91	2.20	3.34	3.95	4.48	3.49	2.29	2.16	3.20	2.36	5.29*

Continued on next page

Table 4.2 – *Continued from previous page*

			Jan	**Feb**	**Mar**	**Apr**	**May**	**Jun**	**Jul**	**Aug**	**Sep**	**Oct**	**Nov**	**Dec**	**Annual**
Station 4		Slope	0.05	0.08	0.07	0.04	0.05	0.04	0.05	0.04	0.04	0.04	0.06	0.06	0.05
	DTR	Z	-0.84	-0.64	-0.92	-2.40	-2.07	-1.04	-1.25	0.36	-0.45	0.31	-1.53	-2.46	-2.43*
		Slope	-0.02	-0.01	-0.02	-0.04	-0.04	-0.02	-0.01	0.00	-0.01	0.01	-0.04	-0.05	-0.02
Station 5	Tmax	Z	1.20	0.00	-1.75	-1.14	1.56	0.94	-1.01	0.10	-1.88	0.00	1.53	2.40*	0.26
		Slope	0.06	0.00	-0.11	-0.08	0.06	0.03	-0.04	0.01	-0.06	0.00	0.06	0.12	0.00
	Tmin	Z	0.16	0.88	1.30	0.00	1.30	1.46	0.29	1.30	0.68	0.36	-0.42	1.04	0.23
		Slope	0.00	0.05	0.06	0.00	0.04	0.05	0.01	0.04	0.01	0.02	-0.02	0.06	0.01
	DTR	Z	0.55	-1.20	-2.05*	-1.01	0.32	0.00	-1.14	-1.23	-2.66*	-0.29	0.84	1.33	-0.36
		Slope	0.02	-0.05	-0.16	-0.07	0.02	0.00	-0.05	-0.04	-0.06	-0.02	0.05	0.10	-0.01

Table 4.3: Sen's slope (°C/yr) values of Tmax, Tmin and diurnal temperature range (DTR) for RCP2.6

		Jan	**Feb**	**Mar**	**Apr**	**May**	**Jun**	**Jul**	**Aug**	**Sep**	**Oct**	**Nov**	**Dec**	**Annual**
(a) Tmax	2011-2100	-0.003	0.001	0.003	0.003	0.002	-0.001	0.000	0.001	0.004	0.003	0.007	0.005	0.002
	2011-2040	-0.018	-0.005	0.007	-0.003	-0.002	-0.007	-0.003	0.000	0.003	0.007	-0.001	-0.001	0.000
	2041-2070	0.005	-0.001	0.005	0.007	-0.012	-0.007	0.005	0.001	-0.002	0.008	0.021	0.008	0.003
	2071-2100	0.008	0.004	0.016	0.003	-0.002	0.005	-0.001	0.006	-0.004	0.020	-0.007	0.004	0.005
(b) Tmin	2011-2100	-0.002	-0.001	0.004	0.005	0.003	0.001	0.000	0.001	0.003	0.001	0.007	0.005	0.002
	2011-2040	-0.011	-0.003	0.008	-0.017	0.001	0.000	0.000	0.003	0.006	-0.004	-0.014	-0.003	-0.002
	2041-2070	-0.003	-0.018	0.014	-0.001	-0.015	0.000	-0.002	0.002	-0.001	0.004	0.014	0.002	0.000
	2071-2100	0.009	-0.015	0.012	0.011	-0.004	0.002	0.000	0.003	-0.002	0.008	-0.003	-0.002	0.000
(c) DTR	2011-2100	0.000	0.002	-0.002	-0.002	-0.001	-0.001	0.001	-0.001	0.001	0.002	0.000	0.000	0.000
	2011-2040	-0.004	-0.001	0.003	0.010	-0.002	-0.009	-0.002	-0.002	-0.003	0.013	0.015	0.007	0.001
	2041-2070	0.011	0.021	-0.007	0.010	0.002	-0.005	0.006	-0.002	0.003	0.000	0.003	0.003	0.003
	2071-2100	-0.002	0.017	0.005	-0.006	0.003	0.006	0.003	0.001	-0.004	0.013	0.002	0.006	0.005

Table 4.4: Sen's slope (°C/yr) values of Tmax, Tmin and diurnal temperature range (DTR) for RCP6.0

		Jan	**Feb**	**Mar**	**Apr**	**May**	**Jun**	**Jul**	**Aug**	**Sep**	**Oct**	**Nov**	**Dec**	**Annual**
(a) Tmax	2011-2100	-0.004	0.003	0.003	0.006	0.003	-0.001	0.000	0.001	0.006	0.009	0.007	0.010	0.004
	2011-2040	-0.001	0.002	0.004	0.000	0.003	0.002	0.000	0.001	-0.003	0.002	0.003	0.020	0.001
	2041-2070	0.000	0.012	0.018	0.000	0.005	0.005	0.003	0.006	0.001	0.019	0.008	0.019	0.008
	2071-2100	0.006	0.004	0.007	0.016	0.004	0.000	0.003	0.006	0.000	0.021	0.013	0.008	0.007
(b) Tmin	2011-2100	0.000	0.007	0.008	0.012	0.003	0.001	0.000	0.002	0.005	0.005	0.010	0.011	0.005
	2011-2040	0.002	0.010	0.003	-0.005	-0.009	-0.002	-0.002	0.005	-0.001	0.001	0.002	0.026	0.001
	2041-2070	-0.006	0.020	0.012	0.003	0.003	0.000	-0.001	0.003	-0.001	0.010	0.012	0.015	0.006
	2071-2100	-0.004	0.002	0.009	0.034	0.002	0.001	-0.001	0.006	0.001	0.018	0.018	0.012	0.008
(c) DTR	2011-2100	-0.003	-0.004	-0.004	-0.006	-0.001	-0.001	0.001	-0.001	0.001	0.004	-0.002	-0.001	-0.001
	2011-2040	0.001	-0.009	-0.003	0.002	0.007	0.005	0.002	-0.004	-0.004	0.000	-0.004	-0.008	0.000
	2041-2070	0.007	0.000	-0.003	-0.020	0.002	-0.003	0.003	0.001	0.000	0.002	-0.002	-0.001	0.000
	2071-2100	0.004	-0.004	0.006	-0.006	0.000	0.005	0.002	0.003	0.003	0.002	-0.006	0.000	0.002

Similarly, the mean annual and mean monthly Tmin trend Z-statistics are shown in Figure 4.5 for all the RCP scenarios. The figure depicts the significant and non-significant changes in Tmin during the periods of 2011-2100, 2011-2040, 2041-2070 and 2071-2100 at monthly and annual scale. For RCP2.6 annual minimum temperature tends to increase significantly with a magnitude of 0.002°C/yr along with the months of March (0.004°C/yr), August (0.001°C/yr) and November (0.007°C/yr) as shown in Table 4.3(b). The moderate RCP scenario (RCP6.0) trends do not show significant increase at annual scale but the winter and the post monsoon months show significant increasing trend with a highest magnitude in the month of April (0.012°C/yr) to minimum 0.002°C/yr in the month of August (Table 4.4b). For the extreme emission scenario (RCP8.5) although, no significant trend found in long term duration (2011-2100) but Tmin likely to increase significantly during 2041-2070 with a magnitude of 0.013°C/yr (Table 4.5b). The DTR is defined as the difference between the maximum and minimum temperature in a day. The analysis of DTR shows a significant decreasing trend with the magnitude of 0.001°C/yr in diurnal variation at annual temperature scale for RCP6.0 whereas for the RCP2.6 and RCP8.5, trends are not significant at 95% confidence interval . The corresponding magnitude of increasing and decreasing trend of DTR can be seen in the Tables 4.3(c), 4.4(c) and 4.5(c). For the time period of 2040-2070 and 2071-2100, an increasing trend was observed in DTR with a magnitude of 0.003°C/yr and 0.005°C/yr respectively for RCP2.6.

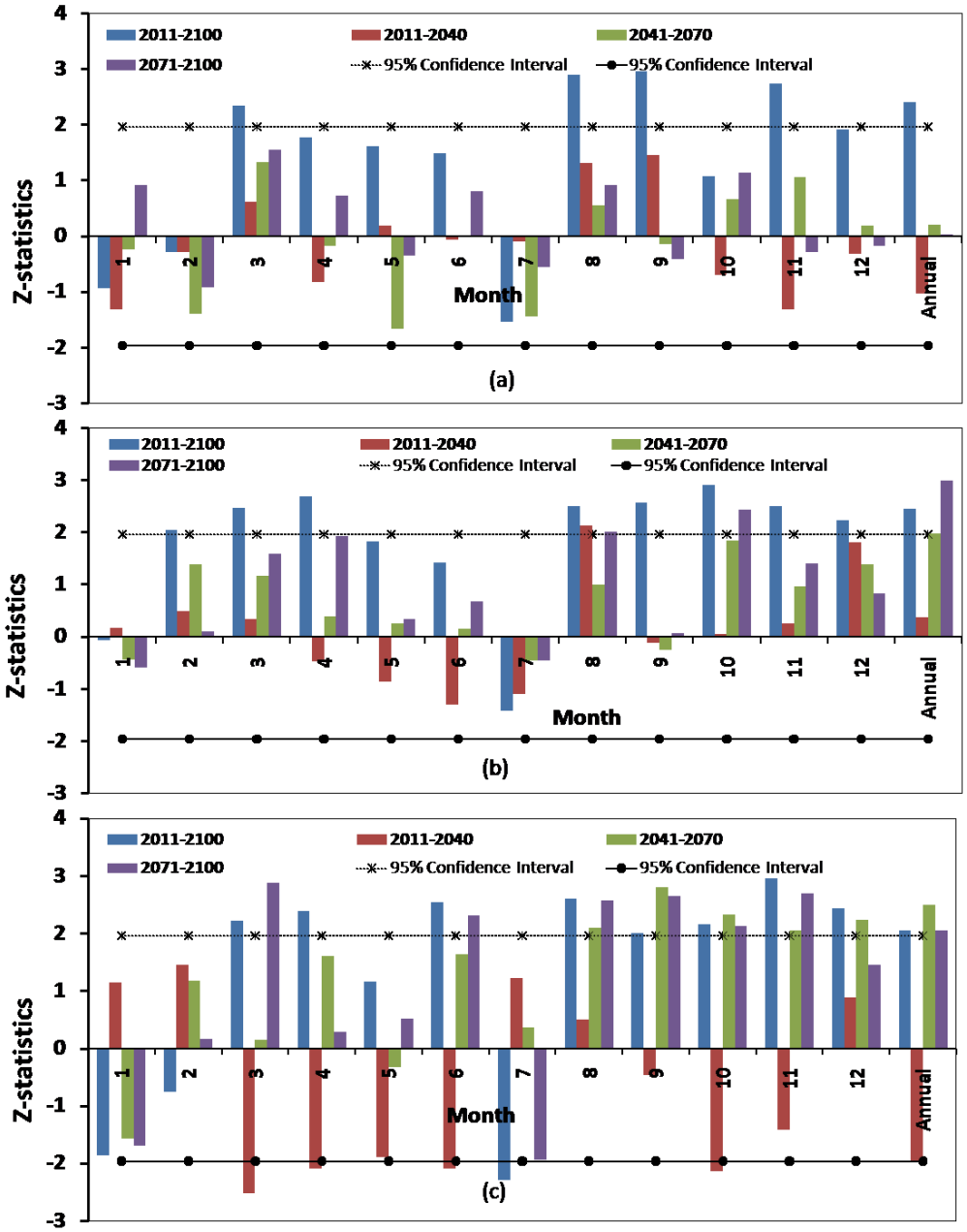

Figure 4.5: Mann-Kendall test Z- statistics showing significant and non-significant trend of minimum temperature for (a) RCP2.6 (b) RCP6.0 and (c) RCP8.5

Table 4.5: Sen's slope (°C/yr) values of Tmax, Tmin and diurnal temperature range (DTR) for RCP8.5

		Jan	**Feb**	**Mar**	**Apr**	**May**	**Jun**	**Jul**	**Aug**	**Sep**	**Oct**	**Nov**	**Dec**	**Annual**
(a) Tmax	2011-2100	-0.005	0.002	0.008	0.005	0.003	0.000	0.000	-0.003	0.004	0.019	0.013	0.007	0.004
	2011-2040	0.021	0.001	-0.015	-0.015	-0.049	-0.001	0.003	0.005	0.045	-0.043	-0.023	-0.014	-0.005
	2041-2070	-0.010	0.005	-0.004	0.015	-0.003	-0.008	0.002	-0.005	0.012	0.030	0.028	0.016	0.005
	2071-2100	-0.012	0.014	0.025	0.007	-0.004	0.012	-0.002	0.001	0.011	0.036	0.025	0.018	0.012
(b) Tmin	2011-2100	-0.003	-0.002	0.007	0.010	0.003	0.003	-0.003	0.001	0.007	0.014	0.018	0.006	0.005
	2011-2040	0.012	0.019	-0.026	-0.027	-0.031	-0.011	0.003	0.002	-0.002	-0.034	-0.038	0.012	-0.008
	2041-2070	-0.013	0.019	0.002	0.026	-0.002	0.003	0.001	0.006	0.017	0.019	0.031	0.026	0.013
	2071-2100	-0.014	0.003	0.032	0.003	0.005	0.008	-0.003	0.006	0.018	0.020	0.037	0.017	0.012
(c) DTR	2011-2100	-0.002	0.004	0.001	-0.005	-0.001	-0.002	0.003	-0.004	-0.006	0.005	-0.004	0.000	0.000
	2011-2040	0.001	-0.015	0.011	0.022	-0.006	0.010	-0.005	0.009	0.047	-0.015	0.017	-0.023	0.004
	2041-2070	-0.001	-0.016	-0.010	-0.014	-0.002	-0.010	0.000	-0.010	-0.005	0.010	-0.002	-0.016	-0.006
	2071-2100	-0.001	0.011	-0.008	0.004	-0.006	0.007	0.003	-0.005	-0.002	0.019	-0.009	-0.004	0.000

The results of the downscaled temperature series for the 21st century indicate increase in temperature over the Subansiri basin for proposed low, moderate and extreme RCP emission scenarios. These results are in agreement with the IPCC report (IPCC, 2014) which reports an increase in temperature because of increased radiative forcing and anthropogenic activity. Sonali and Kumar (2013) conducted a trend analysis study on historical temperature series of 1901-2003 for the all climate zones of India and reported an increase in the maximum and minimum temperature for all the zones. Easterling et al. (1997) in their study on the maximum and minimum temperature trend worldwide reported a significant decrease in diurnal variation of the temperature because increase in maximum temperature is comparatively lower than increase in minimum temperature. Shrestha et al. (1999) studied the temperature trends for the Himalayan range and revealed an increasing trend for most of the part of Nepal and major Himalayan region.

4.8 Precipitation downscaling and projection

After selecting the predictors, downscaling model was prepared using linear regression with conditional sub-model; conditional sub-model implicates separate parameterization for dry days and wet days from the series of precipitation (Wilby et al., 2002). RMSE, R^2 and NSE value for the calibration and validation period are shown in Table 4.6 and graph plot of observed and model generated precipitation is shown in Figure 4.6. As shown in Table 4.6, R^2 vary from 0.76 to 0.81 in calibration period whereas in validation period it ranges from 0.78 to 0.88 for different stations. NSE found to be ranging from 0.78 to 0.88 during calibration and 0.74 to 0.83 in validation. Figure 4.7 represents the comparison of observed annual precipitation and precipitation series of

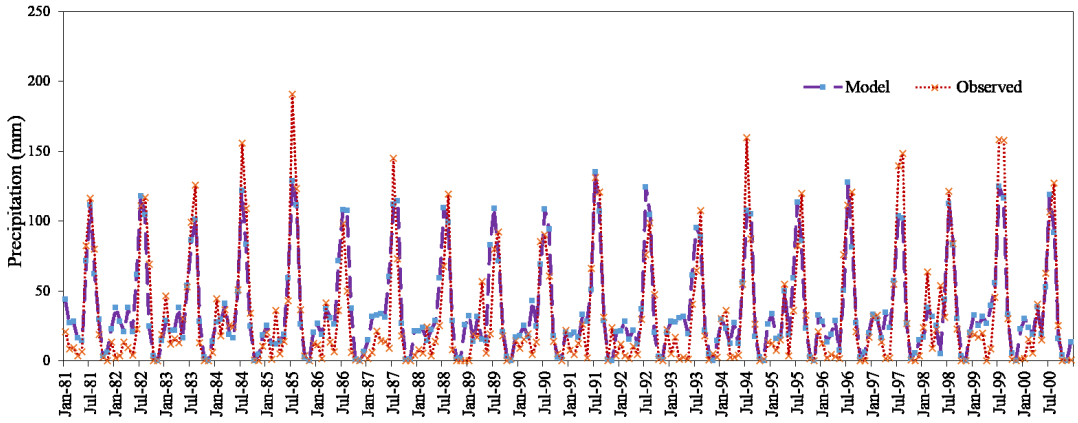

Figure 4.6: Calibration (1980-1995) and validation (1996-2000) result of the precipitation downscaling model for Subansiri river basin

Table 4.6: Calibration and validation results of precipitation downscaling model for all sub-basins

	Station 1		**Station 2**		**Station 3**		**Station 4**		**Station 5**	
	Cal	Val	Cal	Val	Cal	Val	Cal	Val	Cal	Val
RMSE	35.50	36.54	31.10	37.21	29.54	34.43	31.23	35.84	27.13	31.97
R^2	0.81	0.79	0.83	0.79	0.85	0.81	0.83	0.80	0.76	0.74
NSE	0.80	0.78	0.82	0.78	0.88	0.83	0.81	0.79	0.78	0.74

RCP scenarios for 2011-2100.

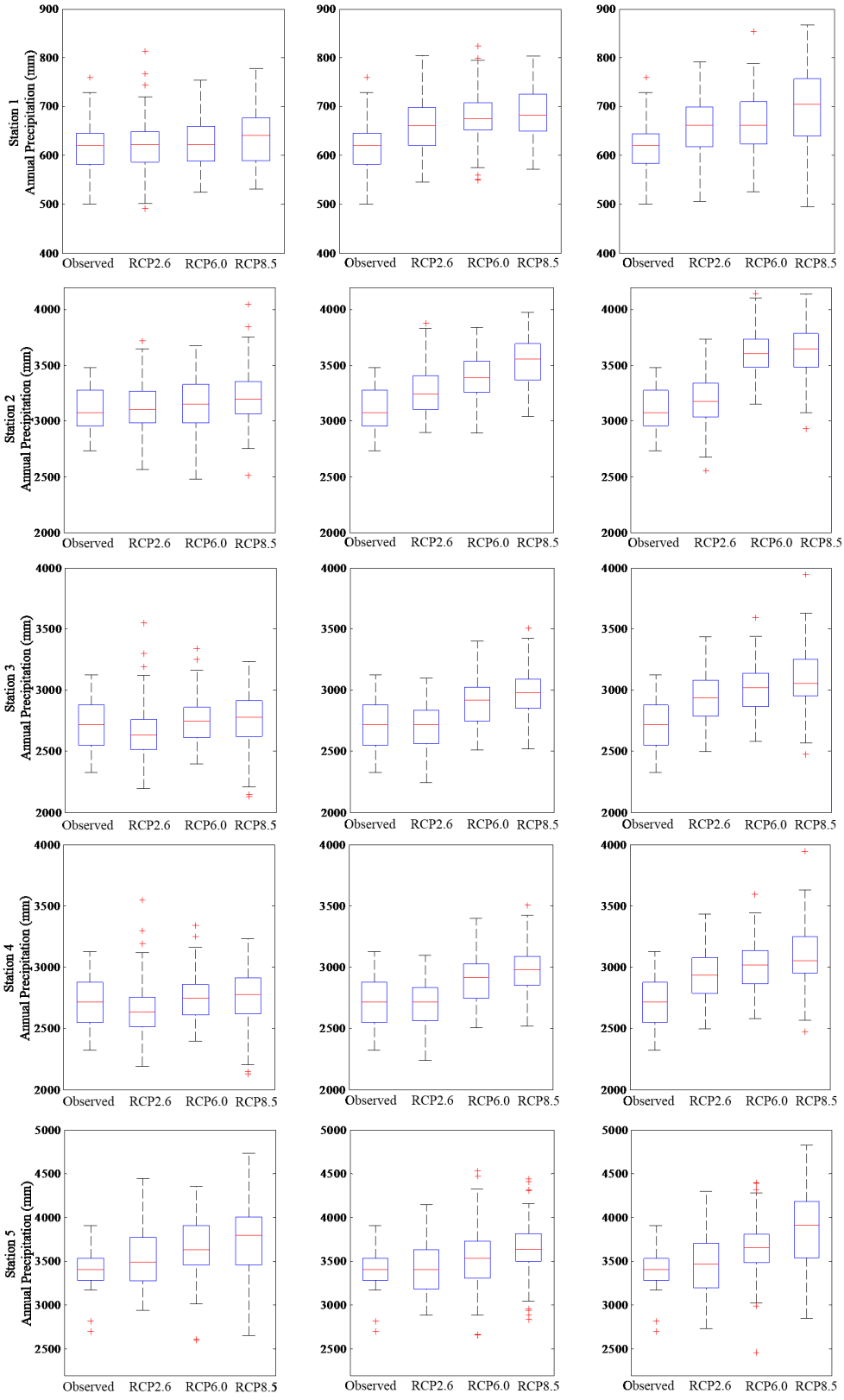

Figure 4.7: Box-plots of the precipitation anomalies for GCM/RCPs over the stations for the period of 2011-2100 compared to controlled scenario GCM run

Figure 4.7(a) shows changes in precipitation over station 1, results shows increase in annual precipitation for all the RCP scenarios with variation in magnitude with GCM. Average of all three GCM shows increase of 4.39% for RCP2.6, 5.17%, 5.88% and 8.86% respectively for RCP4.5, RCP6.0 and RCP8.5. Figure 4.7(b) shows the precipitation in for station 2 and average of three GCM indicates increase of 3.21%, 7.65%, 9.07% and 11.83% respectively for RCP2.6, RCP6.0 and RCP8.5. Similarly Figure 4.7(c), 4.7(d) and 4.7(e) represent annual precipitation for RCP scenario with their respective GCM. Increase in precipitation over station 3 is calculated to be 2.19%, 5.72%, 6.74% and 8.64% respectively for the increasing order of RCP scenarios. In station 4 increments for RCP2.6 to RCP8.5 is calculated to be 4.35%, 3.45%, 4.09% and 8.11% respectively. Changes in annual precipitation over station 5 found to be positive with 2.13%, 5.80%, 6.07% and 10.37% for RCPs. It can be concluded from Figure 4.7 that the changes in precipitation across the basin is positive with magnitude increasing from low RCP scenario to high RCP scenario.

4.9 Extreme precipitation indices

4.9.1 Precipitation indices analysis of the historical data

Precipitation extreme indices are important parameters to analyse the precipitation distribution in a region. In this study several precipitation indices were calculated such as PRCPTOT (total annual precipitation), CDD (consecutive dry days), CWD (consecutive wet days), R1mm (number of rainy days in a year when precipitation is more than 1 mm), R10mm (heavy precipitation days precipitation more that 10mm), R20mm (very heavy precipitation days), SDII (simple daily intensity index), R95p (wet days) and R95p (extremely wet days).

Trend analysis of historical data period gives an insight of existing pattern of the changing climate and also proves helpful for comparing the future changes. Figure 4.8 shows the z-statistics of indices for different stations and their respective Sen's slope magnitude are shown in Table 4.7. From the Figure 4.8 it is clear that station 4 shows significant increasing trend for CWD, PRCPTOT, R10mm, R20mm, R95p and SDII, magnitude of increase of these indices are shown in Table 4.7.

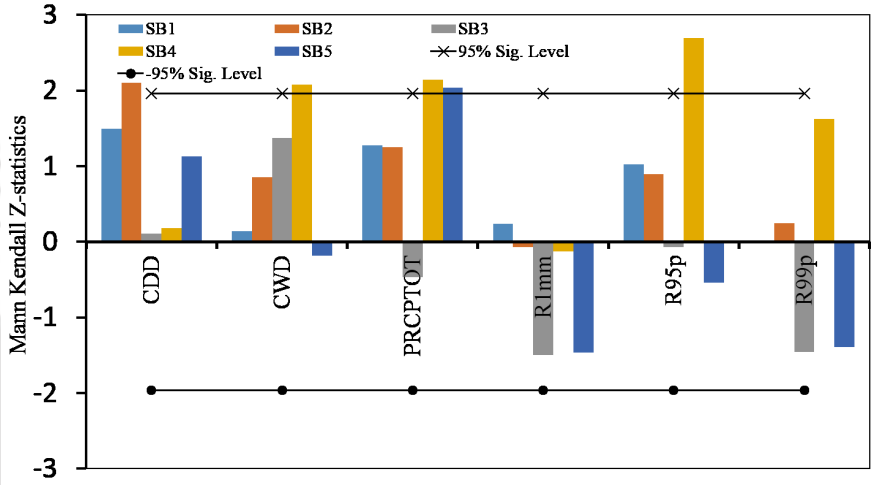

Figure 4.8: Mann-Kendall test Z-statistics of precipitation indices during historical period (1980-2000) over sub basins

No significant trend was observed at any station except station 4. Indices showing increasing or decreasing trend are not statistically significant at 95% confidence level. Average of the increase in annual precipitation of all station s shows increase of 3.63 mm/year which is not very much significant for basin, whereas contribution of very wet days (R95p) is likely to increase. Increasing trend of R95p shows that this increase can create a situation of frequent flood events. Average of all stations annual precipitation gives an idea about the change in precipitation over the basin. Figure 4.9(a) represents the significant and non-significant trends in annual precipitation over the entire basin. Although on 30 year time scale, some decreasing trend was found but it is statistically

Table 4.7: Magnitude of change in precipitation indices during historical period (1980-2000)

Indices	Station 1	Station 2	Station 3	Station 4	Station 5
CDD	0.65	1.00	0.00	0.05	0.03
CWD	0.04	0.17	0.29	0.50	0.00
PRCPTOT	3.20	0.42	-3.13	17.57	0.09
R1mm	0.06	-0.92	-1.45	-0.25	-0.06
R10mm	0.21	-0.44	0.00	1.42	0.05
R20mm	0.05	-0.27	0.30	1.18	0.02
R95p	1.33	0.20	-2.76	18.30	-0.03
R99p	0.00	1.52	0.00	0.00	-0.04
SDII	0.03	0.00	0.05	0.20	0.07

non-significant at 95% confidence level. Significant increasing trend were observed for CM3-RCP2.6, CM3-RCP6.0 and CM3-RCP8.5 for different time periods.

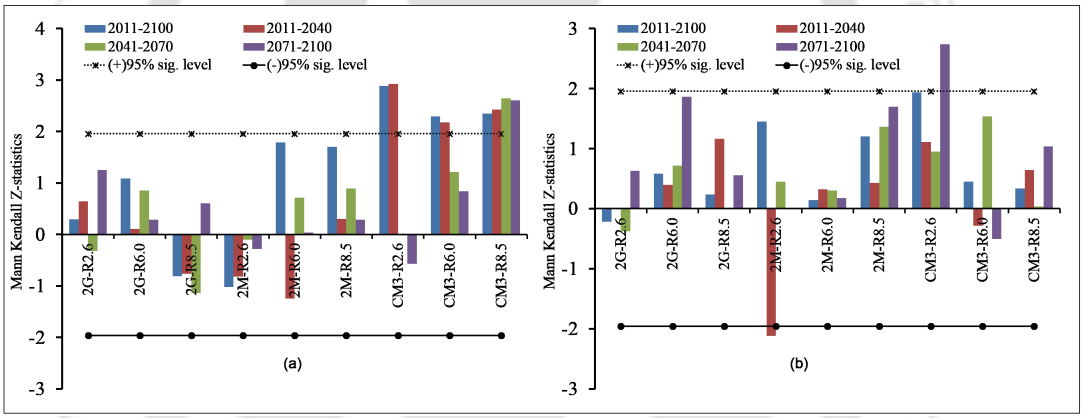

Figure 4.9: Mann-Kendall test Z-statistics of (a) Annual precipitation (b) CDD

Magnitude of change in annual precipitation for different GCM RCPs are shown in Table 4.8 for long-term period of 2011-2100 and three timescale of 30 years i.e. 2011-2040, 2041-2070, 2071-2100. Maximum positive change found at station 5 for the time period during 2041-2070 with magnitude of 138 mm/decade. Average annual precipitation for the entire basin shows increasing trend for all the RCP scenarios with magnitude of 2.31 mm to 31.51 mm/decade.

Table 4.8: Magnitude of change (mm/ decade) in annual precipitation for different GCMs RCP scenarios

			ESM2G			ESM2M			CM3	
		RCP2.6	**RCP6.0**	**RCP8.5**	**RCP2.6**	**RCP6.0**	**RCP8.5**	**RCP2.6**	**RCP6.0**	**RCP8.5**
Station 1	**2011-2100**	0.67	2.75	-2.00	-2.78	3.72	7.67	10.34	13.46	23.28
	2011-2040	5.00	1.10	-8.85	-12.21	-9.86	4.91	39.15	20.93	29.14
	2041-2070	-2.43	13.39	-11.62	-3.13	7.50	13.32	-1.40	15.65	31.33
	2071-2100	16.38	2.30	10.37	-6.00	1.57	5.33	-8.18	12.71	30.55
Station 2	**2011-2100**	3.61	18.24	26.70	-5.42	9.59	22.15	12.64	23.27	38.98
	2011-2040	54.19	80.64	-65.00	89.21	-51.71	-63.58	108.78	-5.00	-7.32
	2041-2070	78.11	-47.25	27.28	-15.29	-4.47	54.00	8.20	-17.38	104.36
	2071-2100	-113.87	-64.45	27.50	-12.06	-2.91	21.06	71.19	-16.52	9.33
Station 3	**2011-2100**	0.68	0.73	1.14	0.53	0.97	2.53	5.57	5.82	8.01
	2011-2040	0.86	-18.00	1.78	10.86	-3.50	0.69	15.44	-1.91	7.95
	2041-2070	6.80	13.82	12.40	1.45	9.00	7.80	-0.20	-2.35	9.38
	2071-2100	-10.14	5.26	-8.55	-2.67	-6.24	-1.00	-3.11	9.76	11.67
Station 4	**2011-2100**	5.00	23.47	34.67	-4.93	11.58	11.53	-13.66	30.00	64.05
	2011-2040	36.64	57.54	-151.55	30.20	-39.36	29.00	25.96	95.00	51.13
	2041-2070	-10.64	67.64	-18.70	-48.50	66.06	-15.33	29.94	-30.36	132.20
	2071-2100	-71.17	11.60	2.85	-12.62	-45.20	-14.55	-62.25	24.90	-24.54
Station 5	**2011-2100**	-1.38	23.96	54.72	-9.28	17.77	48.90	40.84	68.43	129.48
	2011-2040	123.94	80.90	-68.03	76.79	-71.82	-94.57	100.50	-4.40	92.75
	2041-2070	-0.04	29.00	-35.67	-95.87	138.00	14.00	92.12	57.81	88.08
	2071-2100	-196.38	67.60	66.00	13.71	-116.25	23.50	3.10	134.47	6.37

4.9.2 Trend in precipitation indices

Figure 4.9(b), 4.10(a) and 4.10(b) represents the Mann-Kendall z-statistics of consecutive dry days (CDD), consecutive wet days (CWD), and number of rainy days (R1mm) over the basin for different GCM RCP scenario during different time periods. Consecutive dry days index represent the longest spell of days without any precipitation (>1mm) events. For the long-term period (2011-2100) no significant trend is observed over the basin whereas 30 years' time series (2011-2040, 2041-2070 and 2071-2100) analysis indicates significant increasing trend for 2071-2100 in model CM3 RCP2.6 as shown in Figure 4.9(b). Maximum change in CDD was found to be positive with 8.46 days/decade in station 1 for CM3 RCP2.6 scenario during period of 2071-2100, likewise maximum decreasing trend of CDD observed in station 3 with magnitude 4.35 days/decade for RCP2.6 scenario. Average of three GCMs for RCP scenarios shows an increase of 3.46 day/decade in station 1 and in other station magnitude of increase is not very significant.

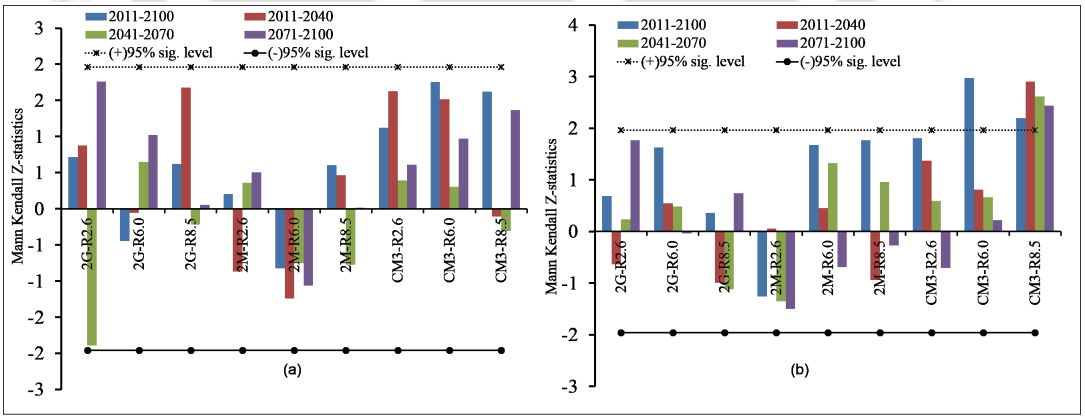

Figure 4.10: Mann-Kendall test Z-statistics of (a) CWD and (b) number of rainy days (R1mm)

Z-statistics of CWD trends show no significant increase over the period of 2011-2100 as shown in Figure 4.10(a). Maximum positive trend in CWD was observed

in station 1 with magnitude of 3.81 days/decade for period of 2011-2040 under CM3 RCP2.6 scenario. Average of GCM values for respective RCPs shows no large magnitude increase or decrease in CWD. Figure 4.10(b) shows z-statistics for number of rainy days and from the figure it is evident that the trend is significantly increasing for CM3 RCP8.5. Magnitude of change in number of rainy days per decade over the stations and average of the three GCMs indicates increase of 5.46 days/decade for RCP8.5.

4.9.3 Trend in the intensity of precipitation

Number of heavy precipitation days (R10mm) is the number of days with precipitation more than 10 mm whereas number of very heavy precipitation days (R20mm) defined as number of days with precipitation more than 20mm. Z-statistics of R10mm shows increasing trend over the basin for CM3 RCP4.5 and CM3 RCP 8.5 for different time scales as shown in Figure 4.11(a). Z-statistics of SDII trend analysis is shown in Figure

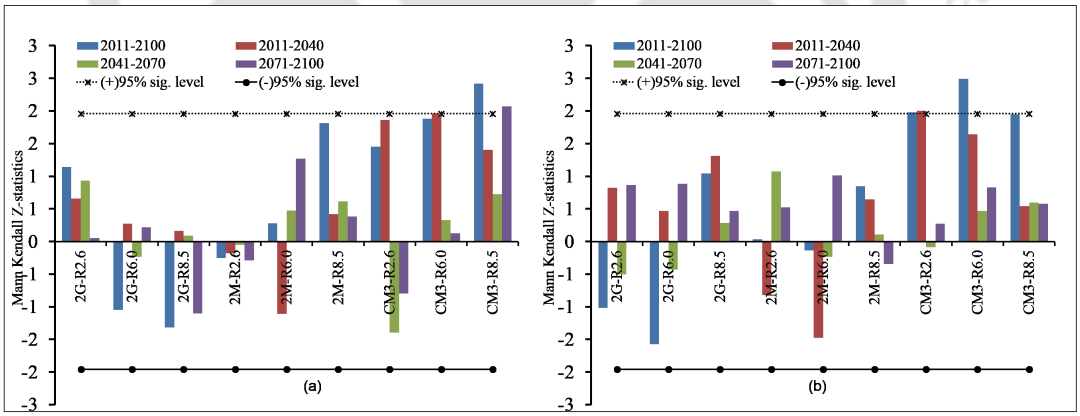

Figure 4.11: Mann-Kendall test Z-statistics of (a) R10mm (b) SDII

4.11(b) which shows significant increasing trend for CM3 RCP6.0. Magnitude of change in R95p for five stations shows maximum increase of 97mm/decade at station 4 for CM3 RCP6.0 whereas maximum decrease observed at station 5 for ESM2G R2.6 during period of 2071-2100 with a magnitude of 133.35 mm/decade. Very wet days precipitation

(R95p) are the sum of the precipitation of days when precipitation was more than 95th percentile of the wet day precipitation distribution derived over base period and extremely wet days precipitation (R99p) defined as amount of precipitation received from the days when precipitation was more than 99th percentile of the wet day precipitation derived over the base period. These two indices provide an idea of the contribution of very wet days and extremely wet days precipitation to the annual precipitation. Figure 4.12(a) represents Z-statistics of R95p and it shows significant increasing trend for CM3 RCP8.5 over the period of 2011-2100, 2011-2040 and 2041-2070. In case of R99p significant increasing trend observed for long-term period of 2011-2100 for CM3 RCP6.0 and over the period of 2011-2100, 2011-2040 and 2041-2070 as shown in Figure 4.12(b). Similarly Sen's slope analysis results of R99p for long-term (2011-2100) duration shows no significant change but maximum magnitude of decrease observed as 46 mm/decade at station 2 during 2011-2040 followed by maximum increase of 46.91 mm/decade for extreme scenario (RCP8.5) over station 5 at the end of the century (2071-2100).

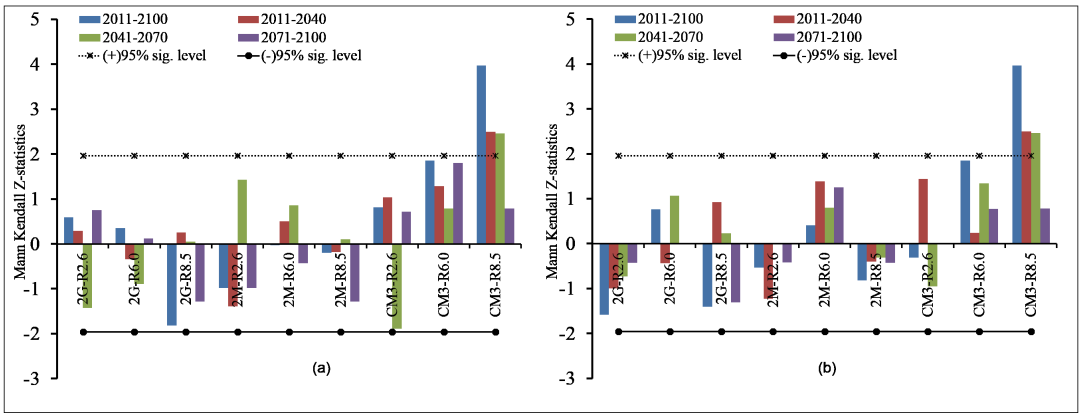

Figure 4.12: Mann-Kendall test Z-statistics of (a) R95p (b) R99p

4.9.4 Spatio-temporal distribution of Precipitation indices

Precipitation varies drastically on spatial as well as on the temporal scale (Nel, 2009; Parthasarathy et al., 1995), which necessitate to analyze this variable on the spatial and different time scale domain. this section analyzes the spatio-temporal variation within the Subansiri river basin for different timescale i.e. 2011-2100, 2011-2040, 2041-2070 and 2071-2100. Spatial and temporal distribution of indices PRCPTOT, R1mm, SDII for historical period (Figure 4.13) and average of the three GCMs for RCP scenarios at different time scale are shown in Figure 4.14 , 4.15 and 4.16. Figure 4.13 shows the spatial distribution of annual precipitation, number of rainy days in a year and daily intensity of precipitation for observed time period (1980-2000). It is observed from the

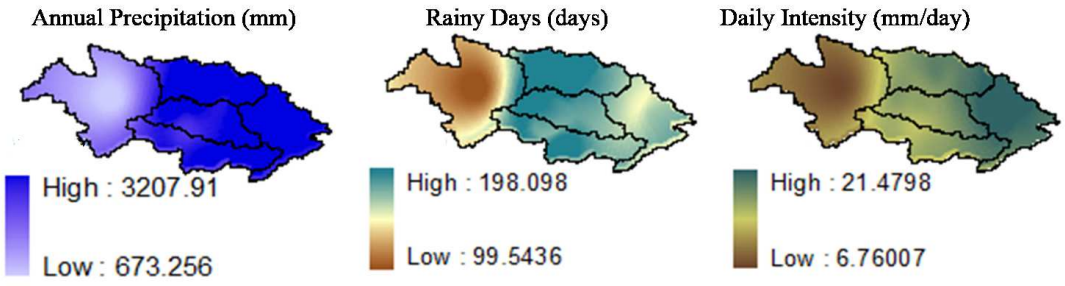

Figure 4.13: Spatio-temporal distribution of precipitation indices observed period (1980-2000) annual precipitation (mm), rainy days (days/yr) and intensity of precipitation (mm/day)

historical data analysis of the precipitation that annual precipitation in basin ranges from 673.25 mm to 3207.91 mm, whereas number of rainy days in a year varies from 99 days to 198 days and daily intensity of the precipitation varies from 6.7 mm/day to 21.47 mm/day, spatial distribution of these indices are shown in Figure 4.13. Upper part of the basin comes under the Tibet region which receives lesser rainfall as compared to the lower part of the basin. 4.14 shows the spatial distribution of annual precipitation at four different time domain i.e. for the long term period of 2011-2100 and three inter-

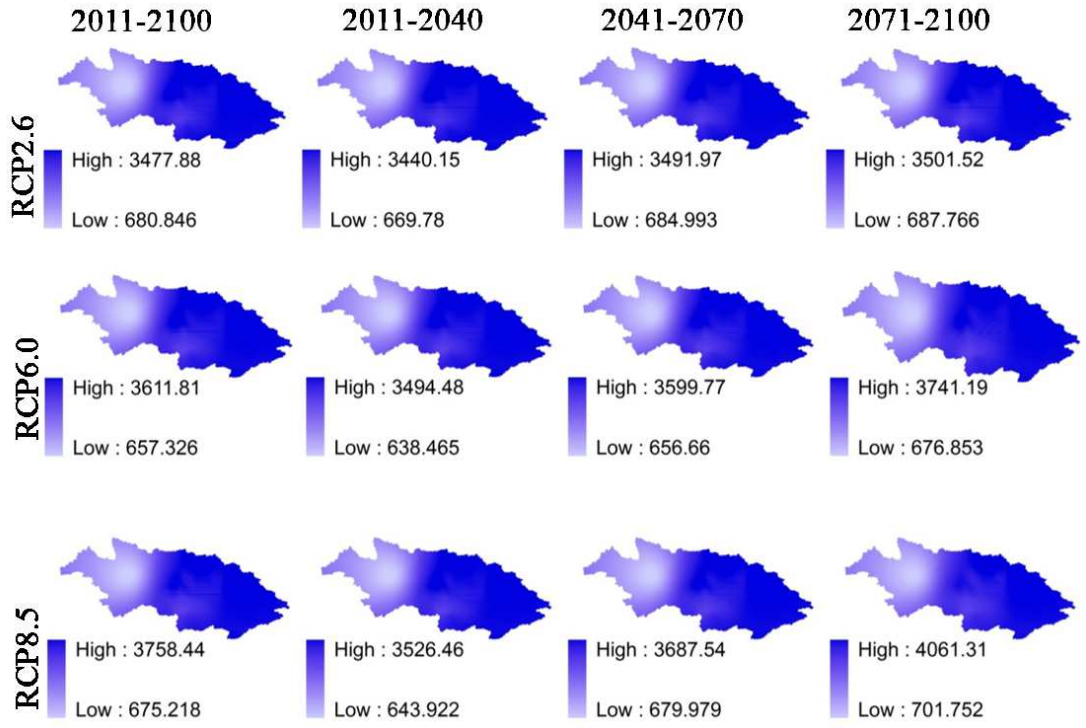

Figure 4.14: Spatio-temporal variation of annual precipitation (mm/yr) over the basin for RCP scenarios

decadal time scale of 2011-2040, 2041-2070 and 2071-2100 for three RCP scenarios. Comparison of the historical values of annual precipitation and projected precipitation spatio-temporal plot it is evident that the amount of annual precipitation increasing at different time scale and also on long-term duration of 2011-2100 over entire basin for the RCP scenarios. Figure 4.15 represents spatial variation of number of rainy days over the basin for different timescale and RCP scenarios. R1mm is likely to decrease when compared to historical period values, as during historical period R1mm ranges from minimum 99 days to maximum of 198 days but in future RCP scenarios R1mm reflects decreasing trend in lower part whereas increasing in the upper station i.e. station 1. For the long term period of 2011-2100 R1mm shows the values upto 113 days in the upper portion and in the lower portion of the basin it reduces to 188 days. Although the magnitude at different inter-decadal timescale varies but a uniform increment in R1mm

is observed for the upper portion followed with the decrease in the lower portion.

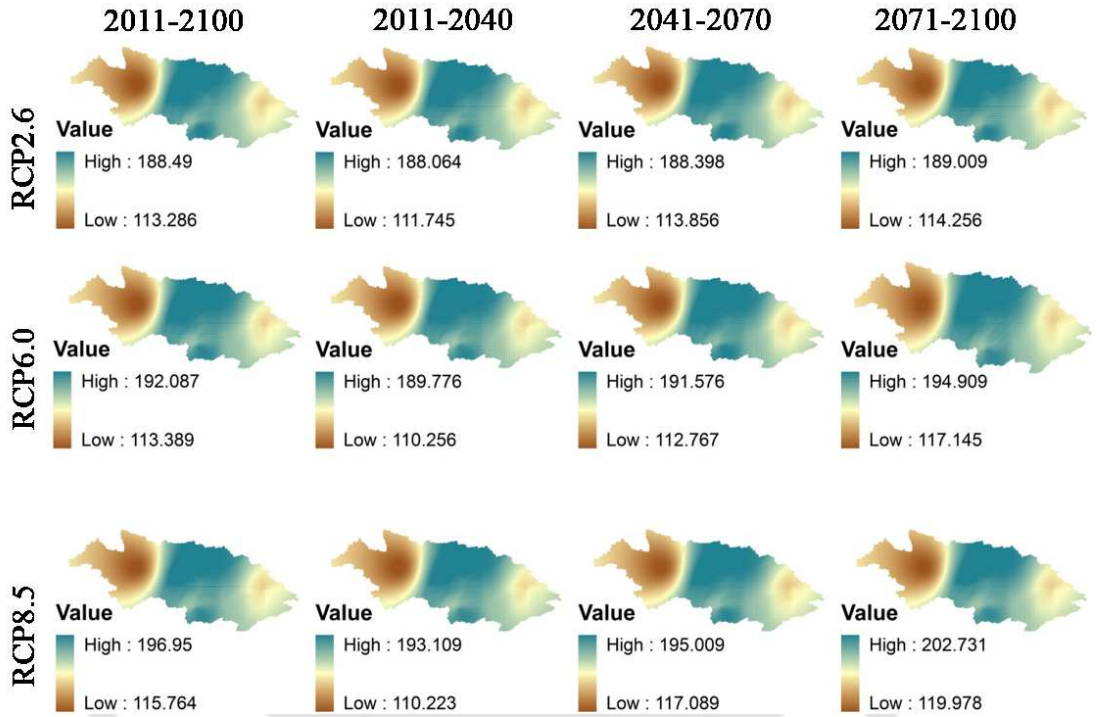

Figure 4.15: Spatio-temporal distribution of number of rainy days (R1mm) over the basin for RCP scenarios.

Figure 4.16 depicts the increase in daily precipitation intensity index for RCP scenarios over stations except the station 1. Decrease in SDII over station 1 is followed by the increase of number of rainy days as shown in Figure 4.16 whereas station 2, station 3, station 4 and station 5 where number of rainy days is likely to decrease are prone to increase in daily rainfall intensity. Variation of daily intensity for RCPs over inter decadal periods are shown in Figure 4.16.

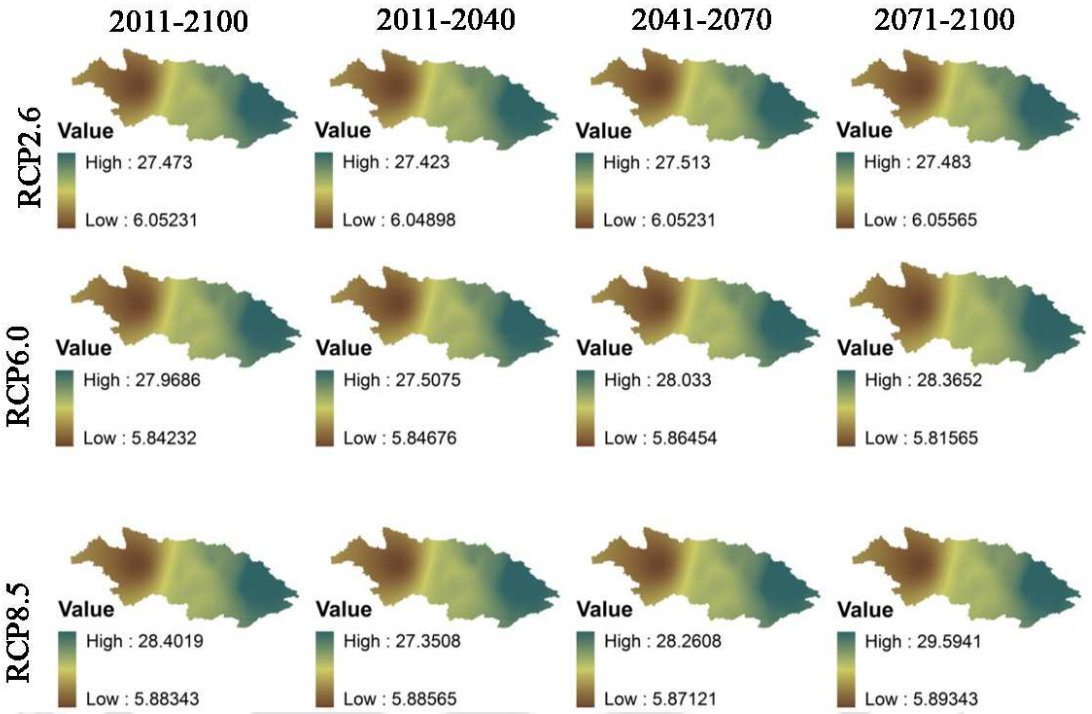

Figure 4.16: Spatio-temporal distribution of simple daily intensity index (mm/day) over the basin for RCP scenarios.

4.10 Uncertainty analysis of GCM projections

Uncertainty associated with the climate change studies on a regional and spatial scale need to be addressed for the projections and better assessment of the change in hydro-climatic variables. In climate change impact studies, uncertainty in impact assessment occurs because of the different sources such as inter-model variability, uncertainty due to downscaling methods adopted and scenario uncertainty. GCM uncertainty involves because of the procedure adopted for the simulation of the GCM for different grid resolutions and using different geophysical processes, scenario uncertainties are inevitable because of the inaccuracy in the processes for prediction of the possible changes in greenhouse gas emission, socio-economic changes etc.

In present study, statistical downscaling is performed with SDSM, since the downscaling

model performance was satisfactory for the precipitation and temperature data series in the calibration and validation process, no other method of downscaling was adopted. Downscaling model prepared with establishing the regression relation between the observed data and NCEP predictors. Downscaling model were further used to simulate the precipitation from the GCM run for historical period as well as for the projection of the precipitation and temperature series over the 21 century time domain for the three RCP scenarios i.e. RCP2.6, RCP6.0 and RCP8.5 using three GCMs namely ESM2G, ESM2M and GFDL-CM3. GCM projection uncertainty has been addressed with the cumulative distribution function (CDF) plots of the historical model run and the projected data series.

Figure 4.17 shows a boxplot of the monthly observed precipitation, the monthly model generated precipitation data series and monthly precipitation series generated from historical run of GCM data. Station-wise results of the precipitation downscaling model on monthly basis show good agreement with the observed precipitation but a comparison of the annual precipitation of observed data and model generated data shows that model overestimates the annual precipitation whereas the historical run GCM precipitation data shows an almost similar pattern to that of the model generated data.

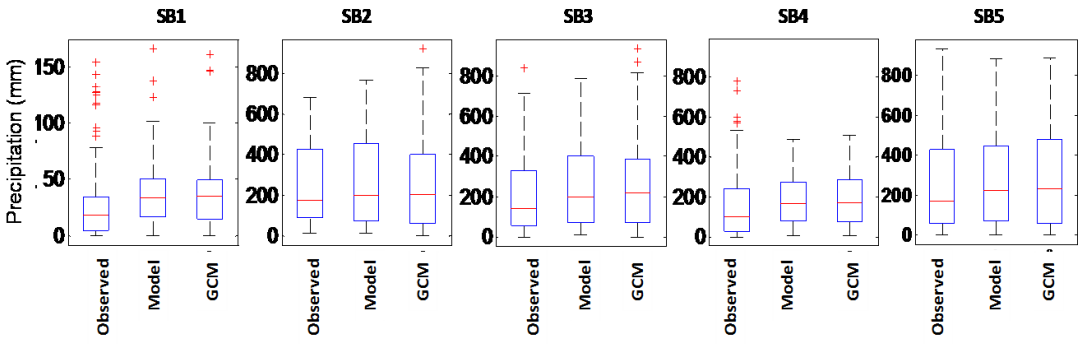

Figure 4.17: Boxplot of the precipitation data series from observed, NCEP and GCM historical run to compare variation.

Figure 4.18 shows the cdf plot of the observed precipitation, NCEP simulated precipitation series and precipitation simulated from GCM datasets of historical run for all the five stations. It shows that the variation in the NCEP and GCM simulated precipitation series captures the observed precipitation very well and there is very less uncertainty involve in the model generated precipitation. For station 1 (SB1) and station 4 (SB4) NCEP simulated precipitation underestimate the lower values of precipitation whereas for station 3 (SB3) GCM simulated precipitation underestimating the precipitation. Results of the CDF plots for the historical simulation period shows the less variation in the simulation of precipitation from both the datasets i.e. NCEP and GCM datasets and captures the trends well. This implicates that the GCM projection will have the lesser uncertainty in the future simulation of the precipitation, which could be analysed by the CDF plots of the precipitation indices for projected timeseries i.e. from 2011-2100. Previous studies on the SDSM efficiency for simulating the precipitation patterns have been explained (Khan et al. 2006, Samadi et al. 2013).

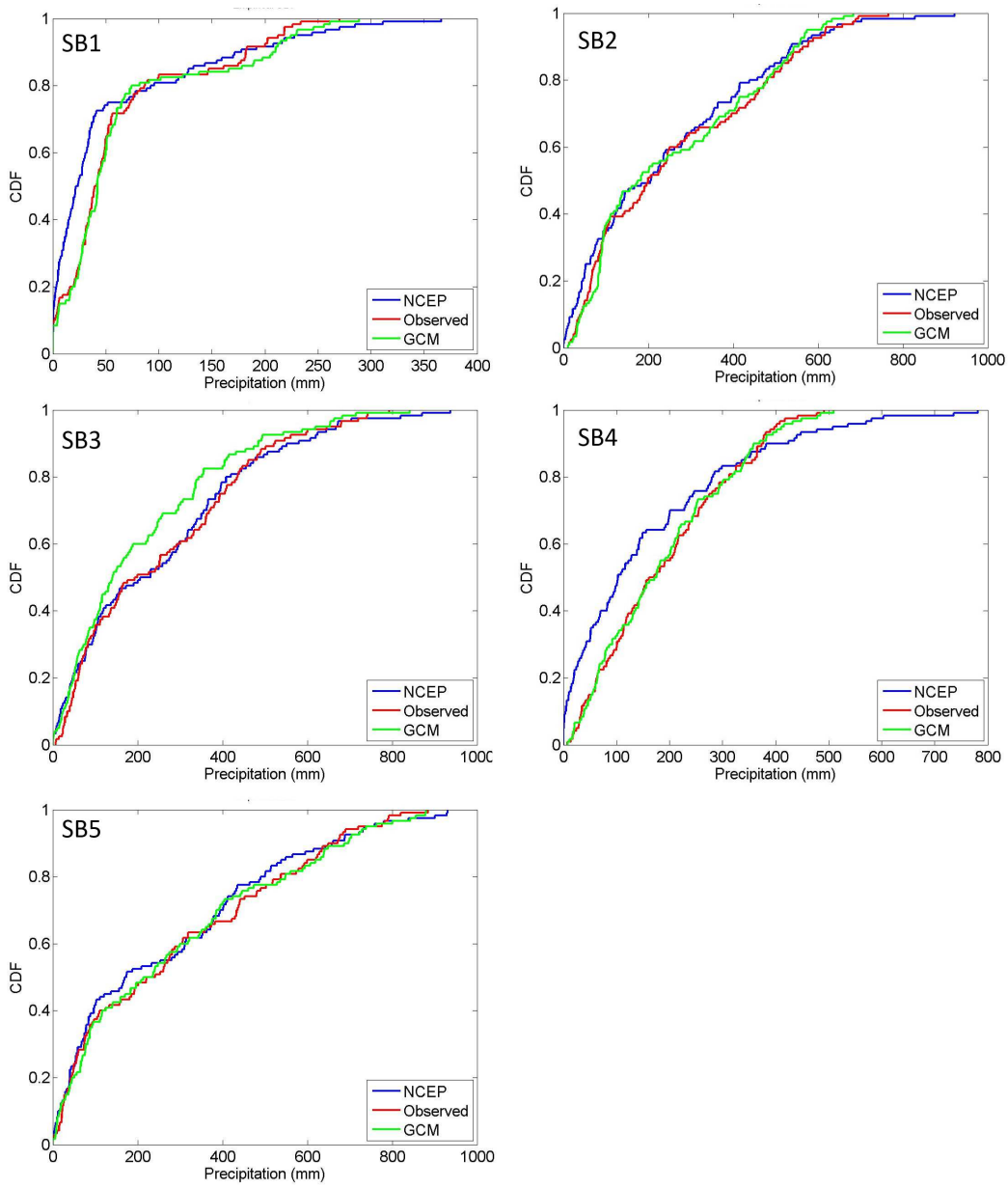

Figure 4.18: CDF plot of the observed precipitation and simulated precipitation from NCEP and GCM datasets for all the stations.

Precipitation indices time series provide a good insight of the distribution of the precipitation in a given time period and this could help in identifying the uncertainties in case of multi GCM model projections of the precipitation in climate change studies. Precipitation indices such as annual precipitation, simple daily precipitation intensity index (SDII), dry days spells (CDD) and wet days spells (CWD) were analyzed for

the projected precipitation time series with their CDF plots for the respective RCP scenarios with the three GCMs.

Fig 4.19 a shows the average annual precipitation for the observed period and projected period precipitation data series for station 5 (SB5) with three GCM i.e. ESM2G, ESM2M and CM3 and their respective RCP scenarios R2.6, R6.0 and R8.5. It is clear from the Fig 4.19 a that the variation amongst the GCMs for annual precipitation projection is very less and it represents almost the similar scenario for all the ensembles. Similarly Fig 4.19 b shows the CDF plots of simple daily intensity index for the observed period along with the projected precipitation series.

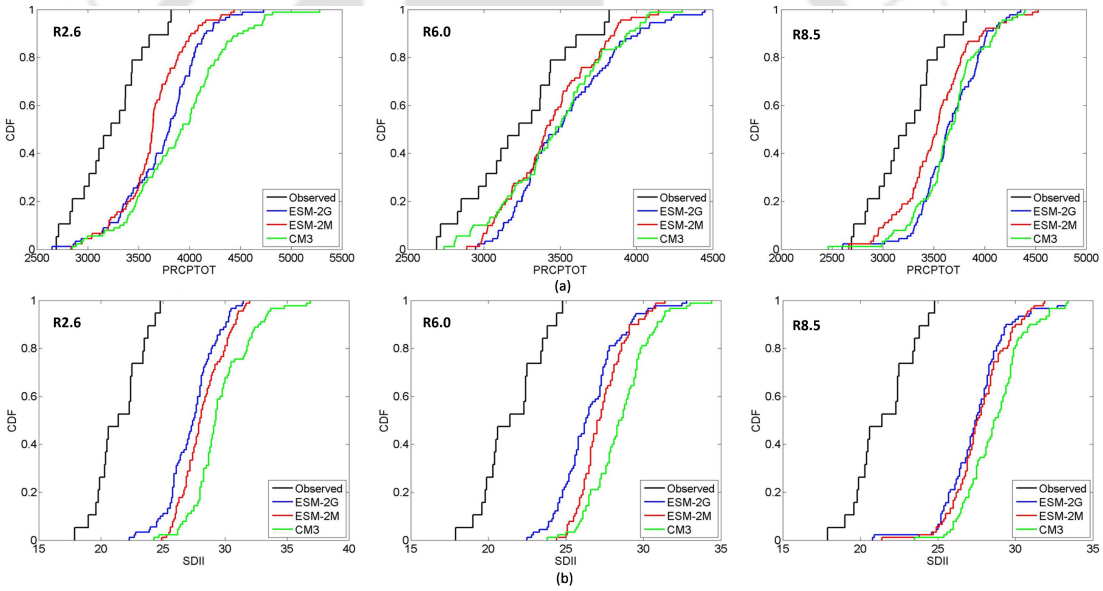

Figure 4.19: CDF plot of (a) annual precipitation and (b) simple daily intensity index (SDII) of observed precipitation and projected precipitation for three RCP scenarios for station 5.

Similarly, Fig 4.20 a shows the CDF plots for dry days index for three RCP scenarios with observed period dry days series and projected GCM ensembles for station 5. Although the average of the GCM ensembles indicate the increase in dry days spells as compared to observed duration dry days spells for all the RCP scenarios but individ-

ual ensemble represents large uncertainty for example CM3 model indicates decrease in the dry days spells for the RCP2.6 scenario whereas ESM2G and ESM2M models show increase in the dry days spell. In case of RCP 6.0 and RCP8.5 also, the GCM ensembles shows uncertainty in dry days spells. Fig 4.20 b shows the wet days spells for all the three RCP scenarios and GCM ensembles compared with observed period wet days spells. All the GCM ensembles depicts less variation in the wet days spell for the projected RCP scenarios and show less uncertainty associated for this index.

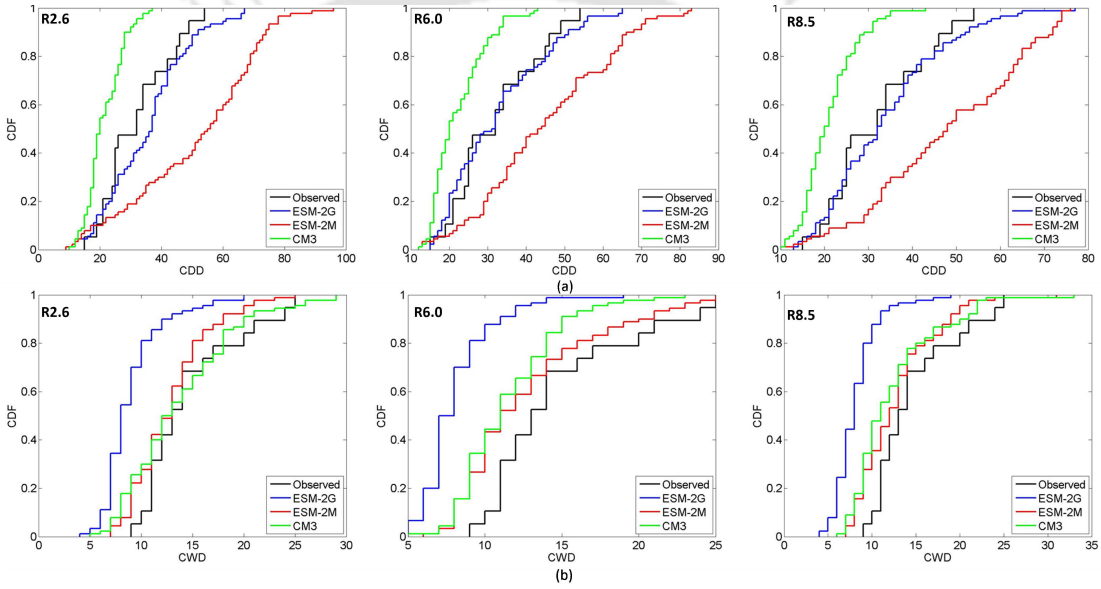

Figure 4.20: CDF plot of the (a) dry days and (b) wet days of observed precipitation and projected precipitation for three RCP scenarios of station 5.

SDSM model performs on the dry days and wet days concept and divides the precipitation series in dry days and wet days and then downscaling is performed on the basis of the wet days. CDF plot of the dry days indices and wet days indices indicates that the model is efficient to capture the wet days pattern and hence it reduces the uncertainty in the projection.

4.11 Conclusions

This chapter covers the downscaling of maximum temperature, minimum temperature and precipitation in Subansiri river basin for three RCP scenarios for the long term period of 2011-2100. Analysis of the downscaling temperature series shows the increase in minimum and maximum temperature for all the RCP scenarios. Precipitation projection also indicates increase in the annual precipitation.

Precipitation indices analysis is also carried out to understand the variability of the precipitation. Temporal variation of SDII indicates a direct proportionality to the emission scenario as the value of daily intensity increasing from low to high emission scenario. Increase in the precipitation can be explained in the terms of annual precipitation and number of rainy days. Annual precipitation shows increasing trends over the basin for all the RCP scenarios but contrary to this, number of rainy days shows contradictory behavior as the upper portion of the basin shows increasing number of rainy days followed by the decrease in the lower portion it is decreasing. So the intensity in the upper portion is showing decreasing trends whereas for the lower portion it shows increasing pattern for all the RCP scenarios.

CHAPTER 5

Hydrological Modeling and streamflow projections

5.1 General

Himalayan region is vulnerable to the climate change because of increasing temperature of the region (Bhutiyani et al., 2007; Khadka et al., 2014). Increasing temperature is the serious threat to the glacier dominated Himalayan region (Singh and Kumar, 1996; Singh and Bengtsson, 2005).Bhutiyani et al. (2010) correlates the increasing trend in temperature to decreased winter snowfall in the north-western Himalayan region. Alteration in temperature and precipitation is subsequently affecting the hydrology of the Himalayan region (Immerzeel et al., 2009). Dahal et al. (2016) in their study over an east Himalayan river basin, reported increase in precipitation which eventually increase the water yield in the basin. Many recent studies reveals the continuously increasing trend in temperature and precipitation in Himalayan range (Bhutiyani et al., 2007; Khadka et al., 2014). This chapter describes the hydrological models of the Subansiri basin and the projection of streamflow for different emission scenarios to assess the changes in streamflow and other water balance component of the river basin.

5.2 Model Framework

In this chapter, hydrological modeling, parameterization and uncertainty analysis of the Subansiri river basin is explained. Apart from the parameterization and uncertainty analysis, future projection of the streamflow in the river for different emission scenarios is also covered in this chapter. Soil and water assessment tool (SWAT) is used for the hydrological modeling of Subansiri River for simulating the streamflow. SWAT is a semi-distributed, lumped model (Neitsch et al., 2011). Sequential uncertainty parameter fitting approach (SUFI2) methods under the framework of SWAT Calibration and Uncertainty Program (SWATCUP) are utilized for the parameterization and uncertainty analysis of the prepared hydrological model. Various water balance component i.e. streamflow, evapotranspiration, snow melt contribution to the discharge of river were calculated after calibration and validation of the hydrological model.

Downscaled temperature and precipitation series (Chapter 4) were taken as the primary variables to assess the change in projections. Future projected temperature and precipitation time series were further utilized for the projections of the streamflow in the river for different RCP scenarios over the period of 2011-2100. Trends and magnitude of change in water balance component in the river basin for different climate change scenarios have been calculated using Mann-Kendall trend test and Sen's slope estimator.

5.3 SWAT Model description

SWAT is lumped, semi distributed, deterministic model which simulates streamflow on the basis of water balance equation, it divides the entire catchment in sub-catchments

and hydrological response units (HRU) and calculates all the water balance component for each HRU. These HRU represents the homogeneous hydrological units where all the physical parameters (e.g. soil group, land use land cover class) remains homogeneous in all directions. Water balance equation can be written as below (Neitsch et al., 2011).

$$SW_t = SW_a + \Sigma_{i=1}^{n} \left(R_{day} - Q_{sur} - E_a - W_{seep} - Q_{gw}\right) \tag{5.1}$$

Where SW_t is the final soil water content (mmH_2O), SW_a the initial soil water content (mmH_2O), t time in days, R_{day} amount of precipitation on day i (mmH_2O), Q_{surf} the amount of surface runoff on day i (mmH_2O), E_a the amount of evapotranspiration on day i (mmH_2O), W_{seep} the amount of percolation and bypass exiting the soil profile bottom on day i (mmH_2O) and Q_{gw} is the amount of return flow on day i (mmH_2O). SWAT works on the methodology suggested by United States Department of Agriculture (USDA) for the runoff calculation from a catchment based on the physical and climatic parameters of the basin, known as soil conservation services (SCS) curve number (CN) method which is given as:

$$Q_{surface} = \frac{(R - I_a)^2}{R - I_a + S} \tag{5.2}$$

Where, $Q_{surface}$ is total surface runoff (mm), R is daily rainfall (mm), I_a is the initial abstraction such as infiltration and interception prior to runoff (mm), S is a retention parameter (in mm) based on the combination of soil and Land use land cover.

$$S = \frac{25400}{CN} - 254 \tag{5.3}$$

Where CN is the curve number for the day and the initial abstractions I_a, is generally approximated as 0.2S and the equation will be as

$$Q_{surface} = \left(\frac{R - 0.2S}{R + 0.8S}\right)^2 \tag{5.4}$$

Runoff starts if the amount of rainfall is higher than the initial abstraction losses ($R_{day} > I_a$) SWAT model requires physical datasets such as soil map, elevation map, land use and land cover map as well as meteorological datasets such as precipitation, minimum and maximum temperature, humidity etc. for model preparation. Apart from this it requires hydrological datsets (e.g. streamflow) for calibration and validation purpose. Apart from the complex input dataset requirement, this model also uses large number parameter coefficients for calibration and validation purposes. SWAT model primarily delineate the whole catchment into numbers of sub-catchments based on the area threshold. Each sub-catchment contains a main channel and many hydrologic response units (HRUs), which consist of homogeneous land use, soil type, and management practices. The contributions of each HRU are then aggregated for the sub catchment by a weighted average. In SWAT, the main hydrological component such as runoff is then simulated for each HRU, and the contributions of each HRU are then aggregated for the sub-basin by a weighted average. Water is then routed to the outlet of the watershed. Likewise, SWAT also simulates other water balance components at each HRU and the contributions of each HRU, are then aggregated for the sub-catchment.

5.4 SWAT model preparation

SWAT requires digital elevation model (DEM) for the delineation of the watershed boundary, sub-watersheds and stream networks, soil map, land use/land cover map

for calculating all the components of hydrological process. Shuttle radar topographic mission (SRTM) (90 m spatial resolution) data was used for morphological mapping of the river basin. Similarly land use/land cover data and soil map data (Chapter 3) were utilized for preparation of the hydrological model. SWAT creates hydrological response unit (HRU) for simplifying the calculations of hydrological response from different type of soil and LULC groups. Each HRU represents the spatial homogeneity for a particular type of physical property (e.g. soil type, LULC class). After providing the physical maps to the, next step is to prepare the weather data for the model. In weather data SWAT mainly requires minimum temperature (Tmin), maximum temperature (Tmax) and precipitation data with several statistical characteristics on the monthly timescale e.g. mean monthly maximum temperature, mean monthly minimum temperature.

In this study, the Subansiri river basin is divided into five sub-basins based on the major tributaries of the Subansiri river,five sub basins (SB) are devided on the basis of major tributaries of the river basin (Figure 5.1) and HRU were created by model on the basis of physical parameters of the input data with a threshold of 5% similarity (Neitsch et al., 2011), and one weather stations was selected for each sub-basin (Figure 5.1). Within a sub-watershed, several HRUs are created based on soil, LULC map and slope map. All the water balance components of hydrological process are computed for each HRU and the final runoff to the main channel is computed through the Muskingum routing method (Neitsch et al., 2011). As shown in the Figure 5.1 sub basins are divided and each sub basin is provided with the one weather station. In this study streamflow is simulated upto the Gerukamukh outlet as shown in the figure. Observed streamflow dataset from 2002-2013 has been utilized for the calibration and validation of the prepared hydrological model.

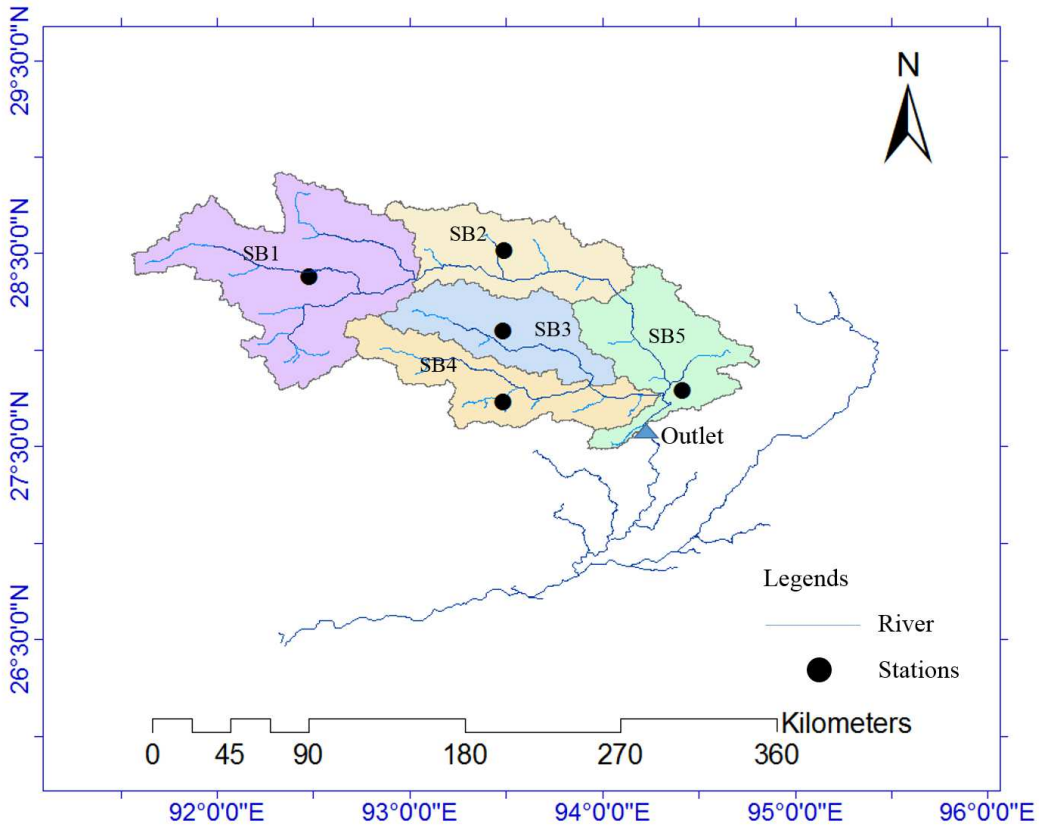

Figure 5.1: Sub-basins of the Subansiri river for SWAT model preparation

5.5 Parameterization and uncertainty analysis of the hydrological model using SUFI2 algorithm

The SWAT simulated results calibrated and validated in SWAT CUP packages. SUFI2 algorithm has been used for model parameterization, sensitivity analysis and uncertainty analysis. The model calibration was performed using the concept of aggregate parameter selection Yang et al. (2007). An 'aggregate parameter' is defined by adding a term such as $v\_$, $a\_$ and $r\_$ to the front of the original parameter to mean a replacement, an absolute increase and a relative change to the initial parameter value, respectively (Abbaspour et al., 2007b). SWAT CUP comprises all sources of uncertainties such as model structure based uncertainty, parameter uncertainty and data input errors.

Parameter uncertainty is usually caused as a result of inherent non-uniqueness of parameters (involved model calibration parameters) in inverse modeling due to wrong data inputs and parameterization. The adaptation of inverse modeling approach is a very popular method for the model calibration(Abbaspour et al., 2007b).

The parameter sensitivity analysis helps to identify the significance of the particular parameter for the calibration process, whether the process is influenced by the parameter values if it changes. For this current study, a global sensitivity analysis approach has been applied. The parameter's sensitivity can be determined by the multiple regression system, which regresses Latin hypercube generated parameters against the objective function. The Latin Hypercube Sampling (LHS) method is considered as a highly efficient sampling method. In this study, the significance level P value test and statistical t-test are used to rank the high sensitive and non-sensitive parameter. If the P-values corresponded to 0 then it means that parameter is highly sensitive for the process. In global sensitivity outcomes, a t significance test (t-stat) is evaluated based on the significance level alpha ($\alpha = 0.05$) and P-values. The alpha value of 0.05 was chosen as the local significance level. Based on this significance level, values larger than 1.96 or lower than -1.96, respectively, indicate a significant ($p < 0.05$) positive or negative trend. If the P values will be closer to zero, the corresponding values will be more significant for the trend (Abbaspour et al., 2007b).

For calibration, SUFI2 follows an iterative process to update the old coefficient parameters to get a new estimate of the parameters. It adopts sequential and fitting processes for incorporating the parameter uncertainty, where the parametric errors are identified in terms of overestimation and underestimation (Abbaspour et al., 2007a). Additionally, it utilizes prior knowledge of the parameter's coefficients and data quality

checks in order to minimize the uncertainty. The algorithm assumes a large parameter uncertainty, which represents a physically meaningful range, to ensure the observed data lies in the 95PPU (95 % prediction uncertainty) band for the first iteration. In the following iterations, it decreases the uncertainty while monitoring the p-factor and r-factor (Abbaspour et al., 2007a).

The 95PPU is calculated between the 2.5% and 97.5% levels of the cumulative distribution of an output variable obtained through Latin hypercube sampling, disallowing 5% of the very bad simulations (Abbaspour et al., 2007a; Yang et al., 2007). SUFI2 algorithm aims at minimization of the overestimation or underestimation of modeling outcomes through iterative parameterization and it tried to bracketing most of the observed data with the smallest possible uncertainty band, which means the good results should have a relatively large p-factor with relatively small r-factor. The p-factor determines the percentage of simulated data falls into the observed dataset and the r-factor determines the uncertainty thickness in the simulated datasets when compared to observed datasets. Theoretically, the value of p-factor ranges between 0 to 100% and r-factor ranges between 0 to infinity. The values of p-factor equal to 1 and r-factor equal to 0 corresponds to a condition where measured data is equivalent to observed data. A larger p-factor can be achieved at the expense of a larger r-factor (Abbaspour et al., 2007a). The mathematical expressions of SUFI2 algorithm are defined into the following steps

1 First the objective function $g\theta$ and other parameter ranges $\theta_{absmin}, \theta_{absmax}$ are defined.

2 Latin hypercube sampling is carried out for the hypercube$[\theta_{min}, \theta_{max}]$, the corresponding objective functions are evaluated and the sensitivity matrix J and the

parameter covariance matrix C are calculated according to equations 5.5 and 5.6

$$J_{ij} = \frac{\Delta g_i}{\Delta \theta_j}, i = 1, \ldots .., C_2^m, j = 1, \ldots .n \tag{5.5}$$

$$C = S_g^2 (J^T J)^{-1} \tag{5.6}$$

Where S_g^2 is the variance of the objective function values resulting from the number of model runs.

3 A 95% predictive interval of a parameter θ_j is computed as follows (Equation 5.7):

$$\theta_{j,lower} = \theta_j^\star t_{v,0.025} \sqrt{(C_{jj}} \theta_{j,upper} \theta_j^\star + t_{v,0.025} \sqrt{C_{jj}} \tag{5.7}$$

Where $\theta_j^\star$ is the parameter θ_j for the best estimates (i.e. parameters which produce the optimal objective function), and v is the degrees of freedom (mn).

4 The 95PPU is calculated at the 2.5% and 97.5% levels of the cumulative distribution of an output variable obtained through Latin hypercube sampling, disallowing 5% of the very bad simulations (Equation 5.8).

$$r - factor = \frac{\frac{1}{n} \Sigma_{t_i=1}^{n} \left(y_{t_i,97.5\%}^M - y_{j,2.5\%}^M \right)}{\sigma_{obs}} \tag{5.8}$$

Where $y_{t_1,97.5\%}^M$ and $y_{j,2.5\%}^M$ represents the upper and lower boundary of the 95PPU and σ_{obs} stands for the standard deviation of the measured data.

5 The goodness of fit and the degree to which the calibrated model accounts for the uncertainties are assessed by the above two measures. A uniform distribution in the parameter hypercube $[\theta_{min}, \theta_{max}]$ is interpreted as the posterior parameter distribution. Otherwise $[\theta_{min}, \theta_{max}]$ is updated according to the given Equations

5.9 and 5.10

$$\theta_{j,min,new} = \theta_{j,lower} - max\left(\frac{\theta_{j,lower} - \theta_{j,min}}{2}, \frac{\theta_{j,max} - \theta_{j,upper}}{2}\right) \tag{5.9}$$

$$\theta_{j,max,new} = \theta_{j,upper} + max\left(\frac{\theta_{j,lower} - \theta_{j,min}}{2}, \frac{\theta_{j,max} - \theta_{j,upper}}{2}\right) \tag{5.10}$$

6 Finally the model performs different iterations for initialization of the best parameter ranges.

5.6 Model performance evaluation

5.6.1 Calibration and Validation

Subansiri river basin was divided in 5 sub-basins on the basis of major tributaries of the river (Figure 5.2). Hydrological model was calibrated and validated first, considering the main parameters as shown in the Table 5.1. Parameters were optimized using the SWAT-CUP SUFI2 algorithm. Observed streamflow data is available for the period of 2002-2013, model was run for 2000-2010 with warmup period of two years i.e. 2000-2002, further the data from 2002-2010 was selected for calibration and remaining 2011-2013 data was used for validation of the model. Figure 5.2 shows the scatter plot for calibration and validation. Model performance were evaluated on the basis of coefficient of determination (R^2) and Nash-Sutcliffe efficiency (NSE) Eq. 5.11 and Eq. 5.12,

Coefficient of determination

$$R^2 = \left(\frac{\sum_{i=1}^{n}(T_{O_i} - \overline{T_O})(T_{P_i} - \overline{T_p})}{\left(\sqrt{\sum_{i=1}^{n}(T_{O_i} - \overline{T_O})^2}\right)\left(\sqrt{\sum_{i=1}^{n}(T_{P_i} - \overline{T_P})^2}\right)}\right)^2 \tag{5.11}$$

Nash-Sutcliff Efficiency

$$NSE = 1 - \frac{\Sigma_{i=1}^{n}(T_{O_i} - T_{P_i})^2}{\Sigma_{i=1}^{n}(T_{O_i} - \overline{T_O})^2} \tag{5.12}$$

Where T_{O_i} and T_{P_i} are the i^{th} data point of observed and model generated temperature dataset respectively and $\overline{T_O}$ and $\overline{T_P}$ are the mean of observed and model generated temperature data series respectively. Model was calibrated and validated for daily and monthly timescale and results shown in the scatter plot in the Figures 5.2 and 5.3. For calibration R^2 found to be 0.86 (Figure 5.2a) and for validation it is 0.80 (Figure 5.2b) whereas NSE of monthly model for calibration period is 0.82 and for validation period it is 0.80.

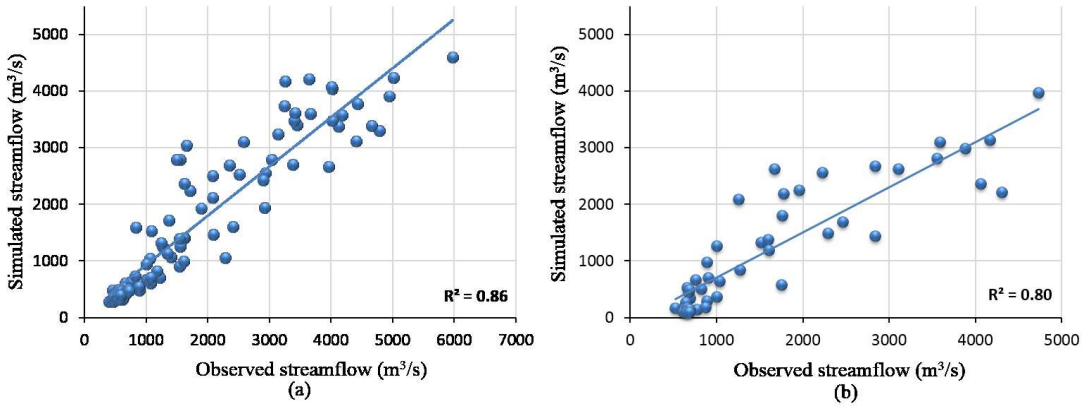

Figure 5.2: (a) Calibration and (b) validation results of streamflow simulation of Subansiri river for monthly model

Daily scale model calibration and validation results shows comparatively poor results as compared to the monthly model results. Model fails to simulate the high peaks of the streamflow but in monthly model it simulates well. For calibration of daily model R^2 found to be 0.54 (Figure 5.3a) and for validation period it was 0.45 (Figure 5.3b). Subansiri river is a perennial river with very high flow during the monsoon season and daily model fails to predict these peak value.

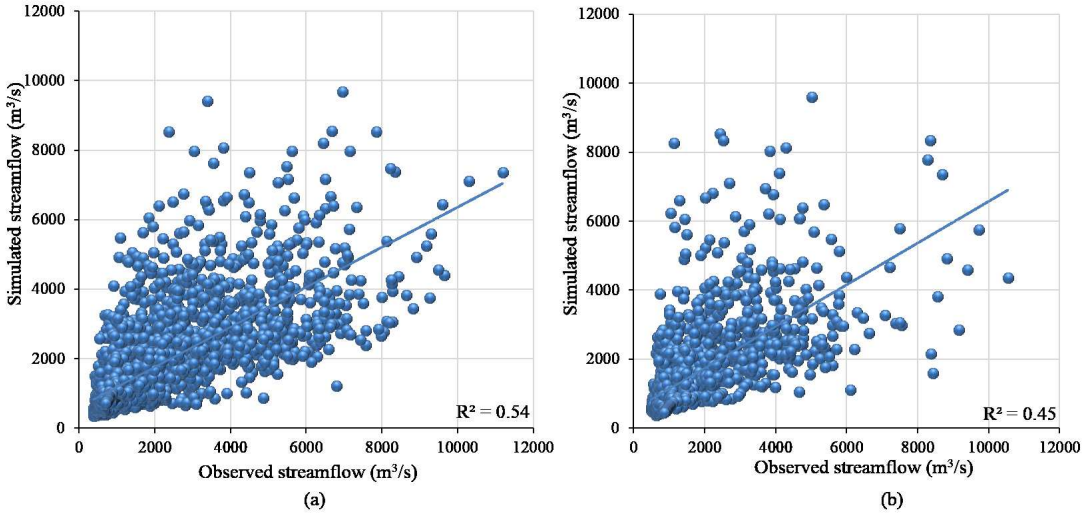

Figure 5.3: (a) Calibration and (b) validation results of streamflow simulation of Subansiri river for daily model

5.6.2 Sensitivity and uncertainty analysis

SWAT model is a semi distributed model which works on sub-basin and hydrological response unit (HRU) approach. Therefore, Subansiri river basin was divided into five sub basins, on the basis of the major tributaries of the river and each sub basin has one weather station. Land use and land cover data, soil map, slope map as explained in chapter 3 were used for the model preparation. Further, several model parameters were selected for calibration and validation purpose. Parameters selected for the calibration purpose affect the output variables and hence it is important to check the sensitivity of the parameters. Range of the parameter values impart the uncertainty in the model output variable, this uncertainty analysis and sensitivity analysis was analyzed using SUFI2 algorithm. Table 5.1 shows the initial range of the selected parameter and fitted values along with the t-stats and p-value of the sensitivity test. Prefix R (relative) and V (value) used with the parameter names in Table 5.1 shows the method applied for changing the parameter values for each iteration. Uncertainty in the model represented

Table 5.1: SWAT parameters list used for calibration of the model with sensitivity analysis t-stat and p-value

Parameter Name	**Min value**	**Max value**	**Fitted Value**	**t-Stat**	**P-Value**
1:R_CN2.mgt	-0.25	0.25	0.21	6.94	0.000
2:V_ALPHA_BF.gw	0	1	0.51	1.23	0.220
3:V_GW_DELAY.gw	10	250	136.36	-3.32	0.001
4:V_GWQMN.gw	0	1000	234.50	-2.17	0.030
5:V_GW_REVAP.gw	0.02	0.2	0.04	-6.98	0.000
6:V_ESCO.hru	0.8	1	0.98	3.80	0.000
7:V_CH_N2.rte	0	0.3	0.01	-3.44	0.001
8:V_CH_K2.rte	5	130	44.81	-2.99	0.003
9:V_ALPHA_BNK.rte	0	1	0.22	12.01	0.000
10:R_SOL_AWC	-0.2	0.4	0.05	-1.33	0.185
11:R_SOL_K	-0.8	0.8	0.66	20.94	0.000
12:R_SOL_BD	-0.5	0.6	-0.25	5.74	0.000
13:V_SFTMP.bsn	-5	5	1.11	-1.76	0.078
14:V_SMTMP.bsn	-5	5	4.42	-0.82	0.414
15:R_SNOCOVMX.bsn	0	10	7.42	1.67	0.096
16:R_SURLAG.bsn	-0.25	0.25	0.01	-1.57	0.118
17:V_CANMX.hru	0	3	0.08	-1.16	0.245
18:V_SMFMX.bsn	1.4	6.9	5.80	-0.83	0.408
19:V_SMFMN.bsn	1.4	6.9	5.49	0.68	0.500
20:R_SNOCOVMX.bsn	0	300	164.25	-1.56	0.120
21:R_SNO50COV.bsn	0.01	0.99	0.51	-0.47	0.642
22:V_TIMP.bsn	0.1	1	0.41	0.59	0.554

by two metrics i.e. p-factor and r-factor as discussed in methodology section. R-factor found to be 0.38 and p-factor 0.68. Figure 5.4 shows the plot of observed monthly streamflow along with simulated streamflow and 95ppu band. Sensitivity analysis shows that curve number parameter is most sensitive in order to simulate the streamflow, whereas some other sensitive parameters are baseflow factor, groundwater delay etc. as shown in Table 5.1. Since the Subansiri river basin contains some snow covered portion, some parameter related to snowmelt hydrology were also found sensitive.

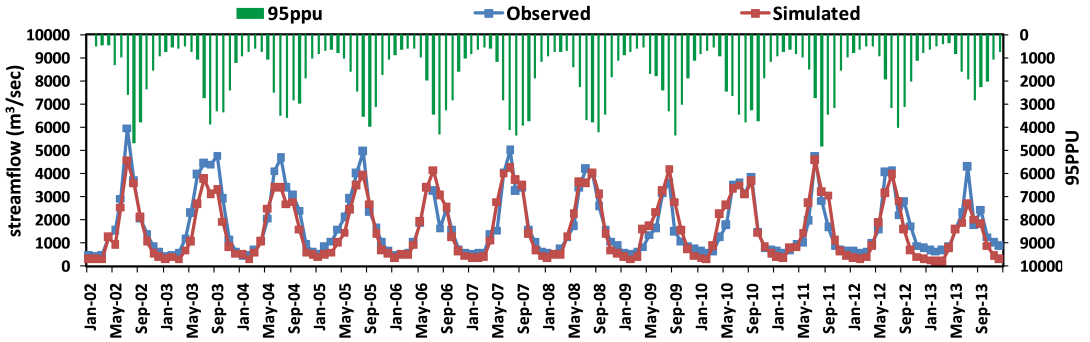

Figure 5.4: Observed streamflow and simulated streamflow plot with 95ppu plot

Prefixes with parameters indicates the methods use for changing the values of parameters in each iteration as explained in the previous section. R indicates the relative method where the optimized fraction value of the parameter is added or subtracted to the original value such as for curve number. Similarly, a shows the absolute change in the parameter value. Model starts calibration with the initial values of the parameters and with each iteration, model changes the value of the parameters with user defined methods and compares the output value with the provided observed value and tries to minimize or maximize the user defined objective function, coefficient of determination and Nash-Sutcliffe efficiency in this case.

5.7 Projection of streamflow and changes in hydrological components

Hydrological model of the Subansiri river was calibrated and validated using the observed streamflow for the period of 2002-2013, paramterization and uncertainty analysis was performed using SUFI2 algorithm. further, the prepared model was used for the projection of streamflow for selected RCP scenarios. Downscaled precipitation and temperature series were taken as the primary inputs in the calibrated SWAT model and

streamflow, evapotranspiration and other water balance component were projected for 2016-2100 period. To assess the change and trends in these component for future time series domain MK test was applied and further flow duration curve plot were created to check the dependable flow available in the stream for the future scenarios.

Mann-Kendall (MK) non parametric test (Mann, 1945; Kendall, 1968) was applied to test the existing trends in the data series, MK test z-statistic provides an idea about the significance of existing trend at 95% confidence interval. Further Sen's slope (Sen, 1968) formula was used to check the magnitude of trends. Table 5.2 shows the Mann-Kendall trend test analysis results and Sen's slope magnitude for all the variables, table suggests that for all the scenarios amount of precipitation and streamflow in the river are likely to increase exceptionally in case of RCP scenarios where it tends a decreasing trend but not statistically significant. Although the evapotranspiration in SB2 and SB3 show a significant decreasing trend but the total water yield likely to increase for the RCP6.0 and RCP8.5 scenarios. Figure 5.5 represents the sub-basin analysis of the precipitation pattern, evapotranspiration and water yield from the sub-basin. Figure suggest that the precipitation as well as the water yield in all the sub-basins are going to increasing for the future period. Mann- Kendall (MK) non parametric test was applied to test the existing trends in the precipitation, evapotranspiration and streamflow data series, further Sen's slope (Sen, 1968) formula was used to check the magnitude of trend in the data series. MK test z-statistics provide an idea about the significance of existing trend at 95% confidence interval. Table 5.2 shows the Mann-Kendall trend test analysis results and Sen's slope magnitude for all the variables. Table suggest that for all the scenarios amount of precipitation and streamflow in the river are likely to increase exceptionally in case of RCP scenarios where it tends a decreasing trend but

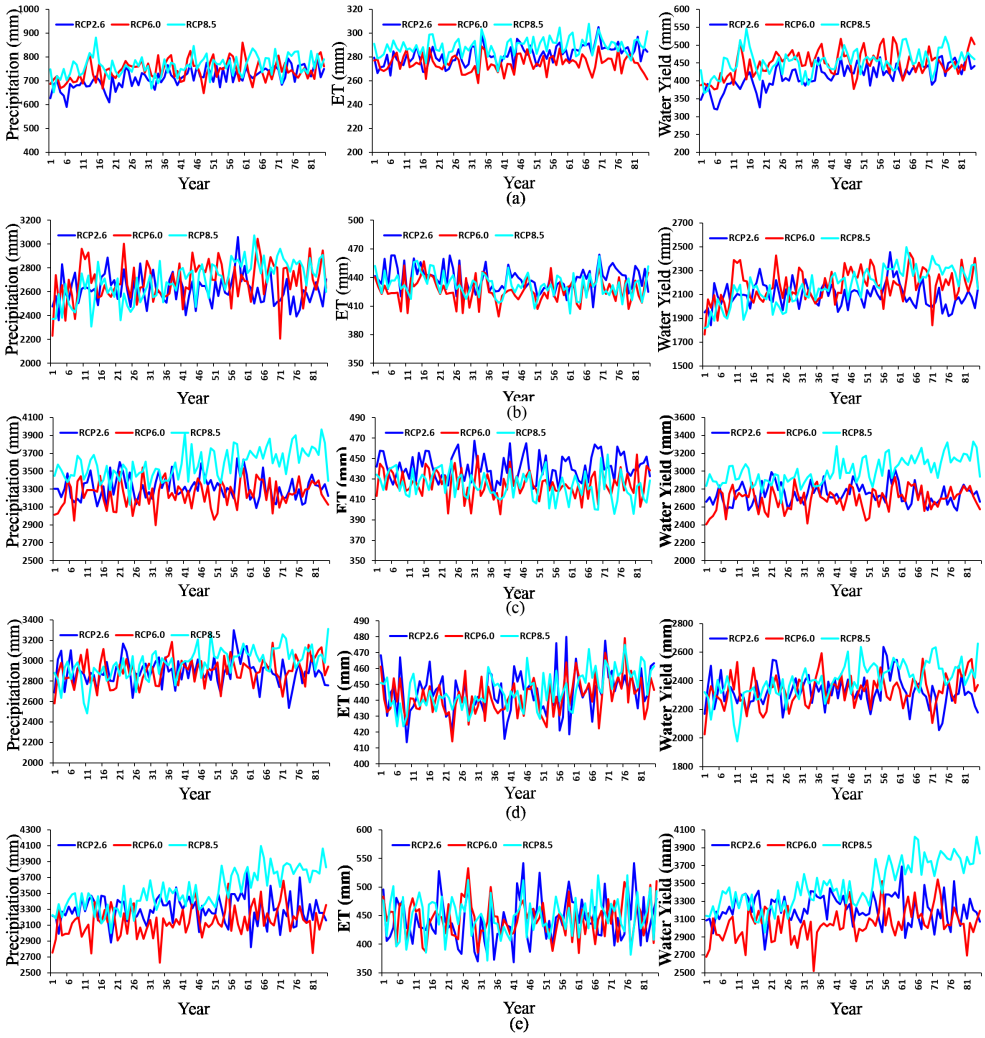

Figure 5.5: Trends on annual precipitation, evapotranspiration and water yield (a) SB1 (b) SB2 (c) SB3 (d) SB4 and (e) SB5

not statistically significant. Although the evapotranspiration in SB2 and SB3 show a significant decreasing trend but the total water yield likely to increase for the RCP6.0 and RCP8.5 scenarios. Downscaled precipitation and temperature data were used as primary input in the calibrated hydrological model for assessing the change in amount of streamflow for different RCP scenarios. Major concern of the changing climate for a region is the availability of the water for different season, it can be assess with the help of exceedance percentage of the streamflow or the flow-duration curve.

Table 5.2: Mann-Kendall test statistics of precipitation, evapotranspiration and water yield for each sub-basin

		Precipitation			**Evapotranspiration**			**Water Yield**		
		RCP2.6	**RCP6.0**	**RCP8.5**	**RCP2.6**	**RCP6.0**	**RCP8.5**	**RCP2.6**	**RCP6.0**	**RCP8.5**
SB1	**Z-stats**	6.26	2.44	3.15	4.88	0.37	2.17	7.00	2.76	3.28
	Sen's Slope	1.07	0.48	0.59	0.16	0.01	0.07	0.92	0.52	0.50
	p-value	0.00	0.01	0.00	0.00	0.71	0.03	0.00	0.01	0.00
		RCP2.6	**RCP6.0**	**RCP8.5**	**RCP2.6**	**RCP6.0**	**RCP8.5**	**RCP2.6**	**RCP6.0**	**RCP8.5**
SB2	**Z-stats**	-0.98	2.22	6.74	-2.90	-2.99	-4.70	-0.77	3.26	7.78
	Sen's Slope	-0.56	1.63	4.57	-0.20	-0.21	-0.34	-0.40	1.91	4.72
	p-value	0.33	0.03	0.00	0.00	0.00	0.00	0.44	0.00	0.00
		RCP2.6	**RCP6.0**	**RCP8.5**	**RCP2.6**	**RCP6.0**	**RCP8.5**	**RCP2.6**	**RCP6.0**	**RCP8.5**
SB3	**Z-stats**	-0.19	1.26	4.92	-1.13	-1.98	-3.54	-0.16	1.61	6.27
	Sen's Slope	-0.12	0.91	3.63	-0.08	-0.13	-0.25	-0.10	0.95	3.72
	p-value	0.85	0.21	0.00	0.26	0.05	0.00	0.87	0.11	0.00

Continued on next page

Table 5.2 – *Continued from previous page*

		Precipitation			Evapotranspiration			Water Yield		
		RCP2.6	**RCP6.0**	**RCP8.5**	**RCP2.6**	**RCP6.0**	**RCP8.5**	**RCP2.6**	**RCP6.0**	**RCP8.5**
SB4	**Z-stats**	-0.33	2.36	6.03	1.75	2.35	4.99	-0.41	2.60	6.32
	Sen's Slope	-0.15	1.39	3.34	0.11	0.13	0.26	-0.14	1.23	2.98
	p-value	0.74	0.02	0.00	0.08	0.02	0.00	0.68	0.01	0.00
		RCP2.6	**RCP6.0**	**RCP8.5**	**RCP2.6**	**RCP6.0**	**RCP8.5**	**RCP2.6**	**RCP6.0**	**RCP8.5**
SB5	**Z-stats**	0.03	2.77	7.50	1.25	-0.28	0.33	-0.32	3.08	8.13
	Sen's Slope	0.02	2.16	7.37	0.22	-0.04	0.04	-0.23	2.23	8.27
	p-value	0.98	0.01	0.00	0.21	0.78	0.74	0.75	0.00	0.00

Flow duration curve is plotted by arranging the streamflow data in descending order and then ranking them and calculating the probability of each value of streamflow. This methodology provides an idea about the probability of the dependable flow.

Figure 5.6 shows the flow-duration curve for different GCM/RCP scenarios. Figure provides a good insight of the dependable flow in term of the probability, almost for all the dependable flow percent the magnitude of streamflow is increasing, figure also suggest that the for a particular percent exceedance discharge the RCP8.5 scenario has the highest value. The figure also indicates that the flow in river is likely to increase for all the scenarios and discharge value for all the percent exceedance is going to increase in any case of RCP scenarios.

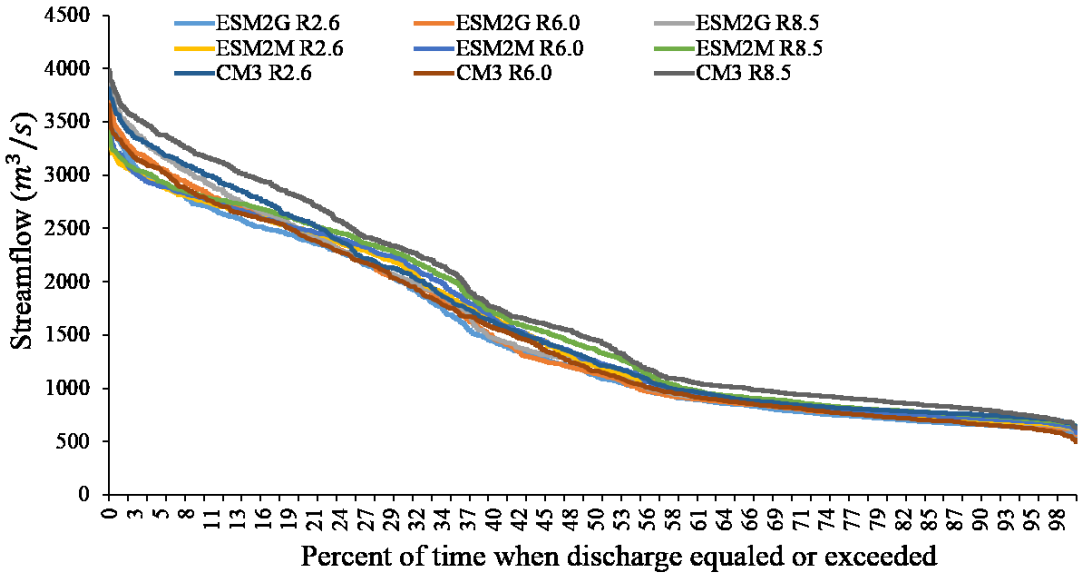

Figure 5.6: Comparison of exceedance flow for all the GCM/RCP ensembles for the period of 2016-2100

5.8 Conclusions

This chapter covers the hydrological modeling of the Subansiri river, which provides the information of the physical characteristics of the river basin and model parameters sensitive for the streamflow generation in the basin. Parameterization and uncertain analysis of the model provided a feasible range of the parameters included in the calibration of the streamflow. Calibration and uncertainty analysis were performed using SUFI2 approach. Model calibrated for the monthly time series performed better than the model prepared for the daily time series. Reason behind the poor daily model results could be the extreme values in the observed streamflow series, to which the model failed to capture. After calibrating the model with acceptable range of selected objective function i.e. coefficient of determination and Nash-Sutcliffe efficiency, the projection of the streamflow were made for 2016-2100 for three GCMs and three RCP smission scenarios. For the projection of stremflow, downscaled precipitation and temperature data series were taken as the input. Streamflow projection and its trend analysis suggests the increase in streamflow for the emission scenarios, MK trend analysis test of the streamflow and evapotranspiration shows the increasing magnitude for the period of 2016-2100.

CHAPTER 6

Integrated simulation-management model

6.1 General

This chapter, covers the integrated approach for river basin planning of Subansiri river under three emission scenarios i.e. RCP2.6, RCP6.0 and RCP8.5. In previous chapters downscaling of precipitation and temperature were covered along with the hydrological modeling and changes in the water resources of the basin were also evaluated. this chapter proposes a integrated simulation-management approach for the river management for upto the mid-century (upto 2050) time duration.

Under the threat of climate change, water availability and allocation of water for different sectors are the major concern for the planners and policymakers. Different demand sectors like municipal demand, industries and agricultural demand are increasing with the passes of time. Unplanned development, excessive withdrawal of the groundwater, increasing water demand for the population will be the major challenge for river basin planning and management. It should also be remembered that water also needs to be allocated for the aquatic environment alongside the demands of other users. Increasing water demands to fulfill the diverse societal developmental needs has led to increasing

exploitation of rivers.

Water allocation is central to the management of water resources. Due to uneven precipitation distribution and increasing population the water demand is increasing. Conflicts often arise when different water users compete for limited water supply. The need to establish appropriate water allocation methodologies and associated management institutions and policies is recognized by researchers, water planners and governments. Subansiri river basin drains the districts of Arunachal Pradesh and Assam, downstream of the LSHE reservoir consist of the districts North Lakhimpur, Dhemaji and Papumpare. Since the main objective of the LSHE is power production and flood control, but under the threat of climate change and population increase the available water resources may not be sufficient for the requirement. Taking into consideration the challenges of climate change impact on the water resources availability and demand, this chapter deals with the simulation-optimization model which addresses the water availability and water demand in particular sector such as drinking water demand.

6.2 Water evaluation and planning (WEAP) model

Under the threat of climate change, water availability and allocation of water for different sectors are the major concern for the planners and policymakers. Different demand sectors like municipal demand, industries and agricultural demand are increasing with the passes of time. Unplanned development, excessive withdrawal of the groundwater, increasing water demand for the population will be the major challenge for river basin planning and management. It should also be remembered that water also needs to be allocated for the aquatic environment alongside the demands of other users. Increasing water demands to fulfill the diverse societal developmental needs has led to increasing

exploitation of rivers.

The Water Evaluation and Performance (WEAP) model developed by the Stockholm Environmental Institute (SEI) is a tool for estimating the water demand and supply balance of different stakeholders for the available water resources. It is mainly applicable to the wide range of the water allocation problems, reservoir simulation, and demand and supply analysis. WEAP model can simulate the hydrological processes (e.g., evapotranspiration, runoff and infiltration) for assessment of the water resources in catchment and estimation of the human activities within the watershed boundary to influence water resources and their allocation.

WEAP model uses mass balance to allocate available water to the various sectors according to the priorities set by the user. Catchment of the stream or waterbody is defined with shapefiles prepared in the GIS interface and other important components such as the tributaries diversion points, dam or reservoir location are demarcated. After providing the streamflow time series to the model, reservoir specification and elevation-capacity curve data, model simulates the available water quantity which is available for the allocation to the different stakeholders.

6.3 Integrated simulation-management model

Water management model for future climate change scenario was prepared by linking the SWAT hydrological model outputs and temperature and precipitation downscaling results along with socio-economic data obtained from Census of India. Streamflow data generated for different RCP scenarios were utilized for providing inflow volume to the reservoir for different scenarios and water demand in the command area were calculated through a conceptual approach of total population and per capita water re-

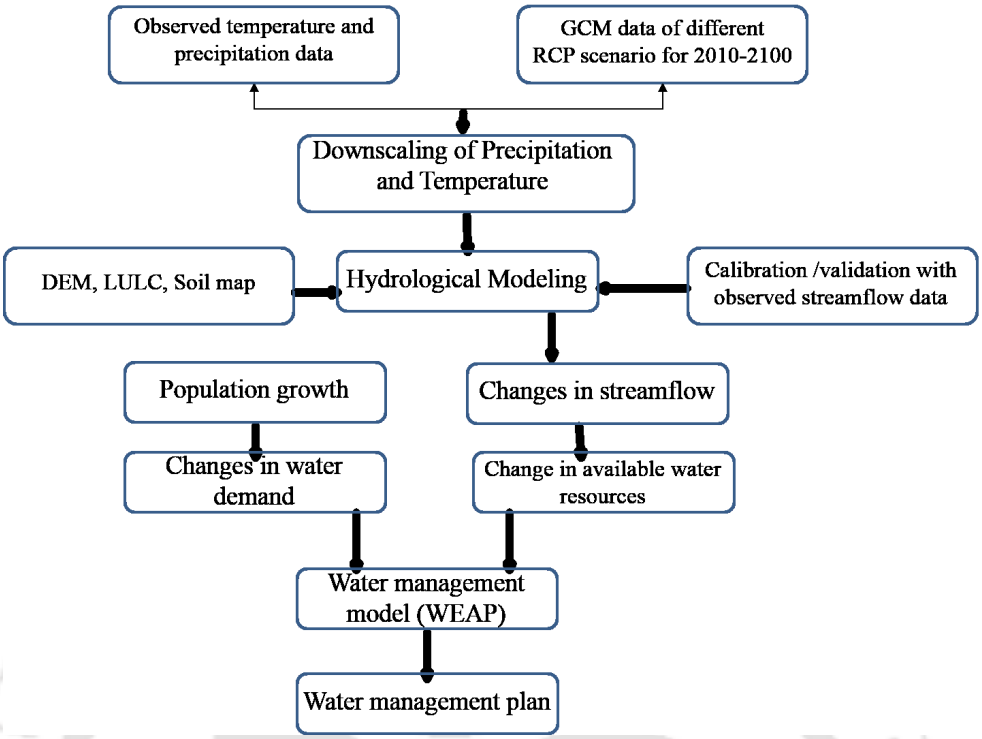

Figure 6.1: Flowchart of the methodology

quirement. Future projection of increased population was calculated from the linear equation prepared from census data of 2001 and 2011. Three main districts namely Papumpare (Arunachal Pradesh), Lakhimpur (Assam), and Dhemaji (Assam) which covers the major portion of command area were selected for defining the future changes in water demand and population growth. A schematic flowchart of the coupled approach is shown in Figure 6.1. Climate change is most likely to introduce an additional stress to already stressed water systems in developing countries. Climate change is inherently linked with the hydrological cycle and is expected to cause significant alterations in regional water resources systems necessitating measures for adaptation and mitigation. Increasing temperatures, for example, are likely to change precipitation patterns resulting in alterations of regional water availability, evapotranspirative water demand of crops and vegetation, extremes of floods and droughts, and water quality. A comprehensive assessment of regional hydrological impacts of climate change is thus

necessary. General circulation model simulations provide future projections of the climate system taking into consideration changes in external forcing, such as atmospheric carbon-dioxide and aerosols, a coupled approach of hydrological modeling and ware management modeling was used for planning of optimal use available water resources in the river basin.

6.4 A top-down approach for river basin planning

Climate change impacts on the water resources have been discussed widely in the scientific community and research literatures. Feasible adaptation options under the available resources and in context of the geographical and economic situation is the demand of the hour (Bhave et al., 2013; Safavi et al., 2015; Arnell, 2010). Recent developments in the field of climate change studies do not just focus on the impact assessment but also to the adaptation strategies, taking into consideration the various stakeholders' priorities. In climate change impact and adaptation studies, it is necessary to consider the various stakeholders while deciding any policy for a feasible solution. Population growth, increased agricultural water demand and extreme pace of industrialization along with climate changes in the recent past have created immense burden on land and water resources around the world. The main challenge in front of the scientific community and policymakers is, how to improve the management of water resources for present and future generations under the threat of climate change. Water resources planning and management requires involvement of all sectors of the society which can be called as the stakeholders. Participation of all the stakeholders in decision making process help the policymakers to avoid any regret adaptation policy. Conflict of the interests are the major challenge in the water resources planning process, in a case of conflict, first

priority should be given to the human population. Situation of conflict has become a normal scene in water allocation in large basins (Sandoval-Solis and McKinney, 2012). Previous section (6.3) discusses the linked simulation-management model and this section proposes a top down approach for the decision making considering the three main stakeholders i.e. population in the downstream, farmers and the power production.

6.5 Application of integrated approach for Subansiri river basin

6.5.1 Lower Subansiri reservoir and its command area description

6.5.1.1 Physical specifications of Lower Subansiri reservoir

Lower Subansiri hydropower project (LSHE) is located near North Lakhimpur town of the Assam which covers a part of district of Lower Subansiri of Arunachal Pradesh and Dhemaji district of Assam. Location of the dam site is 27° 33' 15" N latitude and 94° 15' 30"S Longitude. LSHE is mainly a hydropower project, which can be utilized for flood control as well in the monsoon period to accommodate the excess inflow. In this way the reservoir can be considered as a multipurpose reservoir. Hydropower project on the reservoir is estimates to produce 2000 MW of hydropower for a minimum of 4 hour peaking period (Ray, 2010). Designed total power production from the hydropower project is 2000 MW, project proposes to have eight turbines each with 250 MW production capacity in this way total 2000 MW power production is expected for a minimum of 4hr in a day. Downstream district of the Subansiri reservoir i.e. Dhemaji, Lakhimpur are prone to flood in monsoon period, so the reservoir can be used as flood control structure during the high flow season by accommodating the flood

volume. LSHE project is proposed for a full reservoir level (FRL) of elevation 205 m corresponding to storage of 1365 Mm^3 and maximum water level (MWL) of elevation 208.25 m with storage volume of 1470 Mm^3. The flood cushion of about 441.6 Mm^3 is provided for the period of high inflow like June July August months which is volume between elevation 205 m and 190 m. Maximum draw down level (MDDL) is 181m with storage volume of 720 Mm^3. Height of the dam above river bed level is 116 m and from the deepest foundation level is 133 m (Ray, 2010).

6.5.1.2 Capacity elevation relationship

Capacity elevation curve is the indicator of the storage of reservoir at a given water level in reservoir, following capacity elevation curve was collected from Ray (2010). Figure 6.2 shows the elevation capacity curve of the reservoir.

$$S_t = 0 - 46 \quad Mm^3$$

$$Elevation(m) = \frac{128.5S_t + 1412}{S_t + 15.033}$$

$$S_t = 46 - 509 \quad Mm^3$$

$$Elevation(m) = 3.555 \times 10^{-7} S_t^3 - 0.00045 S_t^2 + 0.2561 S_t + 9.40$$

$$S_t = 509 - 1532 \quad Mm^3$$

$$Elevation(m) = 5.7 \times 10^{-9} S_t^3 - 3.319 \times 10^{-5} S_t^2 + 0.08358 S_t + 135.13$$

where S_t is the storage in Mm^3 and elevation is in meter unit.

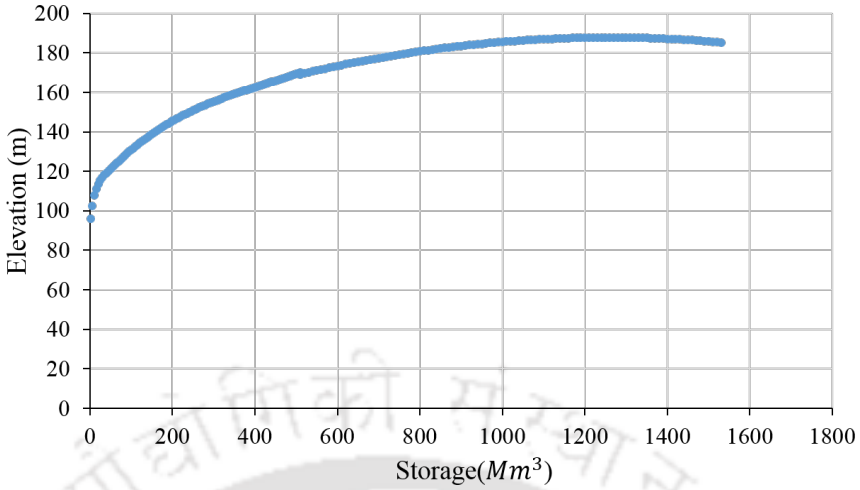

Figure 6.2: Elevation storage graph of Lower Subansiri reservoir

6.5.1.3 Command area description of Lower Subansiri reservoir

In India, Subansiri River drains two states partially namely Arunachal Pradesh and Assam. In Arunachal Pradesh, parts of Lower Subansiri district, Upper Subansiri district and Papumpare is covered whereas in Assam major part of Dhemaji and North Lakhimpur district of Assam falls in Subansiri river basin. River. A hydroelectric power plant is constructed on the Subansiri River at the foothill near Gerukamukh where it enters the Assam state, which is named as Lower Subansiri hydro-electric project (LSHE). Main objective of project is the electricity production and flood control, capacity of the power plant is 2000 MW (Ray, 2010). State of Arunachal Pradesh is mostly mountainous and less populated whereas the parts of Assam state which is covered by Subansiri river basin, is plain and more populated as compared to state of Arunachal Pradesh.

6.5.1.4 Demography of the reservoir command area

LSHE is constructed at Gerukamukh in Assam where it enters the Assam state, length of the river from Lower Subansiri reservoir to the confluence of Brahmaputra is 126

km with a command area of 9598 sq km. Lakhimpur and Dhemaji districts of Assam have the 968 revenue villages as per 2001 Census. Economy of the villages rely mainly on the agriculture and livestock including fishing as the off-form economic activity. Population data of the three districts in the downstream of the river were collected from the Census of 2001 and 2011 (http://censusindia.gov.in/). Lakhimpur district consist seven tehsils with total population of 0.88 million (2001) and 1.04 million (2011) with a total population increase of 17.22% with respect to 2001 population in one decade. Rural population constitutes of 0.82 million whereas urban population constitute only 0.065 million.

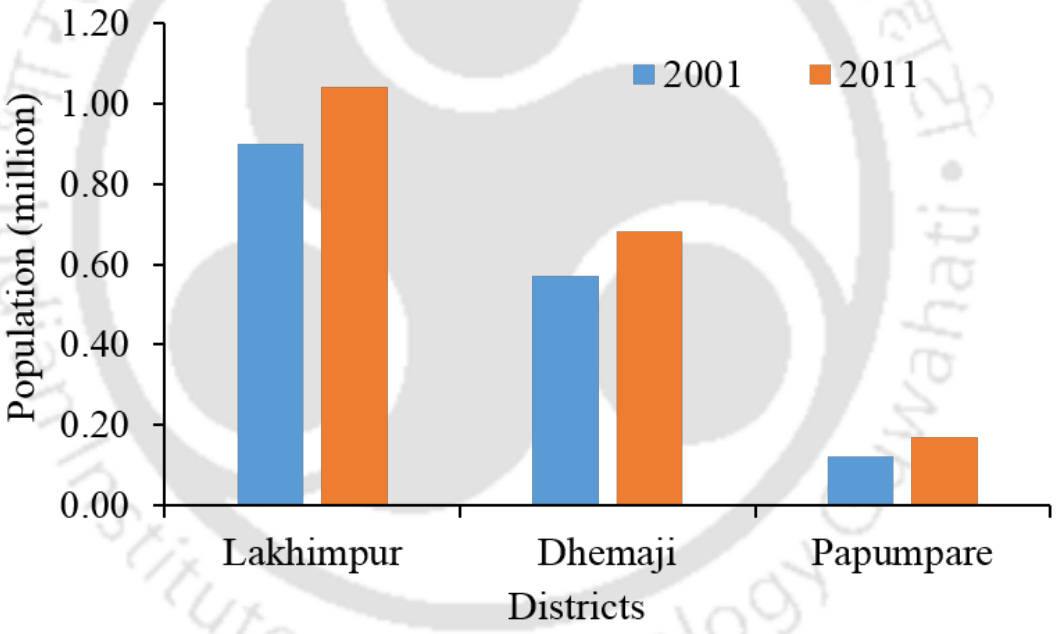

Figure 6.3: Population of the districts from two Census data

Similarly Dhemaji district consists of six districts with population of 0.57 million and 0.63 million in 2001 and 2011 respectively with a population growth rate of 19% in a decade. Papumpare district of Arunachal Pradesh consist of 15 districts with total population of 0.12 million with a growth rate of 44% in a decade. Figure 6.3 show the

population of three districts for Census 2001 and 2011, major portion of the population in these district reside in rural area with agriculture as a major source of earning along with fishing.

6.5.2 Population projection and change in water demand

6.5.2.1 Population projection methods

Although there are several methods for population projections such as arithmetical increase method, geometrical increase method, incremental increase method, graphical method and logistic curve method etc. Methods used for the population projections does not consider the saturation capacity of the population, except logistic curve method. Arithmetic increase method is suitable small, average or comparatively new cities it projects lower population than the actual situation. In this method constant growth rate is assumed for the projection. Two consecutive Census data are taken as the basis for finding the population increase rate and the difference is added to the present population estimate the population for the future duration.

Geometric increase method depends on the assumption that the increase in population percentage remains constant over the decades. Geometric mean increase is used to find out the future increment in population. This method gives slightly higher value as compared to the actual value. This method is modification of arithmetical increase method and it is suitable for an average size town under normal condition where the growth rate is found to be in increasing order. While adopting this method the increase in increment is considered for calculating future population. The incremental increase is determined for each decade from the past population and the average value is added to the present population along with the average rate of increase.

Logistic curve method when the growth rate of population due to births, deaths and migrations takes place under normal situation and it is not subjected to any extraordinary changes like epidemic, war, earth quake or any natural disaster, etc., and the population follows the growth curve characteristics of living things within limited space and economic opportunity. If the population of a city is plotted with respect to time, the curve so obtained under normal condition looks like S-shaped curve and is known as logistic curve.

6.5.2.2 Population projection for Lower Subansiri reservoir command area

Future projection of the population were carried out on the basis of the Census data of 2001 and 2011. Increase in the population between two census and percent growth in population were taken as the basis for estimating the annual population growth. Further, the population growth were projected up to the mid-century (2050) duration following the geometric increase method. Three districts of the downstream of the reservoir were selected for the projection of the population, as this population will be considered as the one among the various stakeholders in the water resources management planning. Figure 6.4 shows the population projection of three districts up to 2050. Population growth in Lakhimpur district was recorded with increase of 17.22% whereas for Dhemaji and Papumpare district the growth was recorded with 19.65% and 44.6% respectively. The average increase in population of these districts were used as the average growth rate for projecting the population on the basis of the geometric increase method.

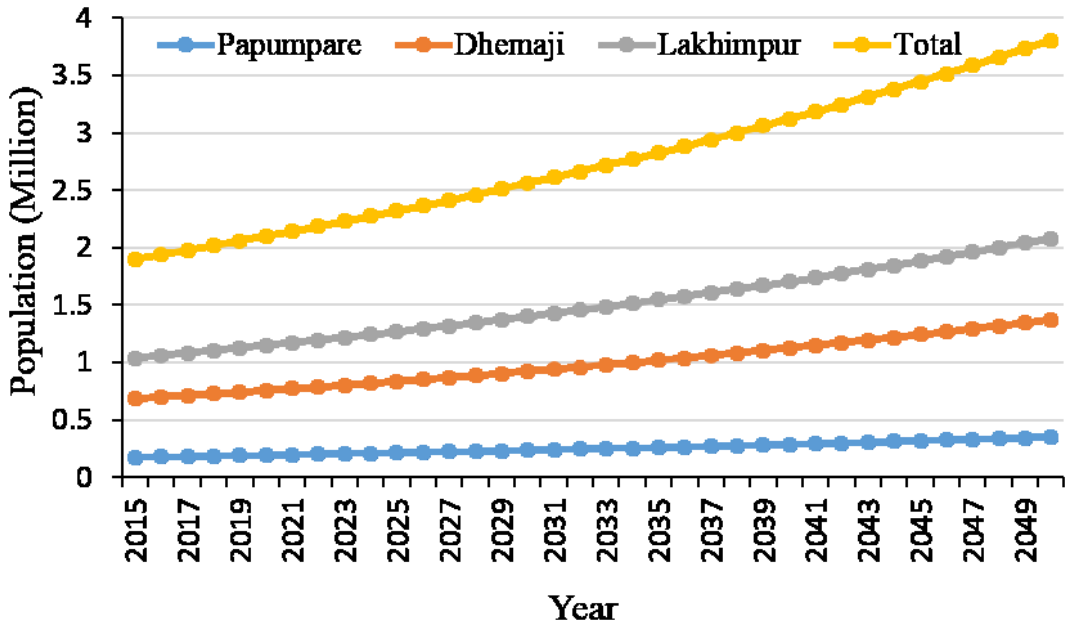

Figure 6.4: Population projection of the districts

6.5.2.3 Projections of water resources and water availability

Change in water availability were calculated on the basis of the projected streamflow by calibrated hydrological model for all the RCP scenarios. On the basis of the reservoir specification and elevation capacity curve of the reservoir, capacity of the reservoir was calculated for each of the inflow value. Streamflow for the future climate change scenarios for all the RCP scenarios were taken into consideration for the water availability in the future. Streamflow of the river was projected for the RCP2.6, RCP6.0 and RCP8.5 for the period of 2016-2100. Since the management plan is proposed for the upto 2050, the streamflow was considered for this period only. Changes in streamflow is discussed in details in the Chapter 4.

6.5.2.4 Changes in water demand

Change in water demand was made on the basis of the population growth in the downstream districts and the per capita water requirement of the population following the standard guideline. Figure 6.5 shows the three major demand sites in the reservoir command area which was identified in the WEAP model and change in water demand was calculated for the period of 2016-2050.

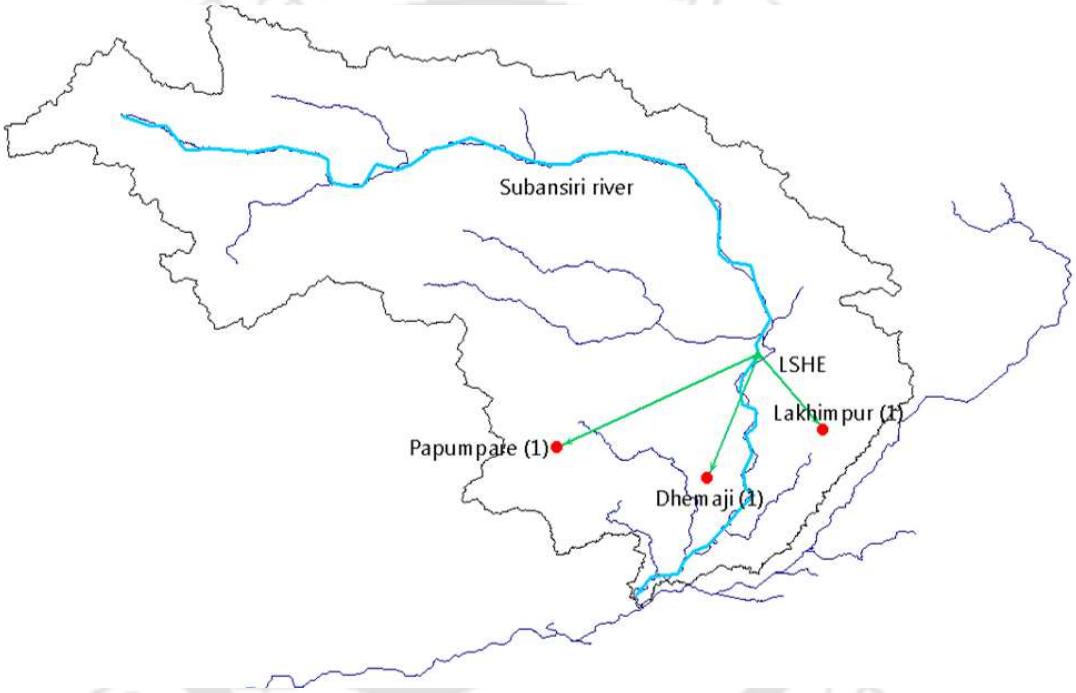

Figure 6.5: Location of demand sites in the water management model

Inflow to the reservoir were generated from the hydrological modeling and it provides the information of available water. Water demand was calculated for the three districts and it was compared with the available water as the storage in the reservoir and unmet demand was calculated for the downstream districts for the projected population. Figure 6.6 shows the unmet water demand for the three RCP scenarios.

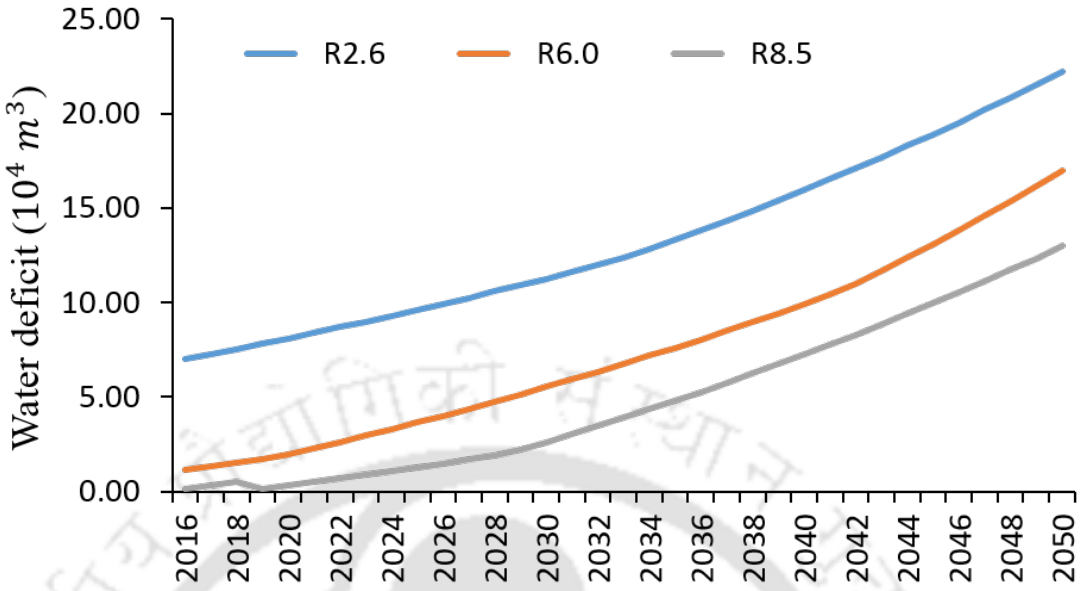

Figure 6.6: Unmet demand of command area districts for RCP scenarios

6.5.3 Proposed water storage structure

It was observed from the water resources availability and the water demand calculation that the available surface water resources are not enough to fulfill the water demand in the command area. Seasonal variation in the water availability intensifies the scarcity situation,such situation encourages for the alternative water resources in the river basin. In management plan to overcome the seasonal scarcity of the command area it is required to rely on the local surface water resources, since the groundwater level and utility data is not available for the region, the management plan is focused on the surface water resources only.

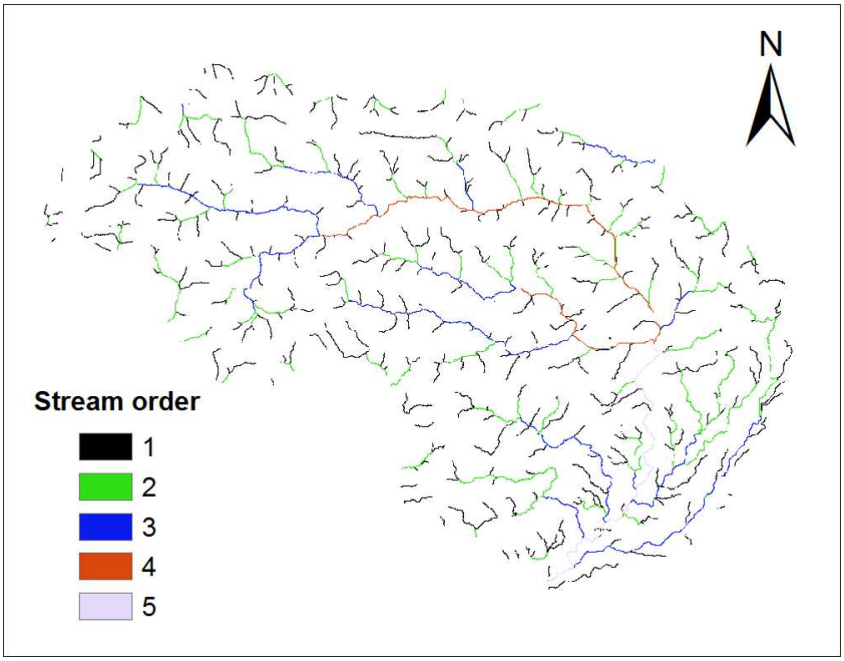

Figure 6.7: Stream order map of the Subansiri river basin

One of the popular approach for such situation is the construction of the water storage structures which check the drain of water and conserve it for the scarcity situation. To identify the potential location for the water storage structure in the river basin a overlay approach was adapted (Ramakrishnan et al., 2009), where the cite selection were based on the hydrological characteristics, morphological characterstics of the stream, slope of the land ware taken as the basic input for prioritization in a GIS environment. This approach uses the potential runoff generation zone which will largely depend upon the sub-basin area, slope and stream order which ultimately provides the suitable location for the structure. Fig. 6.7 shows the stream network and the order of the streams in river basin, order of stream provides idea about the amount of runoff a stream will receive. Apart from the stream order, slope map and runoff potential map were used for identification of the potential zone. Figure 6.8 shows the proposed water storage structures in the downstream small tributaries. These proposed water

storage structure would check the drain of water to conserve it for the lean period. It was observed from the model that local water storage structure are sufficient enough to fulfill the water requirement in the lean period and low flow season.

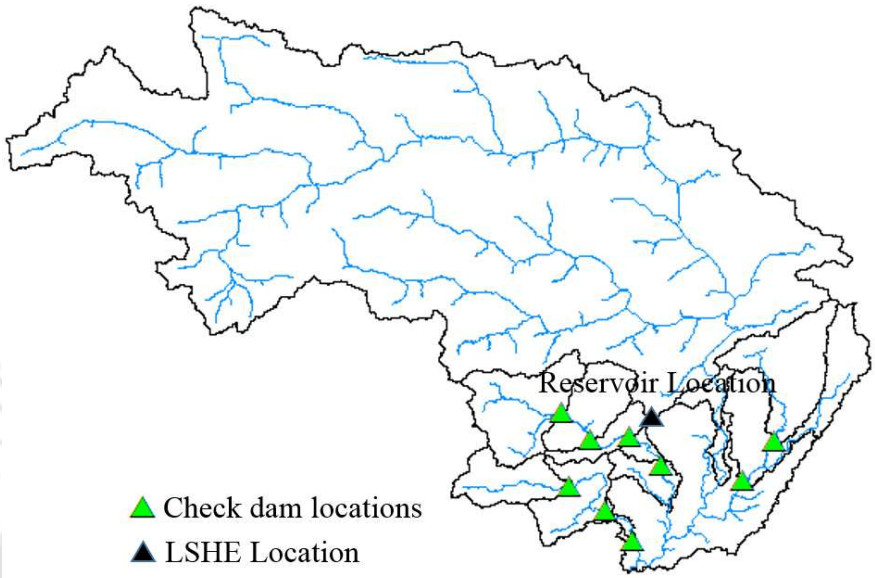

Figure 6.8: Location of proposed checkdam sites in the command area

On the basis of the morphological and hydrological characteristics of the watershed finally nine water conservation structures were proposed for the storage of water to fulfill the requirement in the water deficit condition. Practical implementation of the construction on the selected cites involves much more practicality such as the agricultural land or settlement area should not be disturbed with such constructions. Analysis of the streamflow availability in these water storage structures suggest that the water stored in these structured will be sufficient enough to fulfill the requirement in short term deficit situation.

6.6 Advantages of the linked approach in river basin planning

Linked simulation-management approach combined with the top down decision making approach for the river basin planning has several advantage over traditional management approach. Decision making process involves the several stakeholders into account along with the climatic and hydrological processes which are going to be affected by the climate change impacts. Expanding modeling approach beyond the river basin and streamflow simulation and including the reservoir command area improves the representation of water resources characteristics in upstream as well as in the downstream and provides a platform for the management strategies. Further advantages of the linked approach is that it accounts the climatic variabilty which is inherent on the climate change process such as change in precipitation and temperature, which affects the seasonal water availability for the agricultural demand in command area. Linked approach addresses the water availability in terms of quantity and timing which is more important in planning purposes because of better understanding of relative ability to address the adaptation requirement. Along with the advantages there are several limitations as well with such approach, such as modeling reservoir and command areas requires large data of the downstream such as population, agricultural practices and canal release which are not available always in many river basins. Large involvement of the resource presents a challenge for large scale applicability in such studies which requires resources necessary for data collection, stakeholder consultations and modeling analyses. WEAP model has the limitations such as it works on the a monthly time step which may not be appropriate for all studies or for a particular adaptation option.

6.7 Conclusions

Earlier studies (Ray, 2010) on the Subansiri river was conducted for the environmental impact assessment and effect of Lower Subansiri reservoir on the downstream of the reservoir, focus was mainly on the loss in agricultural and fish production because of the large diurnal variation in the river flow because of the turbine operation. Since no study was carried out for the climate change impact assessment on the water availability and water demand, this study focuses on this aspect and found that the increasing population will cause extra burden on the water resources of the basin and need to be addressed for management plans. Several other similar studies were carried out for the water management under climate change scenarios which are compared here. Sapkota et al. (2013) conducted a study on the Upper Ganges river basin in India for the available water resources in the river basin under the past and future climate change scenarios. Water evaluation and planning model was utilized for the assessment of the water demand for the different sectors e.g. municipal demand, agricultural demand and industrial demand. It was found that, for the available amount of water resources a water deficit arises in the months of December and January for the historical period. Future projection of the water demand for the climate change scenarios indicated the deficit in the months of December, January and February. Considering the essential environmental flow in the stream, water deficit increases significantly for all the sectors. As a remedy measures, several option were suggested including the change in cropping pattern and emphasize conjunctive use. Bhave et al. (2013) suggested climate change adaptation option in the Kangsabati river basin of West Bengal. Study utilized the combined bottom-up and top-down approach for the adaptation options including the

several stakeholders of the river catchment. Study explores the various in-situ management options for the water conservation in the catchment such as increasing the forest area and construction of the check-dams at several locations in order to check the drainage of rainfall generated surface water. Yates et al. (2015) proposed a multistage decision support process for the basin planning of Upper Colorado river considering the city and farms as the stakholders in management plan. Approach was achieved by management model WEAP and downscaling model SDSM. Future scenarios of the water resources in the basin and drought occurrence were the main focus of management plan. It was found that drought mitigation strategies will only provide short term benefits and suggested engagement of water managers and stakeholders participation in decision making process.

CHAPTER 7

Conclusions and recommendations for the future work

Present study has been carried out to explore the changes in the hydro-climatological variables such as streamflow, precipitation and temperature of the Subansiri river basin which is the largest tributary of Brahmputra river basin in Northeast India. To accomplish the study, three general circulation models with three representative concentration pathways were selected for the study. To carry out the climate change impact studies on the precipitation and temperature, statistical downscaling technique was utilized for projection of mentioned climatic variables for the future period of 2011-2100. Impact of climate change on the hydrology of the river basin were further estimated using the Soil and water assessment tool (SWAT) model. Further, a integrated simulation-management model was proposed for the river basin for the different climate change scenarios, on the basis of the population growth of the river basin and increase in the water demand. Based on the selected objectives, following are the conclusive points notified in the overall study discussed further

7.1 Downscaling of the temperature and precipitation

Trends in the historical precipitation and temperature were calculated using Mann-Kendall trend test and Sen's slope methods. Further, temperature and precipitation were projected for the three RCP scenarios i.e. RCP2.6, RCP6.0 and RCP8.5 for three GCM scenarios using statistical downscaling technique. For the downscaling technique, historical observed precipitation an temperature series were used for the model preparation with the NCEP predictors. After calibration and validation of the models, future projection of the variables were performed by using the GCM variables for the three RCP scenarios. The downscaling results show uniform increase in minimum and maximum temperature for the basin whereas inter-decadal analysis of temperature shows that increase in minimum temperature is more than increase in maximum temperature which subsequently shows a decreasing trend for diurnal temperature range. A worldwide study on the trend of temperature shows an increase in the maximum temperature which is low as compared to the minimum temperature. The Subansiri River originates from Himalayan glaciers; an increase in the temperature of the basin may cause an alteration in the hydrology of the basin. This analysis of the change in temperature can be helpful in the assessment of the changes in the hydrological cycle of the region. Precipitation downscaling and precipitation indices analysis for 2011-2100 was performed using three GCM datasets for four RCP scenarios. Average of precipitation generated using three GCMs gives a clear picture of increasing trend of annual precipitation and intensity in Subansiri river basin. Subansiri river originates from Tibetan plateau which is rain shadow zone and receives as less than thousand millimeter precipitation whereas precipitation in stations station 2,3,4 and 5 which fall in Arunachal

Pradesh and Assam states receive high annual precipitation in thousands of millimeters. The study reveals possibility of increase in annual precipitation in intensity in station 1 which is in agreement with a previous study (Song et al., 2011). Changes in annual precipitation magnitude vary for RCP2.6, RCP6.0 and RCP8.5 from 3.26mm/year, 6.39mm/year and 9.57mm/year, respectively. (IPCC, 2013) report indicates increase in annual precipitation for mountainous region which justifies the findings of the study. Physical reasons behind the probable change was not the part of the study but the results shows a good agreement with the previous studies done for the region and ongoing possible greenhouse gas emission scenarios. Though the present study focuses mainly on Subansiri river catchment in the eastern Himalayan region. Many other river catchments in eastern Himalayan regions shares the same hydro-climatology, for example, all are fed by Southwest Monsoon during same period of the year and have same wind circulation patterns. Hence, the outcomes of this study can be related to the climatic changes happening in other catchments in the region. Apart from this, methods used in this study (statistical downscaling and precipitation indices analysis) can provide a framework for similar kind of studies in the future.

7.2 Hydrological modeling and analysis of changes in streamflow

Hydrological modeling of the Subansiri river was carried out to simulate the streamflow in the Subansiri river with the help of soil and water assessment tool (SWAT). Digital elevation map, land use land cover map and soil map along with the weather data such as precipitation and temperature were utilized for the model preparation. Further the model was calibrated using the SWAT-CUP tool, along with the model calibration and

validation, uncertainty analysis of the model was also performed using the SUFI2 algorithm. After calibration and validation of the model, downscaled precipitation and temperature data were utilized as the primary input in the model for the future projections of the streamflow in the river. Three CMIP5 GCMs with three RCP emission scenarios were selected for the study, total 9 ensembles of precipitation, temperature and streamflow were generated for comparing the changes in these variables as compared to the baseline scenario. Results show significant increase in annual precipitation and annual average Tmax and Tmin of the basin for all the RCP scenarios which is incremental in nature according to the extremity of the RCP scenarios. Since the hydrology of any region depend largely on the climatology factors along with the physical factors of the region, study shows that the changes in precipitation and temperature subsequently affecting the runoff and water yield in the river basin. Subansiri river is glacier induced perennial river which causes massive flood during the monsoon period in the downstream portion of Lakhimpur and Dhemaji districts.

7.3 Integrated approach for water management under climate change scenarios

Lower Subansiri hydropower project which is situated at the Gerukamukh in Assam is mainly operated for the flood control and hydro-power generation. Taking into consideration the increasing population and changes in the climate parameters along with the hydrological variables, it is important to have some more aspects of the reservoir utilization apart from the hydropower generation. An integrated approach was used for the water management plans under different climate change scenarios. Integrated simulation-management model proposed by integrating the SWAT model and water

management model i.e. water evaluation and planning model (WEAP). The assessment of the water demand in the different future scenarios and management plan. Results show that the water availability in the reservoir will not be sufficient to meet the municipal water demand along with the hydro power generation. As the study suggests possible increase in precipitation and discharge in the basin, situation may become more serious in the future climate change scenarios. Top down approach were adapted to overcome the seasonal scarcity of the water and water storage structure were suggested for water conservation and checking the runoff. This study could be helpful for policy making, planning and mitigation strategies to curb the possible flood hazard situations for the climate change scenarios in the region.

7.4 Recommendations for the future study

Following work may be taken as the future extension of the present works:

- In downscaling of the temperature and precipitation, three GCMs were selected for the study. Although in the climate change studies, uncertainties are inherent in nature because of the adaptation of different methods in the GCM simulation, which imparts uncertainty in the downscaling results. For the future extension of the work, more number of GCM could be selected for minimizing the uncertainty.

- GCMs are the coarser grid products, regional climate models (RCM) could provide even more accurate results for the projection of temperature and precipitation. Apart from the datasets, more methodologies for the downscaling could have provided the better comparison for selection of the suitable methods.

- Change in the streamflow were assessed on the basis of the hydrological modeling

of the river basin, primary variable taken into consideration were the precipitation and temperature whereas the other variables were taken constant such as LULC, which can be considered for the future studies.

- Simulation management model has the several limitations which can be improved with the use of several advanced optimization techniques.

References

Abbaspour, K., Vejdani, M., and Haghighat, S. (2007a). SWAT-CUP calibration and uncertainty programs for SWAT. In *MODSIM 2007 International Congress on Modelling and Simulation, Modelling and Simulation Society of Australia and New Zealand*.

Abbaspour, K. C., Johnson, C. A., and van Genuchten, M. T. (2004). Estimating Uncertain Flow and Transport Parameters Using a Sequential Uncertainty Fitting Procedure. *Vadose Zone Journal*, 3(4):1340.

Abbaspour, K. C., Rouholahnejad, E., Vaghefi, S., Srinivasan, R., Yang, H., and Kløve, B. (2015). A continental-scale hydrology and water quality model for Europe: Calibration and uncertainty of a high-resolution large-scale SWAT model. *Journal of Hydrology*, 524:733–752.

Abbaspour, K. C., Yang, J., Maximov, I., Siber, R., Bogner, K., Mieleitner, J., Zobrist, J., and Srinivasan, R. (2007b). Modelling hydrology and water quality in the pre-alpine/alpine Thur watershed using SWAT. *Journal of Hydrology*, 333(2-4):413–430.

Ahmed, J. A. and Sarma, A. K. (2005). Genetic algorithm for optimal operating policy of a multipurpose reservoir. *Water Resources Management*, 19(2):145–161.

Alemayehu, T., McCartney, M., and Kebede, S. (2010). The water resource implications of planned development in the Lake Tana catchment, Ethiopia. *Ecohydrology and Hydrobiology*, 10(2):211–221.

Alexander, L., Zhang, X., Peterson, T., Caesar, J., Gleason, B., Klein Tank, A., Haylock, M., Collins, D., Trewin, B., Rahimzadeh, F., et al. (2006). Global observed changes in daily climate extremes of temperature and precipitation. *Journal of Geophysical Research: Atmospheres*, 111(D5).

Anandhi, A., Srinivas, V., Nanjundiah, R. S., and Nagesh Kumar, D. (2008). Downscaling precipitation to river basin in India for IPCC SRES scenarios using support vector machine. *International Journal of Climatology*, 28(3):401–420.

Arnell, N. W. (2003). Relative effects of multi-decadal climatic variability and changes in the mean and variability of climate due to global warming: Future streamflows in Britain. *Journal of Hydrology*, 270(3-4):195–213.

Arnell, N. W. (2010). Adapting to climate change: an evolving research programme. *Climatic Change*, 100(1):107–111.

Arnell, N. W. and Lloyd-Hughes, B. (2013). The global-scale impacts of climate change on water resources and flooding under new climate and socio-economic scenarios. *Climatic Change*, 122(1-2):127–140.

Bahremand, A. and De Smedt, F. (2010). Predictive Analysis and Simulation Uncertainty of a Distributed Hydrological Model. *Water Resources Management*, 24(12):2869–2880.

Barnett, T. P., Adam, J. C., and Lettenmaier, D. P. (2005). Potential impacts of a warming climate on water availability in snow-dominated regions. *Nature*, 438(7066):303–9.

Bates, B., Kundzewicz, Z., Wu, S., and Palutikof, J. (2008). Observed and projected changes in climate as they relate to water. *Climate Change and Water*, pages 13–31.

Bhave, A. G., Mishra, A., and Groot, A. (2013). Sub-basin scale characterization of climate change vulnerability, impacts and adaptation in an Indian River basin. *Regional Environmental Change*, 13(5):1087–1098.

Bhave, A. G., Mittal, N., Mishra, A., and Raghuwanshi, N. S. (2016). Integrated assessment of no-regret climate change adaptation options for reservoir catchment and command areas. *Water Resources Management*, 30(3):1001–1018.

Bhutiyani, M. R., Kale, V. S., and Pawar, N. J. (2007). Long-term trends in maximum, minimum and mean annual air temperatures across the Northwestern Himalaya during the twentieth century. *Climatic Change*, 85(1-2):159–177.

Bhutiyani, M. R., Kale, V. S., and Pawar, N. J. (2010). Climate change and the precipitation variations in the northwestern Himalaya: 1866-2006. *International Journal of Climatology*, 30(4):535–548.

Block, P. (2011). Tailoring seasonal climate forecasts for hydropower operations. *Hydrology and Earth System Sciences*, 15(4):1355–1368.

Box, J. E., Bromwich, D. H., Veenhuis, B. A., Bai, L. S., Stroeve, J. C., Rogers, J. C., Steffen, K., Haran, T., and Wang, S. H. (2006). Greenland ice sheet surface mass balance variability (1988-2004) from calibrated polar MM5 output. *Journal of Climate*, 19(12):2783–2800.

Brekke, L. D., Maurer, E. P., Anderson, J. D., Dettinger, M. D., Townsley, E. S., Harrison, A., and Pruitt, T. (2009). Assessing reservoir operations risk under climate change. *Water Resources Research*, 45(4).

Burn, D. H., Sharif, M., and Zhang, K. (2010). Detection of trends in hydrological extremes for Canadian watersheds. *Hydrological Processes*, 24(13):1781–1790.

Cayan, D. R., Maurer, E. P., Dettinger, M. D., Tyree, M., and Hayhoe, K. (2008). Climate change scenarios for the california region. *Climatic change*, 87(1):21–42.

Chen, H., Guo, J., Zhang, Z., and Xu, C. Y. (2012). Prediction of temperature and precipitation in Sudan and South Sudan by using LARS-WG in future. *Theoretical and Applied Climatology*, 113(3-4):363–375.

Chinnasamy, P., Bharati, L., Bhattarai, U., Khadka, A., Dahal, V., and Wahid, S. (2015). Impact of planned water resource development on current and future water demand in the Koshi river basin, Nepal. *Water International*, 40(7):1004–1020.

Chu, J. T., Xia, J., Xu, C. Y., and Singh, V. P. (2009). Statistical downscaling of daily mean temperature, pan evaporation and precipitation for climate change scenarios in Haihe River, China. *Theoretical and Applied Climatology*, 99(1-2):149–161.

Cunderlik, J. M. and Ouarda, T. B. M. J. (2009). Trends in the timing and magnitude of floods in Canada. *Journal of Hydrology*, 375(3-4):471–480.

Dahal, V., Shakya, N., and Bhattarai, R. (2016). Estimating the impact of climate change on water availability in bagmati basin, nepal. *Environmental Processes*, 3(1):1–17.

Dai, A., Qian, T., Trenberth, K. E., and Milliman, J. D. (2009). Changes in continental freshwater discharge from 1948 to 2004. *Journal of Climate*, 22(10):2773–2792.

Das, A., Ghosh, P. K., Choudhury, D. P., Munda, G. C., Ngachan, S. V., and Chowdhury, P. (2009). Climate change in Northeast INDIA: recent facts and events –worry for agricultural management. In *ISPRS Archives XXXVIII-8/W3 Workshop Proceedings: Impact of Climate Change on Agriculture*.

Deng, Z., Qiu, X., Liu, J., Madras, N., Wang, X., and Zhu, H. (2016). Trend in frequency of extreme precipitation events over ontario from ensembles of multiple gcms. *Climate Dynamics*, 46(9-10):2909–2921.

Dettinger, M. D. (2012). Projections and downscaling of 21st century temperatures, precipitation, radiative fluxes and winds for the Southwestern US, with focus on Lake Tahoe. *Climatic Change*, 116(1):17–33.

Duhan, D. and Pandey, A. (2013). Statistical analysis of long term spatial and temporal trends of precipitation during 1901-2002 at Madhya Pradesh, India. *Atmospheric Research*, 122:136–149.

Duhan, D. and Pandey, A. (2015). Statistical downscaling of temperature using three techniques in the Tons River basin in Central India. *Theoretical and Applied Climatology*, 121(3-4):605–622.

Dunne, J. P., John, J. G., Adcroft, A. J., Griffies, S. M., Hallberg, R. W., Shevliakova, E., Stouffer, R. J., Cooke, W., Dunne, K. A., Harrison, M. J., et al. (2012). GFDL's ESM2 global coupled climate-carbon Earth System Models. Part I: Physical formulation and baseline simulation characteristics. *Journal of Climate*, 25(19):6646–6665.

Dunne, J. P., John, J. G., Shevliakova, S., Stouffer, R. J., Krasting, J. P., Malyshev, S. L., Milly, P. C. D., Sentman, L. T., Adcroft, A. J., Cooke, W., Dunne, K. A., Griffies, S. M., Hallberg, R. W., Harrison, M. J., Levy, H., Wittenberg, A. T., Phillips, P. J., and Zadeh, N. (2013). GFDL's ESM2 global coupled climate-carbon

earth system models. Part II: Carbon system formulation and baseline simulation characteristics. *Journal of Climate*, 26(7):2247–2267.

Easterling, D. R., Horton, B., Jones, P. D., Peterson, T. C., Karl, T. R., Parker, D. E., Salinger, M. J., Razuvayev, V., Plummer, N., Jamason, P., et al. (1997). Maximum and minimum temperature trends for the globe. *Science*, 277(5324):364–367.

Ellison, D., N Futter, M., and Bishop, K. (2012). On the forest cover–water yield debate: from demand-to supply-side thinking. *Global Change Biology*, 18(3):806–820.

Elsner, M. M., Cuo, L., Voisin, N., Deems, J. S., Hamlet, A. F., Vano, J. A., Mickelson, K. E. B., Lee, S. Y., and Lettenmaier, D. P. (2010). Implications of 21st century climate change for the hydrology of Washington State. *Climatic Change*, 102(1-2):225–260.

Fischer, G., Tubiello, F. N., van Velthuizen, H., and Wiberg, D. A. (2007). Climate change impacts on irrigation water requirements: Effects of mitigation, 1990–2080. *Technological Forecasting and Social Change*, 74(7):1083–1107.

Ghosh, S., Luniya, V., and Gupta, A. (2009). Trend analysis of Indian summer monsoon rainfall at different spatial scales. *Atmospheric Science Letters*, 10:285–290.

Ghosh, S. and Mujumdar, P. (2008). Statistical downscaling of GCM simulations to streamflow using relevance vector machine. *Advances in Water Resources*, 31(1):132–146.

Gogoi, C. and Goswami, D. C. (2014). A study on channel migration of the Subansiri river in Assam using remote sensing and gis technology. *Current Science*, 106(8).

Gosain, A. K., S. R. and Basuray, D. (2003). Assessment of vulnerability and adaptation for water sector. In *Proceedings of the workshop on vulnerability assess-ment and adaptation due to climate change on Indian water resources, coastal zones and human health. Ministry of Environment and Forests, New Delhi.*, pages 17–24.

Goswami, U., Sarma, J. N., and Patgiri, A. D. (1999). River channel changes of the Subansiri in Assam, India. *Geomorphology*, 30(3):227–244.

Goyal, M. K., Burn, D. H., and Ojha, C. S. P. (2011). Evaluation of machine learning tools as a statistical downscaling tool: temperatures projections for multi-stations for Thames River Basin, Canada. *Theoretical and Applied Climatology*, 108(3-4):519–534.

Goyal, M. K. and Ojha, C. S. P. (2012a). Downscaling of precipitation on a lake basin: evaluation of rule and decision tree induction algorithms. *Hydrology Research*, 43(3):215.

Goyal, M. K. and Ojha, C. S. P. (2012b). Downscaling of surface temperature for lake catchment in an arid region in India using linear multiple regression and neural networks. *International Journal of Climatology*, 32(4):552–566.

Harou, J. J., Pulido-Velazquez, M., rosenberg, D. E., Medellín-Azuara, J., Lund, J. R., and Howitt, R. E. (2009). Hydro-economic models: Concepts, design, applications, and future prospects. *Journal of Hydrology*, 375(3):627–643.

Hattermann, F. F., Kundzewicz, Z. W., Huang, S., Vetter, T., Gerstengarbe, F. W., and Werner, P. (2013). Climatological drivers of changes in flood hazard in Germany. *Acta Geophysica*, 61(2):463–477.

Immerzeel, W. W., Droogers, P., de Jong, S. M., and Bierkens, M. F. P. (2009). Large-scale monitoring of snow cover and runoff simulation in Himalayan river basins using remote sensing. *Remote Sensing of Environment*, 113(1):40–49.

Immerzeel, W. W., van Beek, L. P. H., Konz, M., Shrestha, A. B., and Bierkens, M. F. P. (2012). Hydrological response to climate change in a glacierized catchment in the Himalayas. *Climatic Change*, 110(3-4):721–736.

IPCC (2007). Climate change 2007: impacts, adaptation, and vulnerability: working group II contribution to the Intergovernmental Panel on Climate Change fourth assessment report, summary for policymakers. IPCC Secretariat, Geneva. Technical report.

IPCC (2013). Climate Change 2013: The Physical Science Basis. Contribution of Working Group I to the Fifth Assessment Report of the Intergovernmental Panel on Climate Change. *Intergovernmental Panel on Climate Change, Working Group*

I Contribution to the IPCC Fifth Assessment Report (AR5)(Cambridge Univ Press, New York), page 1535.

IPCC (2014). *Climate Change 2014: Synthesis Report*. Number 58.

Jothiprakash, V. and Arunkumar, R. (2013). Multi-reservoir optimization for hydropower production using NLP technique. *KSCE Journal of Civil Engineering*, 18(1):344–354.

Kalma, J. D., McVicar, T. R., and McCabe, M. F. (2008). Estimating Land Surface Evaporation: A Review of Methods Using Remotely Sensed Surface Temperature Data. *Surveys in Geophysics*, 29(4-5):421–469.

Karl, T., Jones, P., Knight, R., Kukla, G., Plummer, N., Razuvayev, V., Gallo, K., Lindseay, J., Charlson, R., and Peterson, T. (1993). A new perspective on recent global warming: Asymmetric trends of daily maximum temperature and minimum temperature. *Bulletin of the American Meteorological Society*, 77:279–292.

Kaser, G., Juen, I., Georges, C., Gomez, J., and Tamayo, W. (2003). The impact of glaciers on the runoff and the reconstruction of mass balance history from hydrological data in the tropical Cordillera Bianca, Peru. *Journal of Hydrology*, 282(1-4):130–144.

Kendall (1968). *The advanced theory of statistics*, volume 3. London.

Khadka, D., Babel, M. S., Shrestha, S., and Tripathi, N. K. (2014). Climate change impact on glacier and snow melt and runoff in Tamakoshi basin in the Hindu Kush Himalayan (HKH) region. *Journal of Hydrology*, 511:49–60.

Khan, M. S., Coulibaly, P., and Dibike, Y. (2006). Uncertainty analysis of statistical downscaling methods. *Journal of Hydrology*, 319(1-4):357–382.

Kharin, V. V., Zwiers, F., Zhang, X., and Wehner, M. (2013). Changes in temperature and precipitation extremes in the cmip5 ensemble. *Climatic Change*, 119(2):345–357.

Kron, W. and Berz, G. (2007). Flood disasters and climate change: trends and options–a (re-) insurer's view. *Global change: enough water for all*, pages 268–273.

Kumar, a. R. S., Goyal, M. K., Ojha, C. S. P., Singh, R. D., Swamee, P. K., and Nema, R. K. (2013). Application of ANN, Fuzzy Logic and Decision Tree Algorithms

for the Development of Reservoir Operating Rules. *Water Resources Management*, 27(3):911–925.

Mahmood, R. and Babel, M. S. (2013). Evaluation of SDSM developed by annual and monthly sub-models for downscaling temperature and precipitation in the Jhelum basin, Pakistan and India. *Theoretical and Applied Climatology*, 113(1-2):27–44.

Mann, H. B. (1945). Nonparametric tests against trend. *Econometrica: Journal of the Econometric Society*, pages (245–259).

Mehrotra, D. and Mehrotra, R. (1995). Climate change and hydrology with emphasis on the Indian subcontinent. *Hydrological Sciences Journal*, 40(2):231–242.

Mehrotra, R. (1999). Sensitivity of runoff, soil moisture and reservoir design to climate change in central Indian river basins. *Climatic Change*, 42(4):725–757.

Mehta, V. K., Aslam, O., Dale, L., Miller, N., and Purkey, D. R. (2013). Scenario-based water resources planning for utilities in the lake victoria region. *Physics and Chemistry of the Earth*, 61:22–31.

Milly, P. C., Dunne, K. A., and Vecchia, A. V. (2005). Global pattern of trends in streamflow and water availability in a changing climate. *Nature*, 438(7066):347–350.

Mishra, V. and Lilhare, R. (2016). Hydrologic sensitivity of Indian sub-continental river basins to climate change. *Global and Planetary Change*, 139:78–96.

Mondal, A. and Mujumdar, P. P. (2012). On the basin-scale detection and attribution of human-induced climate change in monsoon precipitation and streamflow. *Water Resources Research*, 48(10).

Mujumdar, P. P. and Nirmala, B. (2007). A bayesian stochastic optimization model for a multi-reservoir hydropower system. *Water Resources Management*, 21(9):1465–1485.

Nash, J. E. and Sutcliffe, J. V. (1970). River flow forecasting through conceptual models Part I—A discussion of principles. *Journal of hydrology*, 10(3):282–290.

Neitsch, S. L., Williams, J., Arnold, J., and Kiniry, J. (2011). Soil and water assessment tool theoretical documentation version 2009. Technical report, Texas Water Resources Institute.

Nel, W. (2009). Rainfall trends in the kwazulu-natal drakensberg region of south africa during the twentieth century. *International Journal of Climatology*, 29(11):1634–1641.

Neupane, R. P., White, J. D., and Alexander, S. E. (2015). Projected hydrologic changes in monsoon-dominated Himalaya Mountain basins with changing climate and deforestation. *Journal of Hydrology*, 525:216–230.

Palazzi, E., Hardenberg, J., and Provenzale, A. (2013). Precipitation in the hindu-kush karakoram himalaya: Observations and future scenarios. *Journal of Geophysical Research: Atmospheres*, 118(1):85–100.

Parthasarathy, B., Munot, A., and Kothawale, D. (1995). Monthly and seasonal rainfall series for all india. *Re RR-065*, 113.

Patil, S. D., Wigington, P. J., Leibowitz, S. G., Sproles, E. a., and Comeleo, R. L. (2014). How does spatial variability of climate affect catchment streamflow predictions? *Journal of Hydrology*, 517:135–145.

Patra, J. P., Mishra, A., Singh, R., and Raghuwanshi, N. S. (2012). Detecting rainfall trends in twentieth century (1871-2006) over Orissa State, India. *Climatic Change*, 111(3):801–817.

Payne, J., Wood, A., and Hamlet, A. (2004). Mitigating the effects of climate change on the water resources of the Columbia River basin. *Climatic Change*, 62(1-3):233–256.

Purkey, D., Joyce, B., Vicuna, S., Hanemann, M., Dale, L., Yates, D., and Dracup, J. (2008). Robust analysis of future climate change impacts on water for agriculture and other sectors: a case study in the Sacramento Valley. *Climatic Change*, 87(1):109–122.

Qian, W., Fu, J., and Yan, Z. (2007). Decrease of light rain events in summer associated with a warming environment in china during 1961–2005. *Geophysical Research Letters*, 34(11).

Rajbhandari, R., Shrestha, A., Kulkarni, A., Patwardhan, S., and Bajracharya, S. (2015). Projected changes in climate over the Indus river basin using a high resolution regional climate model (PRECIS). *Climate Dynamics*, 44(1-2):339–357.

Rajeevan, M., Bhate, J., Kale, J. D., and Lal, B. (2006). Development of a high resolution daily gridded rainfall data set for the Indian region. *Current Science*, 91(3):296–306.

Ramakrishnan, D., Bandyopadhyay, A., and Kusuma, K. (2009). Scs-cn and gis-based approach for identifying potential water harvesting sites in the kali watershed, mahi river basin, india. *Journal of Earth System Science*, 118(4):355–368.

Rani, D. and Moreira, M. M. (2009). Simulation–optimization modeling: A survey and potential application in reservoir systems operation. *Water Resources Management*, 24(6):1107–1138.

Ray, M. R. (2010). *Reservoir operation considering downstream impact of a hydroeletric project*. PhD thesis, Indian Institute of Technology Guwahati.

Ray, M. R. and Sarma, A. K. (2011). Minimizing diurnal variation of downstream flow in hydroelectric projects to reduce environmental impact. *Journal of Hydro-Environment Research*, 5(3):177–185.

Rehana, S. and Mujumdar, P. P. (2013). Regional impacts of climate change on irrigation water demands. *Hydrological Processes*, 27(20):2918–2933.

Sachindra, D., Huang, F., Barton, A., and Perera, B. (2011). Statistical downscaling of general circulation model outputs to catchment streamflows.

Safavi, H. R., Golmohammadi, M. H., and Sandoval-Solis, S. (2015). Expert knowledge based modeling for integrated water resources planning and management in the Zayandehrud River Basin. *Journal of Hydrology*, 528:773–789.

Samadi, S., Wilson, C. a. M. E., and Moradkhani, H. (2013). Uncertainty analysis of statistical downscaling models using Hadley Centre Coupled Model. *Theoretical and Applied Climatology*, 114(3-4):673–690.

Samani, Z., Skaggs, R., and Longworth, J. (2012). Alfalfa water use and crop coefficients across the watershed: From theory to practice. *Journal of Irrigation and Drainage Engineering*, 139(5):341–348.

Sandoval-Solis, S. and McKinney, D. (2012). Integrated water management for environmental flows in the Rio Grande. *Journal of Water Resources Planning and Management*, 140(3):355–364.

Sapkota, P., Bharati, L., Gurung, P., Kaushal, N., and Smakhtin, V. (2013). Environmentally sustainable management of water demands under changing climate conditions in the upper ganges basin, India. *Hydrological Processes*, 27(15):2197–2208.

Sarkar, A., Singh, R., and Sharma, N. (2012). Climate variability and trends in part of brahmaputra river basin. *India Water Week 2012 Water, Energy and Food Security: Call for Solutions, New Delhi, 2012*.

Sarma, B., Sarma, A. K., and Singh, V. P. (2013). Optimal Ecological Management Practices (EMPs) for Minimizing the Impact of Climate Change and Watershed Degradation Due to Urbanization. *Water Resources Management*, 27(11):4069–4082.

Sen, P. K. (1968). Estimates of the regression coefficient based on Kendall's tau. *Journal of the American Statistical Association*, 63(324):1379–1389.

Shrestha, A. B., Wake, C. P., Mayewski, P. A., and Dibb, J. E. (1999). Maximum temperature trends in the Himalaya and its vicinity: An analysis based on temperature records from Nepal for the period 1971-94. *Journal of Climate*, 12(9):2775–2786.

Singh, D. S. and Awasthi, A. (2011). Natural hazards in the Ghaghara River area, Ganga plain, India. *Natural Hazards*, 57(2):213–225.

Singh, P. and Bengtsson, L. (2005). Impact of warmer climate on melt and evaporation for the rainfed, snowfed and glacierfed basins in the Himalayan region. *Journal of Hydrology*, 300(1-4):140–154.

Singh, P. and Kumar, N. (1996). Determination of snowmelt factor in the Himalayan region. *Hydrological Sciences Journal*, 41(3):301–310.

Singh, P. and Kumar, N. (1997). Impact assessment of climate change on the hydrological response of a snow and glacier melt runoff dominated Himalayan river. *Journal of Hydrology*, 193(1-4):316–350.

Singh, V. and Goyal, M. K. (2016). Changes in climate extremes by the use of CMIP5 coupled climate models over eastern Himalayas. *Environmental Earth Sciences*, 75(9):839.

Singh, V., Sharma, N., and Ojha, C. S. P. (2013). *The Brahmaputra basin water resources*, volume 47. Springer Science & Business Media.

Snell, S. E., Gopal, S., and Kaufmann, R. K. (2000). Spatial interpolation of surface air temperatures using artificial neural networks: Evaluating their use for downscaling gcms. *Journal of Climate*, 13(5):886–895.

Sonali, P. and Kumar, N. D. (2013). Review of trend detection methods and their application to detect temperature changes in India. *Journal of Hydrology*, 476:212–227.

Song, X., Song, S., Sun, W., Mu, X., Wang, S., Li, J., and Li, Y. (2015). Recent changes in extreme precipitation and drought over the songhua river basin, china, during 1960–2013. *Atmospheric Research*, 157:137–152.

Song, Y., Achberger, C., and Linderholm, H. W. (2011). Rain-season trends in precipitation and their effect in different climate regions of China during 1961–2008. *Environmental Research Letters*, 6(3):034025.

Steinschneider, S. and Brown, C. (2012). Dynamic reservoir management with real-option risk hedging as a robust adaptation to nonstationary climate. *Water Resources Research*, 48(W05524).

Taylor, K. E., Stouffer, R. J., and Meehl, G. A. (2012). An overview of CMIP5 and the experiment design. *Bulletin of the American Meteorological Society*, 93(4):485–498.

Thomas, A. (2000). Climatic changes in yield index and soil water deficit trends in china. *Agricultural and Forest Meteorology*, 102(2):71–81.

Torres, R. R. and Marengo, J. A. (2014). Climate change hotspots over South America: from CMIP3 to CMIP5 multi-model datasets. *Theoretical and Applied Climatology*, 117(3-4):579–587.

Vano, J. a., Scott, M. J., Voisin, N., Stöckle, C. O., Hamlet, A. F., Mickelson, K. E. B., Elsner, M. M., and Lettenmaier, D. P. (2010). Climate change impacts on water management and irrigated agriculture in the Yakima River Basin, Washington, USA. *Climatic Change*, 102(1-2):287–317.

Vidal, J. P., Christierson, B., and Wade, S. D. (2011). Using probabilistic climate information for UK water resource planning. Geophysical research abstracts vol. 13 EGU2011-5663-1. 13.

Vose, R. S., Easterling, D. R., and Gleason, B. (2005). Maximum and minimum temperature trends for the globe: An update through 2004. *Geophysical Research Letters*, 32(23).

Watts, G. (2010). Water for people: climate change and water availability, Chapter 4. In Modelling the impact of climate change on water resource, Fung F, Lopez A, New M (eds.). Blackwell, Oxford.

Whitehead, P., Barbour, E., Futter, M., Sarkar, S., Rodda, H., Caesar, J., Butterfield, D., Jin, L., Sinha, R., Nicholls, R., et al. (2015). Impacts of climate change and socio-economic scenarios on flow and water quality of the Ganges, Brahmaputra and Meghna (GBM) river systems: low flow and flood statistics. *Environmental Science: Processes & Impacts*, 17(6):1057–1069.

Wilby, R. L., Dawson, C. W., and Barrow, E. M. (2002). SDSM a decision support tool for the assessment of regional climate change impacts. *Environmental Modelling & Software*, 17(2):145–157.

Willmott, C. J., Rowe, C. M., and Mintz, Y. (1985). Climatology of the terrestrial seasonal water cycle. *Journal of Climatology*, 5(6):589–606.

Yang, J., Reichert, P., Abbaspour, K. C., and Yang, H. (2007). Hydrological modelling of the Chaohe Basin in China: Statistical model formulation and Bayesian inference. *Journal of Hydrology*, 340(3-4):167–182.

Yatagai, A., Arakawa, O., Kamiguchi, K., Kawamoto, H., Nodzu, M. I., and Hamada, A. (2009). A 44-year daily gridded precipitation dataset for asia based on a dense network of rain gauges. *Sola*, 5:137–140.

Yates, D., Purkey, D., Sieber, J., Huber-Lee, A., Galbraith, H., West, J., Herrod-Julius, S., Young, C., Joyce, B., and Rayej, M. (2009). Climate driven water resources model of the Sacramento Basin, California. *Journal of Water Resources Planning and Management*, 135(5):303–313.

Yates, D., Sieber, J., Purkey, D., and Huber-Lee, A. (2005). WEAP21—A demand-, priority-, and preference-driven water planning model: part 1: model characteristics. *Water International*, 30(4):487–500.

Yates, D. N., Miller, K. A., Wilby, R. L., and Kaatz, L. (2015). Decision-centric adaptation appraisal for water management across Colorado's continental divide. *Climate Risk Management*, 10:35–50.

Zhang, Q., Xu, C. Y., and Zhang, Z. (2009). Observed changes of drought/wetness episodes in the Pearl River basin, China, using the standardized precipitation index and aridity index. *Theoretical and Applied Climatology*, 98(1-2):89–99.

Zhang, Y., Vaze, J., Chiew, F. H., Teng, J., and Li, M. (2014). Predicting hydrological signatures in ungauged catchments using spatial interpolation, index model, and rainfall–runoff modelling. *Journal of Hydrology*, 517:936–948.

Papers and conferences

- Shivam, Goyal, M. K., and Sarma, A. K. (2016) "Analysis of the change in temperature trends in Subansiri River basin for RCP scenarios using CMIP5 datasets" *Theoretical and Applied Climatology*, 1-13. (IF 2.4)
- Shivam, Goyal, M. K., and Sarma, A. K. "Index-based study of future precipitation changes over Subansiri river catchment under changing climate" *Journal of Environmental Informatics* (Accepted) (IF 5.5)
- Shivam, Goyal, M. K., and Sarma, A. K. "Spatial Homogeneity of Extreme Precipitation Indices using Fuzzy Clustering over Northeast India", *Natural Hazards, Springer* (Under review) (IF 1.7)
- An integrated simulation-management approach for river basin planning of Subansiri river under climate change scenarios (to be submitted)

Book chapter

- Study of Subansiri River, a tributary of Brahmaputra River in Northeast India *Journal of Geological Society of India, Springer* (Under review)

Conferences

- Climate change impact assessment on water availability in a North-eastern river of India for sustainable water management. Internation Conference on Sustainability (SusCon-V) March 2016, IIM Shillong.
- Regionalization of Northeast India on Precipitation Indices Basis using Fuzzy Clustering Approach, HYDRO 2015 International conference, IIT Roorkee, India, 17-19 December, 2015.
- Extreme precipitation indices analysis of Northeast India region. International Conference, Assam University Silchar, November 2013.